Redshift distances in curved Friedmann-Lemaître-Robertson-Walker spacetime

Steffen Haase[*1]

[*]Leipzig, Germany

Abstract

In the present paper we use the curved Friedmann-Lemaitre-Robertson-Walker metric describing a spatially homogeneous and isotropic universe to derive the cosmological redshift distance in a way which differs from that which can be found in the general astrophysical literature.

Using the curved Friedmann-Lemaitre-Robertson-Walker metric the radial physical distance is described by $R(t) = a(t)\chi(r)$ with $\chi(r) = \arcsin(r)$ for the curvature parameter $\varepsilon = (+1)$ and $\chi(r) = \operatorname{arsinh}(r)$ for $\varepsilon = (-1)$, respectively. In this equation the radial co-moving coordinate is named r and a(t) means the time-depending scale parameter. We use the co-moving coordinate r_e (the subscript e indicates emission) describing the place of a galaxy which is emitting photons and r_a (the subscript a indicates absorption) describing the place of an observer within a different galaxy on which the photons - which were traveling thru the universe - are absorbed. Therefore the physical distance - the real way of light - is calculated by $D = a(t_0)\chi(r_a) - a(t_e)\chi(r_e) \equiv R_{0a} - R_{ee}$. Here means $a(t_0)$ the today's (t_0) scale parameter and $a(t_e)$ the scale parameter at the time t_e of emission of the photons. The physical distance D is therefore a difference of two different physical distances from an origin of coordinates being on r = 0.

Nobody can doubt this real travel way of light: The photons are emitted on the co-moving coordinate place r_e and are than traveling to the co-moving coordinate place r_a. During this traveling the time is moving from t_e to t_0 ($t_e \leq t_0$) and therefore the scale parameter is changing in the meantime from $a(t_e)$ to $a(t_0)$.

Using this right physical distance D we calculate the redshift distance and some relevant classical cosmological equations (effects) for both possible values of $\varepsilon = (\pm 1)$ and compare these theoretical results with some measurements of astrophysics (quasars, SN Ia and galaxy containing a black hole).

We get the today's Hubble parameter $H_{0a,\varepsilon=(+1)} \approx 65.117$ km/(s Mpc) for $\varepsilon = (+1)$ and $H_{0a,\varepsilon=(-1)} \approx 65.189$ km/(s Mpc) for $\varepsilon = (-1)$, respectively, as a main result. This values are a little smaller than the Hubble parameter $H_{0,Planck} \approx 67.66$ km/(s Mpc) resulting from Planck data 2018.

Furthermore, we find for the radius of the by us so-called Friedmann sphere $R_{0a,\varepsilon=(+1)} \approx 2{,}697.62$ Mpc and $R_{0a,\varepsilon=(-1)} \approx 3{,}011.07$ Mpc. This radius corresponds to a maximum possible distance of seeing within an expanding universe. Photons emitted at this distance are infinite red shifted.

The today's mass density of the Friedmann sphere results in $\rho_{0m,\varepsilon=(+1)} \approx 1.037 \times 10^{-30}$ g/cm^3 and $\rho_{0m,\varepsilon=(-1)} \approx 9.24 \times 10^{-32}$ g/cm^3, respectively. For the mass of the Friedmann sphere we get $M_{Fs,\varepsilon=(+1)} \approx 2.506 \times 10^{54}$ g and $M_{Fs,\varepsilon=(-1)} \approx 3.10 \times 10^{53}$ g, respectively.

The mass of black hole within the galaxy M87 has the value $M_{BH,\ M87,\varepsilon=(+1)} \approx 4.1469 \times 10^{43}$g and $M_{BH,\ M87,\varepsilon=(-1)} \approx 4.1468 \times 10^{43}$ g, respectively. The redshift distance of this object is $D_{\varepsilon=(+1)} \approx 19.60$ Mpc and $D_{\varepsilon=(-1)} \approx 19.60$ Mpc, respectively, but its today's distance is only $D_{0,\varepsilon=(+1)} \approx 8.13$ Mpc and $D_{0,\varepsilon=(-1)} \approx 6.78$ Mpc, respectively.

Key words: relativistic astrophysics, theoretical and observational cosmology, redshift, Hubble parameter, quasar, galaxy, M87, SN Ia, black hole, curved spacetime, open universe, closed universe

PACS NO:

[1] steffen_haase@vodafone.de

Contents:

1. Introduction

The current cosmological standard model assumes the correctness of Einstein's field equations (EFE) containing the cosmological term Λ

$$G_{\mu\nu} = \frac{8\pi G}{c_0^{\,4}} T_{\mu\nu} - \Lambda g_{\mu\nu} \tag{1}$$

and solves these equations with the help of the Friedmann-Lemaitre-Robertson-Walker metric (FLRWM)

$$ds^2 = c_0^{\,2} dt^2 - a^2(t)\left[\frac{dr^2}{1-\varepsilon r^2} + r^2(d\vartheta^2 + \sin^2\vartheta\, d\varphi^2)\right] \quad , \tag{2}$$

which is suitable for the description of a homogeneous and isotropic universe evolving over time.

The solutions found by solving the EFE are the two Friedmann equations (FE)

$$\left(\frac{\dot{a}}{a}\right)^2 = \frac{8\pi G}{3}\rho - \frac{\varepsilon c_0^{\,2}}{a^2} + \frac{\Lambda c_0^{\,2}}{3} \qquad \textit{and} \qquad \frac{\ddot{a}}{a} = -\frac{4\pi G}{3}\left(\rho + \frac{3P}{c_0^{\,2}}\right) + \frac{\Lambda c_0^{\,2}}{3}$$
$$\textit{with} \qquad \rho = \sum_i \rho_i \qquad i = r, m \quad . \tag{3a,b}$$

$G_{\mu\nu}$ is the Einstein tensor, G the gravitational constant, c_0 the velocity of light in vacuum, $T_{\mu\nu}$ the energy-momentum tensor and $g_{\mu\nu}$ the metric tensor. The parameter Λ is the cosmological constant that Einstein added to his original field equations, but later he discarded it. With ε = 0, (+1) or (-1) the constant of curvature was introduced and r, ϑ and φ are spherical polar coordinates. The time-dependent cosmological scale parameter was designated with a(t) and its time derivatives with points above. P is the pressure of matter and ρ is mainly the sum of two different densities: relativistic radiation (index r) and not-relativistic matter (index m).

Using the two well known conservation laws

$$K_r = \frac{8\pi G}{3c_0^{\,2}}\left(\rho_r a^4\right) = const \qquad or \qquad \rho_r = \frac{3c_0^{\,2} K_r}{8\pi G}\frac{1}{a^4} \tag{4a,b}$$

and

$$K_m = \frac{8\pi G}{3{c_0}^2}\left(\rho_m a^3\right) = const \qquad or \qquad \rho_m = \frac{3{c_0}^2 K_m}{8\pi G}\frac{1}{a^3} \tag{5a,b}$$

belonging to the two different densities ρ_r and ρ_m, respectively, we can rewrite the first FE as

$$\frac{\dot{a}^2}{{c_0}^2} = \frac{K_m}{a} + \frac{K_r}{a^2} - \varepsilon + a^2\frac{\Lambda}{3} \quad . \tag{3c}$$

The Eq. (4a,b) describe the development in time of radiation density and Eq. (5a,b) means the equivalent for non-relativistic matter.

In the following, we neglect the mathematical possible cosmological constant Λ. The comparison of the redshift distance derived within this paper with measurement results shows in retrospect that this additional parameter is not required. As a result, the EFE are returned to their historically original form and the Eq. (3c) takes on the simpler form

$$\frac{\dot{a}^2}{{c_0}^2} = \frac{K_r}{a^2} + \frac{K_m}{a} - \varepsilon \quad . \tag{3d}$$

Because we will deal with curved spacetime within this paper we have to set the parameter ε = (+1) on the one site and ε = (-1) on the other site. Therefore, we will get two different equations for the belonging redshift distances at the end of our calculation.

2 Derivation of cosmological relevant relations

2.1 Previews

From the requirement of homogeneity it follows that all extra-galactic objects remain at their co-moving coordinate location r in the course of the temporal development of the universe, i.e. the co-moving coordinate distance between randomly selected galaxies does not change over time, the galaxies rest in this co-moving coordinate system. For this reason, dr/dt = 0 applies to them.
This does not apply to the freely moving photons inside the universe: They detach themselves from a galaxy at a certain point in time at a certain co-moving coordinate location, and are then later absorbed at a completely different co-moving coordinate location.

Here we introduce the designation $r_{\mathbf{e}}$ (the subscript **e** indicates **e**mission of light) for the co-moving coordinate location of the light-emitting galaxy and name the co-moving coordinate location of the galaxy in which the observer resides $r_{\mathbf{a}}$ (the subscript **a** indicates **a**bsorption of light). Both variables mark the co-moving coordinate

distance from an origin of coordinates r = 0. The constant co-moving coordinate distance between the two galaxies is therefore calculated to be $\chi(r_a) - \chi(r_e)$ [see Eq. (7a,b)] if we assume that the galaxy of the observer is more depart from the coordinate origin as the light-emitting galaxy. The light should therefore move from the inside to the outside within a spherical assumed mass distribution (outgoing photons), which serves as a simple model for the universe (using the FLRWM, it is quite easy to arrange that all directions are of a radial kind).

Because of curved space, which is considered in this paper, we introduce

$$\chi(r) = \begin{cases} \int_0^r \frac{d\bar{r}}{\sqrt{1-\bar{r}^2}} = \arcsin(r) & for \quad \varepsilon = (+1) \quad with \quad \bar{r} < 1! \\ \int_0^r \frac{d\bar{r}}{\sqrt{1+\bar{r}^2}} = ar\sinh(r) & for \quad \varepsilon = (-1) \quad with \quad \bar{r} = any \end{cases} . \qquad (6a,b)$$

This results in

$$\chi_a(r_a) = \chi_a = \begin{cases} \arcsin(r_a) \\ ar\sinh(r_a) \end{cases} \quad and \quad \chi_e(r_e) = \chi_e = \begin{cases} \arcsin(r_e) & for \quad \varepsilon = (+1) \\ ar\sinh(r_e) & for \quad \varepsilon = (-1) \end{cases} . \qquad (7a,b)$$

These equations describe the co-moving places of the emitting galaxy and of the galaxy containing the observer, respectively.

Due to the measurable expansion of the universe we know that in the course of cosmic evolution all real physical distances $R(t) = a(t)\chi(r)$ over the time-dependent scale parameter a(t) being stretched according to the solution of Eq. (3b).

For a galaxy resting in the coordinate system of the FLRWM, the real physical distance from the origin of coordinates becomes calculated to

$$R(t) = a(t)\int_0^r \frac{d\bar{r}}{\sqrt{1-\varepsilon\bar{r}^2}} = a(t)\arcsin(r) \quad , \qquad (8a)$$

if $\varepsilon = (+1)$ is considered. On the other hand, we get

$$R(t) = a(t)\int_0^r \frac{d\bar{r}}{\sqrt{1-\varepsilon\bar{r}^2}} = a(t)\,ar\sinh(r) \quad , \qquad (8b)$$

if we use $\varepsilon = (-1)$ for integration.

The radial co-moving coordinate r does not depend on time for galaxies.

The physical distance of the light-emitting galaxy from the origin of coordinates at time t_e (the time at that time) is therefore

$$R_e(t_e) = a(t_e)\chi_e \equiv a_e\chi_e = R_{ee} \quad , \tag{9}$$

while for the analog distance of the galaxy containing the observer at the same time

$$R_a(t_e) = a(t_e)\chi_a \equiv a_e\chi_a = R_{ea} \tag{10}$$

applies. The physical distance of both galaxies at the time t_e is therefore

$$D(t_e) = D_e = a_e\chi_a - a_e\chi_e = a_e(\chi_a - \chi_e) = R_{ea} - R_{ee} \quad . \tag{11}$$

For the physical distance between both cosmic objects at a later time - means today‘s time here - $t_0 > t_e$ then applies

$$D(t_0) = D_0 = a_0\chi_a - a_0\chi_e = a_0(\chi_a - \chi_e) = R_{0a} - R_{0e} \quad . \tag{12}$$

However, both distances mentioned above are worthless for the computation of cosmological relevant distance relations, since the emitted photons make their physical way to the observer, which has to be calculated in accordance with

$$D = a_0\chi_a - a_e\chi_e = R_{0a} - R_{ee} \quad . \tag{13}$$

To see this, imagine a photon that detaches itself at the time $t_e < t_0$ from the emitting galaxy at the coordinate χ_e, where the scale parameter at this time has the value a_e. After the photon has moved freely through the expanding universe, it will arrive at the coordinate point χ_a, the place of the observer within another galaxy, at time t_0, with the scale parameter at that time being a_0. Thus, the photon does not travel the path described by Eq. (11) nor by Eq. (12). The real distance traveled by the photon is always unequal to any one of these two distances. This must be taken into account when deriving the redshift distance.

The real physical light path is illustrated by the green line in Fig. 1:

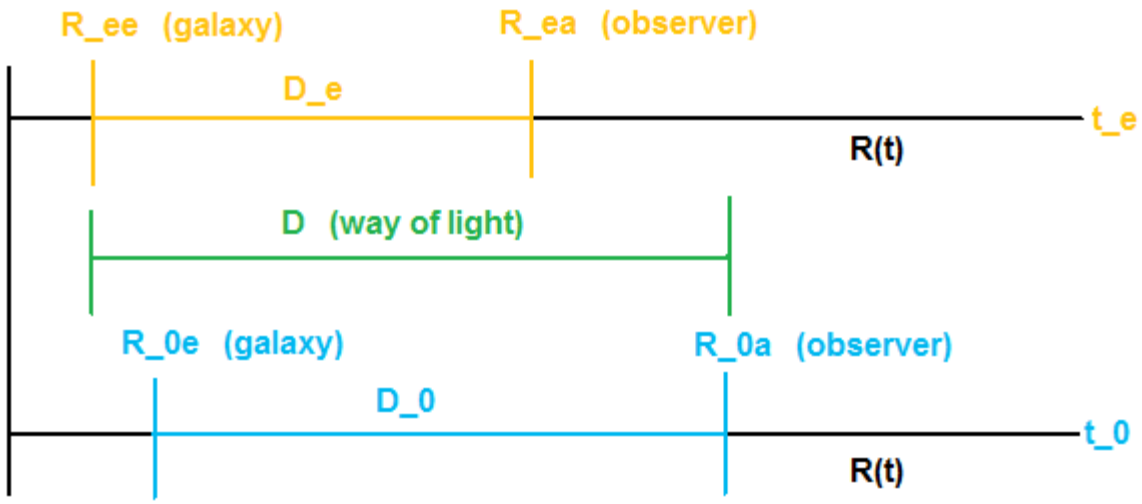

Figure 1. Real physical light path.

These remarks may be sufficient as a preliminary to the now following derivation of the redshift distance.

2.2 ε = (+1)

2.2.1 The redshift distance

In principle, we follow the way demonstrated in our former published papers [11] and [12], respectively.

We now investigate which equation results for the redshift distance (corresponding to the photon path), which depends on the redshift z, if the integral

$$\int_{r_e}^{r_a} \frac{d\bar{r}}{\sqrt{1-\bar{r}^2}} = +\int_{t_e}^{t_0} \frac{c_0 dt}{a(t)} \tag{14}$$

is used. This integral results for ε = (+1) when the line element ds is set equal to zero in the FLRWM (2) and radial (ϑ = φ = const) outgoing photons are considered. Eq. (14) describes the motion of photons inside the universe traveling from the co-moving coordinate $\chi_{e,\varepsilon=(+1)}$ to the co-moving coordinate $\chi_{a,\varepsilon=(+1)}$.
During the travel time of the photons, the scale parameter changes from $a(t_e) = a_e$ to $a(t_0) = a_0$. If the time differential is replaced using the Eq. (3d), follows from Eq. (14)

$$\int_{r_e}^{r_a} \frac{d\bar{r}}{\sqrt{1-\bar{r}^2}} = +\int_{a_e}^{a_0} \frac{da}{\sqrt{K_r + K_m a - a^2}} \quad . \tag{15}$$

After executing the integral we get

$$\arcsin(r_a)-\arcsin(r_e)=\left[\arcsin\left(\frac{\frac{K_{0m}}{a_0}-2}{\frac{K_{0m}}{a_0}\sqrt{1+4\frac{K_{0r}}{{K_{0m}}^2}}}\right)-\arcsin\left(\frac{\frac{K_{em}}{a_e}-2}{\frac{K_{em}}{a_e}\sqrt{1+4\frac{K_{er}}{{K_{em}}^2}}}\right)\right] \quad . \qquad (16)$$

We have used appropriate terms for both involved conservation laws:

$$K_{0m}=\frac{8\pi G}{3{c_0}^2}\rho_{0m}{a_0}^3=\frac{8\pi G}{3{c_0}^2}\rho_{em}{a_e}^3=K_{em}\equiv K_m \qquad and \qquad K_{0r}=\frac{8\pi G}{3{c_0}^2}\rho_{0r}{a_0}^4=\frac{8\pi G}{3{c_0}^2}\rho_{er}{a_e}^4=K_{er}\equiv K_r \qquad (17a,b)$$

or

$$\frac{K_{0r}}{K_{0m}}=\frac{\rho_{0r}}{\rho_{0m}}a_0 \qquad and \qquad \frac{K_{er}}{K_{0m}}=\frac{\rho_{er}}{\rho_{0m}}\frac{{a_e}^4}{{a_0}^3} \qquad and \qquad \frac{K_{em}}{K_{er}}=\frac{\rho_{em}}{\rho_{er}a_e} \quad . \qquad (17c,d)$$

Eq. (17a,b) show us that we can use $K_m = K_{em} = K_{0m}$ and $K_r = K_{er} = K_{0r}$, respectively, because these values are the same constant ones.

Now we insert Eq. (13)

$$a_e\arcsin(r_e)=a_0\arcsin(r_a)-D_{mr,\varepsilon=(+1)} \qquad (13a)$$

in Eq. (16) and get

$$a_0\arcsin(r_a)\left(\frac{a_e}{a_0}-1\right)+D_{mr,\varepsilon=(+1)}=-a_e\left[\arcsin\left(\frac{K_{0m}-2a_0}{\sqrt{{K_{0m}}^2+4K_{0r}}}\right)-\arcsin\left(\frac{K_{em}-2a_e}{\sqrt{{K_{em}}^2+4K_{er}}}\right)\right] \quad . \qquad (18)$$

We now introduce the redshift named z. To this end, we recall the simple relation between the scale parameters a_0 and a_e at the two different times t_e and t_0 and the redshift

$$\frac{a_0}{a_e}=1+z \qquad or \qquad \frac{{a_e}^2}{{a_0}^2}=\frac{1}{(1+z)^2} \qquad (19a, b)$$

and also

$$a_e = \frac{a_0}{(1+z)} \quad . \tag{19c}$$

If Eq. (19b) and (19c) are inserted into Eq. (18), the result is

$$D_{mr,\varepsilon=(+1)} = a_0 \arcsin(r_a)\left[1-\frac{1}{(1+z)}\right] - \frac{a_0}{(1+z)}\left[\arcsin\left(\frac{K_{0m}-2a_0}{\sqrt{{K_{0m}}^2+4K_{0r}}}\right) - \arcsin\left(\frac{K_{em}-2a_e}{\sqrt{{K_{em}}^2+4K_{er}}}\right)\right] \quad . \tag{20}$$

If we unite both arcsin() on the right site we get the equation

$$D_{mr,\varepsilon=(+1)} = a_0 \arcsin(r_a)\left[1-\frac{1}{(1+z)}\right] - \frac{a_0}{(1+z)} * \\ * \arcsin\left\{\frac{\left(\frac{K_m}{a_0}-2\right)\sqrt{\left(\frac{{K_m}^2}{{a_0}^2}+4\frac{K_r}{{a_0}^2}\right)-\left[\frac{K_m}{a_0}-\frac{2}{(1+z)}\right]^2} - \left[\frac{K_m}{a_0}-\frac{2}{(1+z)}\right]\sqrt{\left(\frac{{K_m}^2}{{a_0}^2}+4\frac{K_r}{{a_0}^2}\right)-\left(\frac{K_m}{a_0}-2\right)^2}}{\left(\frac{{K_m}^2}{{a_0}^2}+4\frac{K_r}{{a_0}^2}\right)}\right\} \quad . \tag{21}$$

We have set $K_{0m} = K_m$ and $K_{0r} = K_r$, respectively, in Eq. (21) to can see the generality better.

This yields

$$D_{mr,\varepsilon=(+1)} = R_{0a,\varepsilon=(+1)}\left[1-\frac{1}{(1+z)}\right] - \frac{a_0}{(1+z)} * \\ * \arcsin\left\{\frac{(\gamma_m-2)\sqrt{\left({\gamma_m}^2+4\gamma_r\right)-\left[\gamma_m-\frac{2}{(1+z)}\right]^2} - \left[\gamma_m-\frac{2}{(1+z)}\right]\sqrt{\left({\gamma_m}^2+4\gamma_r\right)-(\gamma_m-2)^2}}{\left({\gamma_m}^2+4\gamma_r\right)}\right\} \quad , \tag{22}$$

if we introduce the following abbreviations

$$R_{0a,\varepsilon=(+1)} = a_0 \arcsin(r_a) \qquad \textit{and} \qquad \gamma_m = \frac{K_m}{a_0} \qquad \textit{and} \qquad \gamma_r = \frac{K_r}{{a_0}^2}$$

$$\textit{and} \qquad \gamma_a = \frac{a_0}{R_{0a,\varepsilon=(+1)}} = \frac{1}{\arcsin(r_a)} \qquad \textit{or} \qquad a_0 = \gamma_a R_{0a,\varepsilon=(+1)} \qquad \textit{and} \qquad [\gamma_m]=[\gamma_r]=[\gamma_a]=1 \quad . \tag{23}$$

After some more calculation steps we find finely

$$D_{mr,\varepsilon=(+1)}\left(z;R_{0a,\varepsilon=(+1)},\gamma_a,\gamma_m,\gamma_r\right)=$$
$$=R_{0a,\varepsilon=(+1)}\left\{1-\frac{1}{(1+z)}\left\{1+\gamma_a\ \arcsin\left\{\frac{\left(\frac{\gamma_m}{2}-1\right)\sqrt{\gamma_r+\frac{1}{(1+z)}\left[\gamma_m-\frac{1}{(1+z)}\right]}-\left[\frac{\gamma_m}{2}-\frac{1}{(1+z)}\right]\sqrt{\gamma_r+\gamma_m-1}}{\left[\left(\frac{\gamma_m}{2}\right)^2+\gamma_r\right]}\right\}\right\}\right\}\quad . \tag{24}$$

This is the equation for the redshift distance, for which we were searching.

The redshift distance $D_{mr,\varepsilon=(+1)}$ is therefore a function of the redshift z and the four parameters $R_{0a,\varepsilon=(+1)}$, γ_a, γ_m and γ_r which all can be determined fundamental by fitting the equation to appropriate astrophysical measurements.

A look at the last root on the right side shows us that we have a condition belonging to the both parameters γ_m und γ_r:

$$\begin{aligned}&\sqrt{\gamma_r+\gamma_m-1}=real \qquad or \qquad \gamma_r+\gamma_m\geq 1\\ &which\ means\\ &\gamma_m\geq 1 \qquad if \qquad \gamma_r=0\\ &\gamma_r\geq 1 \qquad if \qquad \gamma_m=0\quad .\end{aligned} \tag{25}$$

Now we can have a look at some possible values belonging to the four parameters.
At first we can neglect the parameter γ_r if the radiation density is very small in comparison of non-relativistic matter density and find in this way

$$D_{m,\varepsilon=(+1)}\left(z;R_{0a,\varepsilon=(+1)},\gamma_a,\gamma_m\right)=R_{0a,\varepsilon=(+1)}\left\{1-\frac{1}{(1+z)}\left\{1+\gamma_a\ \arcsin\left\{\frac{\left(\frac{\gamma_m}{2}-1\right)}{\sqrt{1+z}}\sqrt{\gamma_m-\frac{1}{(1+z)}}-\left[\frac{\gamma_m}{2}-\frac{1}{(1+z)}\right]\sqrt{\gamma_m-1}}{\left(\frac{\gamma_m}{2}\right)^2}\right\}\right\}\right\}\quad . \tag{24a}$$

In another case, we can neglect the parameter γ_m to can describe a universe containing radiation only

$$D_{r,\varepsilon=(+1)}\left(z;R_{0a,\varepsilon=(+1)},\gamma_a,\gamma_r\right)=R_{0a,\varepsilon=(+1)}\left\{1-\frac{1}{(1+z)}\left\{1+\gamma_a\ \arcsin\left[\frac{\frac{\sqrt{\gamma_r-1}}{(1+z)}-\sqrt{\gamma_r-\frac{1}{(1+z)^2}}}{\gamma_r}\right]\right\}\right\}\quad . \tag{24b}$$

Fig. 2 shows the redshift distance (24) normalized to the distance $R_{0a,\varepsilon=(+1)}$ for various values of the parameter γ_m and $\gamma_r = 0$ as well as $r_a = 1$.

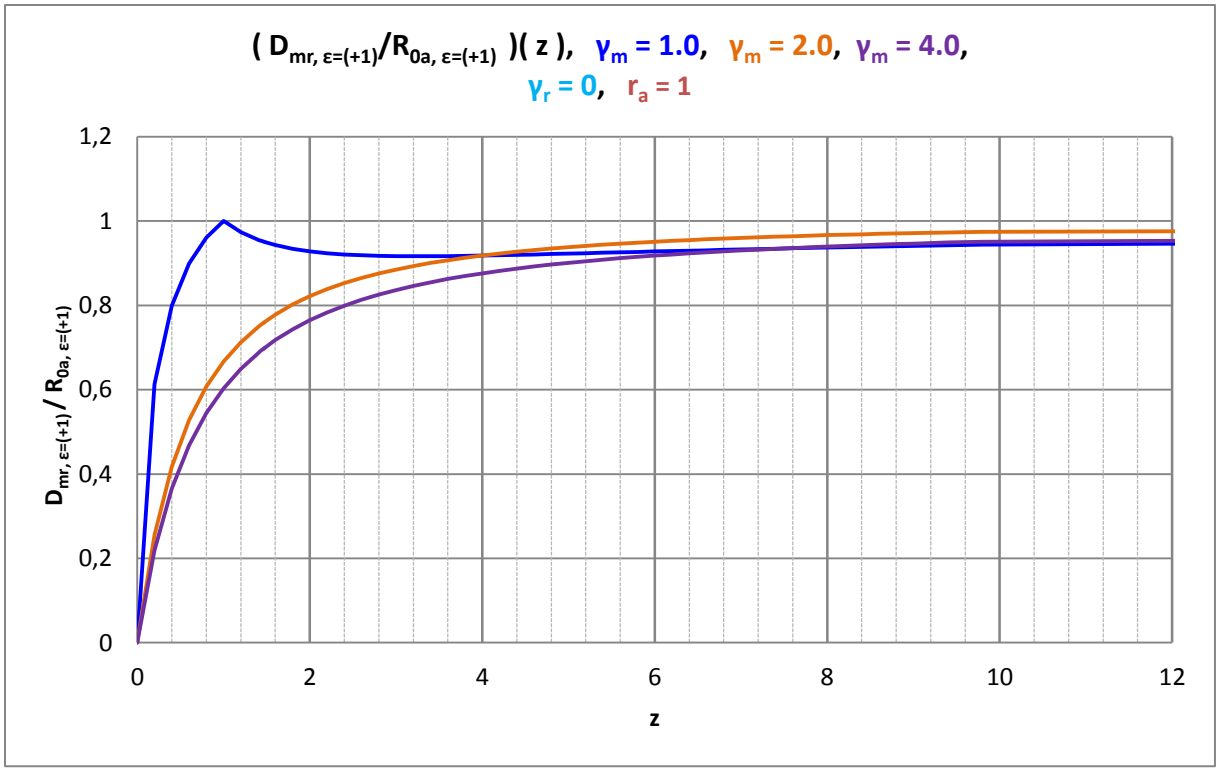

Figure 2. Redshift distance for different values of the parameters γ_m and $\gamma_r = 0$ as well as $r_a = 1$.

The value $\gamma_m = 1$ is the minimal possible value if γ_r is set to zero. Only in this case $D_{mr,\varepsilon=(+1)} = R_{0a,\varepsilon=(+1)}$ is reached a first time for $z = 1$. In all other cases this value is reached only for $z = \infty$.

Fig. 3 shows the redshift distance (24) normalized to the distance $R_{0a,\varepsilon=(+1)}$ for various values of the parameter γ_r and $\gamma_m = 1$ as well as $r_a = 1$.

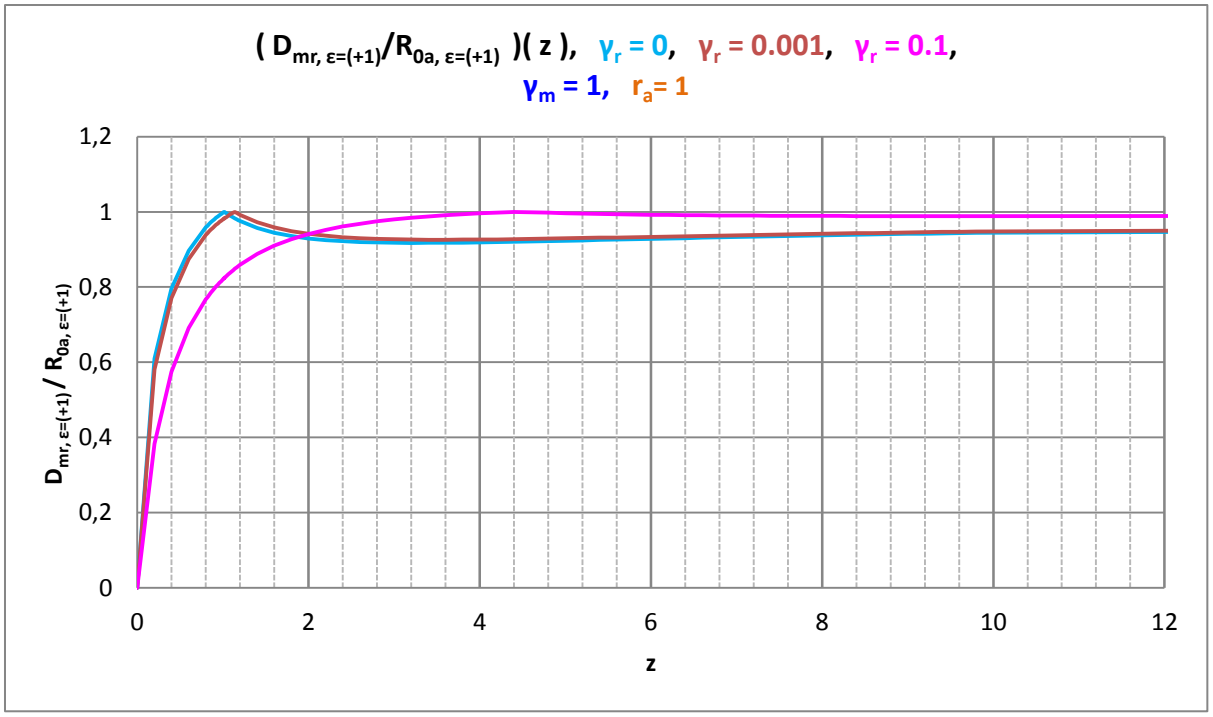

Figure 3. Redshift distance for different values of the parameter γ_r and $\gamma_m = 1$ as well as $r_a = 1$.

The curvature of all the curves is a direct consequence of the Friedmann equation.

The comparison of Eq. (24) and (24a), respectively, with a Hubble diagram thus determines the current radius $R_{0a,\varepsilon=(+1)} = a_0\chi_{a,\varepsilon=(+1)}$ of the Friedmann sphere (the today's physical location of the observer).

2.2.2 The Hubble parameter

For calculating the Hubble parameter we make a Taylor series expansion of our redshift distance (24) up to first order in z and find

$$D_{mr,\varepsilon=(+1)}\left(z;R_{0a,\varepsilon=(+1)},\gamma_a,\gamma_m,\gamma_r\right)\approx R_{0a,\varepsilon=(+1)}\left(1+\frac{\gamma_a}{\sqrt{\gamma_r+\gamma_m-1}}\right)z \quad . \tag{26}$$

This results in

$$c_0 z \approx \frac{c_0}{R_{0a,\varepsilon=(+1)}\left(1+\frac{\gamma_a}{\sqrt{\gamma_r+\gamma_m-1}}\right)} D_{mr,\varepsilon=(+1)}\left(z;R_{0a,\varepsilon=(+1)},\gamma_a,\gamma_m,\gamma_r\right) \quad . \tag{27}$$

This is how we find the today's Hubble parameter

$$H_{0,mr,\varepsilon=(+1)}\left(R_{0a,\varepsilon=(+1)},\gamma_a,\gamma_m,\gamma_r\right)\approx\frac{c_0}{R_{0a,\varepsilon=(+1)}\left(1+\frac{\gamma_a}{\sqrt{\gamma_r+\gamma_m-1}}\right)}\quad . \tag{28}$$

The today's Hubble parameter $H_{0a,mr,\varepsilon=(+1)}$ depends on the four parameters $R_{0a,\varepsilon=(+1)}$, γ_a, γ_m and γ_r and is in this form valid only for small redshifts because of the series expansion made. This means that this $H_{0a,mr,\varepsilon=(+1)}$ is only valid locally near the observer.

Neglecting γ_r in Eq. (28) we find

$$H_{0,m,\varepsilon=(+1)}\left(R_{0a,\varepsilon=(+1)},\gamma_a,\gamma_m\right)\approx\frac{c_0}{R_{0a,\varepsilon=(+1)}\left(1+\frac{\gamma_a}{\sqrt{\gamma_m-1}}\right)}\qquad with\qquad \gamma_m=\frac{K_m}{a_0}\quad . \tag{29}$$

But if we set $\gamma_m = 0$ in Eq. (28) we get

$$H_{0,r,\varepsilon=(+1)}\left(R_{0a,\varepsilon=(+1)},\gamma_a,\gamma_r\right)\approx\frac{c_0}{R_{0a,\varepsilon=(+1)}\left(1+\frac{\gamma_a}{\sqrt{\gamma_r-1}}\right)}\qquad with\qquad \gamma_r=\frac{K_r}{a_0^{\,2}}\quad . \tag{30}$$

The result is that the last both equations show the same mathematical behavior analyzing measurement values, but the physical meaning is different because of the physical structure of the parameter γ_m and γ_r, respectively. Furthermore, we recognize that in both cases γ_m and γ_r, respectively, cannot be equal to one.

The reciprocal of the Hubble parameter (28) is the Hubble time $t_{H0,mr,\varepsilon=(+1)}$ and yields

$$t_{H_{0,mr,\varepsilon=(+1)}}\left(R_{0a,\varepsilon=(+1)},\gamma_a,\gamma_m,\gamma_r\right)=\frac{1}{H_{0,mr,\varepsilon=(+1)}}\approx\frac{R_{0a,\varepsilon=(+1)}}{c_0}\left(1+\frac{\gamma_a}{\sqrt{\gamma_r+\gamma_m-1}}\right)\quad . \tag{31}$$

2.2.3 The magnitude-redshift relation

The magnitude-redshift relation results by the general definition of the apparent magnitude $m_{mr,\varepsilon=(+1)}$

$$m_{mr,\varepsilon=(+1)}-m_{0a,\varepsilon=(+1)}=5\log_{10}\frac{D_{mr,\varepsilon=(+1)}}{R_{0a,\varepsilon=(+1)}}\quad . \tag{32}$$

Here an apparent limit magnitude $m_{0a,\varepsilon=(+1)}$ was introduced instead of $R_{0a,\varepsilon=(+1)}$ which also changes with time. Substituting Eq. (24) into Eq. (32) then provides the sought magnitude-redshift relation

$$m_{mr,\varepsilon=(+1)}\left(z; m_{0a,\varepsilon=(+1)}, \gamma_a, \gamma_m, \gamma_r\right) = \\ = 5\log_{10}\left\{1-\frac{1}{(1+z)}\left\{1+\gamma_a \arcsin\left\{\frac{\left(\frac{\gamma_m}{2}-1\right)\sqrt{\gamma_r+\frac{1}{(1+z)}\left[\gamma_m-\frac{1}{(1+z)}\right]}-\left[\frac{\gamma_m}{2}-\frac{1}{(1+z)}\right]\sqrt{\gamma_r+\gamma_m-1}}{\left[\left(\frac{\gamma_m}{2}\right)^2+\gamma_r\right]}\right\}\right\}\right\}+m_{0a,\varepsilon=(+1)} \quad . \tag{33}$$

The four free parameters $m_{0a,\varepsilon=(+1)}$, γ_a, γ_m and γ_r can be determined by direct comparison with a suitable magnitude-redshift diagram of astrophysical objects.

If we ignore the possible radiation density within our equation, we get the following simpler equation

$$m_{m,\varepsilon=(+1)}\left(z; m_{0a,\varepsilon=(+1)}, \gamma_a, \gamma_m\right) = 5\log_{10}\left\{1-\frac{1}{(1+z)}\left\{1+\gamma_a \arcsin\left\{\frac{\left(\frac{\gamma_m}{2}-1\right)}{\sqrt{1+z}}\sqrt{\gamma_m-\frac{1}{(1+z)}}-\left[\frac{\gamma_m}{2}-\frac{1}{(1+z)}\right]\sqrt{\gamma_m-1}}{\left(\frac{\gamma_m}{2}\right)^2}\right\}\right\}\right\}+m_{0a,\varepsilon=(+1)} \quad . \tag{33a}$$

2.2.4 The angular size-redshift relation

This relation results in for larger distances over

$$\varphi = \arcsin\left(\frac{\delta_{\varepsilon=(+1)}}{D_{mr,\varepsilon=(+1)}}\right) \approx \frac{\delta_{\varepsilon=(+1)}}{D_{mr,\varepsilon=(+1)}} \tag{34}$$

to

$$\varphi_{mr,\varepsilon=(+1)}\left(z; \delta_{\varepsilon=(+1)} / R_{0a,\varepsilon=(+1)}, \gamma_a, \gamma_m, \gamma_r\right) = \\ = \frac{\delta_{\varepsilon=(+1)}}{R_{0a,\varepsilon=(+1)}} \frac{1}{\left\{1-\frac{1}{(1+z)}\left\{1+\gamma_a \arcsin\left\{\frac{\left(\frac{\gamma_m}{2}-1\right)\sqrt{\gamma_r+\frac{1}{(1+z)}\left[\gamma_m-\frac{1}{(1+z)}\right]}-\left[\frac{\gamma_m}{2}-\frac{1}{(1+z)}\right]\sqrt{\gamma_r+\gamma_m-1}}{\left[\left(\frac{\gamma_m}{2}\right)^2+\gamma_r\right]}\right\}\right\}\right\}} \quad . \tag{35}$$

In this equation $\varphi_{mr,\varepsilon=(+1)}$ means the measurable angular size and $\delta_{\varepsilon=(+1)}$ the linear size of the observed extra-galactic object.

Setting $\gamma_r = 0$ we get

$$\varphi_{m,\varepsilon=(+1)}\left(z;\delta_{\varepsilon=(+1)}/R_{0a,\varepsilon=(+1)},\gamma_a,\gamma_m\right)=$$
$$=\frac{\delta_{\varepsilon=(+1)}}{R_{0a,\varepsilon=(+1)}}\frac{1}{\left\{1-\frac{1}{(1+z)}\left\{1+\gamma_a\arcsin\left\{\frac{\left(\frac{\gamma_m}{2}-1\right)}{\sqrt{1+z}}\sqrt{\gamma_m-\frac{1}{(1+z)}}-\left[\frac{\gamma_m}{2}-\frac{1}{(1+z)}\right]\sqrt{\gamma_m-1}}{\left(\frac{\gamma_m}{2}\right)^2}\right\}\right\}\right\}} \quad . \tag{35a}$$

In logarithmic form Eq. (35) becomes to

$$\log_{10}\varphi_{mr,\varepsilon=(+1)}\left(z;\delta_{\varepsilon=(+1)}/R_{0a,\varepsilon=(+1)},\gamma_a,\gamma_m,\gamma_r\right)=$$
$$=\log_{10}\frac{\delta_{\varepsilon=(+1)}}{R_{0a,\varepsilon=(+1)}}-\log_{10}\left\{1-\frac{1}{(1+z)}\left\{1+\gamma_a\arcsin\left\{\frac{\left(\frac{\gamma_m}{2}-1\right)\sqrt{\gamma_r+\frac{1}{(1+z)}\left[\gamma_m-\frac{1}{(1+z)}\right]}-\left[\frac{\gamma_m}{2}-\frac{1}{(1+z)}\right]\sqrt{\gamma_r+\gamma_m-1}}{\left[\left(\frac{\gamma_m}{2}\right)^2+\gamma_r\right]}\right\}\right\}\right\} \quad . \tag{35b}$$

2.2.5 The number-redshift relation

In flat Euclidean space the equation for the light-path sphere becomes to

$$V=\frac{4\pi}{3}D^3 \quad . \tag{36}$$

We use this equation to calculate the number-redshift relation for curved spacetime, because the curvature is contained in the redshift distance. Therefore, we can expect that the error made is not a big one.

If we introduce the redshift distance via Eq. (24)

$$V_{mr,\varepsilon=(+1)}\left(z;R_{0a,\varepsilon=(+1)},\gamma_a,\gamma_m,\gamma_r\right)=$$
$$=\frac{4\pi}{3}R_{0a,\varepsilon=(+1)}{}^3\left\{1-\frac{1}{(1+z)}\left\{1+\gamma_a\arcsin\left\{\frac{\left(\frac{\gamma_m}{2}-1\right)\sqrt{\gamma_r+\frac{1}{(1+z)}\left[\gamma_m-\frac{1}{(1+z)}\right]}-\left[\frac{\gamma_m}{2}-\frac{1}{(1+z)}\right]\sqrt{\gamma_r+\gamma_m-1}}{\left[\left(\frac{\gamma_m}{2}\right)^2+\gamma_r\right]}\right\}\right\}\right\}^3 \tag{37}$$

we get for the number-redshift relation

$$N_{mr,\varepsilon=(+1)}\left(z;N_{0a,\varepsilon=(+1)},\gamma_a,\gamma_m,\gamma_r\right)=$$
$$=N_{0a,\varepsilon=(+1)}\left\{1-\frac{1}{(1+z)}\left\{1+\gamma_a\arcsin\left\{\frac{\left(\frac{\gamma_m}{2}-1\right)\sqrt{\gamma_r+\frac{1}{(1+z)}\left[\gamma_m-\frac{1}{(1+z)}\right]}-\left[\frac{\gamma_m}{2}-\frac{1}{(1+z)}\right]\sqrt{\gamma_r+\gamma_m-1}}{\left[\left(\frac{\gamma_m}{2}\right)^2+\gamma_r\right]}\right\}\right\}\right\}^3 , \quad (38)$$

where $N_{0a,\varepsilon=(+1)}$ means the expected number of objects in the whole light-path sphere $V_{0a,\varepsilon=(+1)}$ and besides

$$N_{0a,\varepsilon=(+1)}=V_{0a,\varepsilon=(+1)}\eta=\frac{4\pi}{3}R_{0a,\varepsilon=(+1)}{}^3\eta \qquad and \qquad N=V\eta \quad (39a,b)$$

applies. With η the number density was named.

In logarithmic form results

$$\log_{10}N_{mr,\varepsilon=(+1)}\left(z;N_{0a,\varepsilon=(+1)},\gamma_a,\gamma_m,\gamma_r\right)=$$
$$=3\log_{10}\left\{1-\frac{1}{(1+z)}\left\{1+\gamma_a\arcsin\left\{\frac{\left(\frac{\gamma_m}{2}-1\right)\sqrt{\gamma_r+\frac{1}{(1+z)}\left[\gamma_m-\frac{1}{(1+z)}\right]}-\left[\frac{\gamma_m}{2}-\frac{1}{(1+z)}\right]\sqrt{\gamma_r+\gamma_m-1}}{\left[\left(\frac{\gamma_m}{2}\right)^2+\gamma_r\right]}\right\}\right\}\right\}+\log_{10}N_{0a,\varepsilon=(+1)} . \quad (40)$$

If we ignore in Eq. (40) the possible radiation density within our equation, we find

$$\log_{10}N_{m,\varepsilon=(+1)}\left(z;N_{0a,\varepsilon=(+1)},\gamma_a,\gamma_m\right)=$$
$$=3\log_{10}\left\{1-\frac{1}{(1+z)}\left\{1+\gamma_a\arcsin\left\{\frac{\left(\frac{\gamma_m}{2}-1\right)}{\sqrt{1+z}}\sqrt{\gamma_m-\frac{1}{(1+z)}}-\left[\frac{\gamma_m}{2}-\frac{1}{(1+z)}\right]\sqrt{\gamma_m-1}}{\left(\frac{\gamma_m}{2}\right)^2}\right\}\right\}\right\}+\log_{10}N_{0a,\varepsilon=(+1)} . \quad (41)$$

2.3 ε = (-1)

2.3.1 The redshift distance

We now want to investigate which equation results for the redshift distance (corresponding to the photon path), which depends on the redshift z, if the integral

$$\int_{r_e}^{r_a} \frac{d\bar{r}}{\sqrt{1+\bar{r}^2}} = +\int_{t_e}^{t_0} \frac{c_0 dt}{a(t)} \tag{42}$$

is used. This integral results for ε = (-1) when the line element ds is set equal to zero in the FLRWM (2) and radial (ϑ = φ = const) outgoing photons are considered. Eq. (42) describes the motion of photons inside the universe traveling from the co-moving coordinate $\chi_{e,\varepsilon=(-1)}$ to the co-moving coordinate $\chi_{a,\varepsilon=(-1)}$.

During the travel time of the photons, the scale parameter changes from $a(t_e) = a_e$ to $a(t_0) = a_0$. If the time differential is replaced using the Eq. (3b), follows from Eq. (42)

$$\int_{r_e}^{r_a} \frac{d\bar{r}}{\sqrt{1+\bar{r}^2}} = +\int_{a_e}^{a_0} \frac{da}{\sqrt{K_r + K_m a + a^2}} \quad . \tag{43}$$

After the execution of the integral we get

$$ar\sinh(r_a) - ar\sinh(r_e) = ar\sinh\left(\frac{2a_0 + K_{0m}}{\sqrt{4K_{0r} - K_{0m}^2}}\right) - ar\sinh\left(\frac{2a_e + K_{em}}{\sqrt{4K_{er} - K_{em}^2}}\right) \quad . \tag{44}$$

We have used appropriate terms for both involved conservation laws how they are given in Eg. (17a,b).

Now we insert the Eq. (13)

$$a_e ar\sinh(r_e) = a_0 ar\sinh(r_a) - D_{mr,\varepsilon=(-1)} \tag{13b}$$

in Eq. (44) and get

$$a_0 ar\sinh(r_a)\left(\frac{a_e}{a_0} - 1\right) + D_{mr,\varepsilon=(-1)} = -a_e\left[ar\sinh\left(\frac{2a_0 + K_{0m}}{\sqrt{4K_{0r} - K_{0m}^2}}\right) - ar\sinh\left(\frac{2a_e + K_{em}}{\sqrt{4K_{er} - K_{em}^2}}\right)\right] \quad . \tag{45}$$

We now introduce the redshift z. If Eq. (19b) and (19c) are inserted into Eq. (45), the result is

$$D_{mr,\varepsilon=(-1)} = a_0 ar\sinh(r_a)\left[1 - \frac{1}{(1+z)}\right] - \frac{a_0}{(1+z)}\left[ar\sinh\left(\frac{2a_0 + K_{0m}}{\sqrt{4K_{0r} - K_{0m}^2}}\right) - ar\sinh\left(\frac{2a_e + K_{em}}{\sqrt{4K_{er} - K_{em}^2}}\right)\right] \quad . \tag{46}$$

If we unite both acsinh() on the right site we get after some simple calculations the equation

$$D_{mr,\varepsilon=(-1)} = a_0 ar\sinh\left(r_a\right)\left[1-\frac{1}{(1+z)}\right]+\frac{a_0}{(1+z)}\ln\left\{\frac{\left[\left(2+\frac{K_m}{a_0}\right)+2\sqrt{1+\frac{K_m}{a_0}+\frac{K_r}{a_0^{\,2}}}\right]}{\left\{\left[\frac{2}{(1+z)}+\frac{K_m}{a_0}\right]+2\sqrt{\frac{1}{(1+z)}\left[\frac{1}{(1+z)}+\frac{K_m}{a_0}\right]+\frac{K_r}{a_0^{\,2}}}\right\}}\right\} \quad . \tag{47}$$

This yields

$$\begin{aligned} &D_{mr,\varepsilon=(-1)}\left(z;R_{0a,\varepsilon=(-1)},\gamma_a,\gamma_m,\gamma_r\right)= \\ &= R_{0a,\varepsilon=(-1)}\left\{1-\frac{1}{(1+z)}\left\{1-\gamma_a\ln\left\{\frac{\left[\left(1+\frac{\gamma_m}{2}\right)+\sqrt{1+\gamma_m+\gamma_r}\right]}{\left\{\left[\frac{1}{(1+z)}+\frac{\gamma_m}{2}\right]+\sqrt{\frac{1}{(1+z)}\left[\frac{1}{(1+z)}+\gamma_m\right]+\gamma_r}\right\}}\right\}\right\}\right\} \quad , \end{aligned} \tag{48}$$

if we introduce the following abbreviations

$$R_{0a,\varepsilon=(-1)} = a_0 ar\sinh\left(r_a\right) \quad and \quad \gamma_m = \frac{K_m}{a_0} \quad and \quad \gamma_r = \frac{K_r}{a_0^{\,2}}$$

$$and \quad \gamma_a = \frac{a_0}{R_{0a,\varepsilon=(-1)}} = \frac{1}{ar\sinh\left(r_a\right)} \quad or \quad a_0 = \gamma_a R_{0a,\varepsilon=(-1)} \quad and \quad \left[\gamma_m\right]=\left[\gamma_r\right]=\left[\gamma_a\right]=1 \quad . \tag{49}$$

Eq. (48) is the equation for the redshift distance, for which we were searching.

The redshift distance $D_{mr,\varepsilon=(-1)}$ is therefore a function of the redshift z and the four parameters $R_{0a,\varepsilon=(-1)}$, γ_a, γ_m and γ_r which all can be determined fundamental by fitting the equation to appropriate astrophysical measurements.

If we neglect the parameter γ_r we get

$$D_{m,\varepsilon=(-1)}\left(z;R_{0a,\varepsilon=(-1)},\gamma_a,\gamma_m\right)= R_{0a,\varepsilon=(-1)}\left\{1-\frac{1}{(1+z)}\left\{1-\gamma_a\ln\left\{\frac{\left[\left(1+\frac{\gamma_m}{2}\right)+\sqrt{1+\gamma_m}\right]}{\left\{\left[\frac{1}{(1+z)}+\frac{\gamma_m}{2}\right]+\sqrt{\frac{1}{(1+z)}\left[\frac{1}{(1+z)}+\gamma_m\right]}\right\}}\right\}\right\}\right\} \quad . \tag{48a}$$

In another case, we can neglect the parameter γ_m to can describe a universe containing radiation only:

$$D_{r,\varepsilon=(-1)}\left(z;R_{0a,\varepsilon=(-1)},\gamma_a,\gamma_r\right)=R_{0a,\varepsilon=(-1)}\left\{1-\frac{1}{(1+z)}\left\{1-\gamma_a\ln\left\{\frac{\left(1+\sqrt{1+\gamma_r}\right)}{\left\{\frac{1}{(1+z)}+\sqrt{\frac{1}{(1+z)}\left[\frac{1}{(1+z)}\right]+\gamma_r}\right\}}\right\}\right\}\right\} \quad . \tag{48b}$$

Fig. 4 shows the redshift distance (48) normalized to the distance $R_{0a,\varepsilon=(-1)}$ for various values of the parameter γ_m and $\gamma_r = 0$ as well as $r_a = 1$.

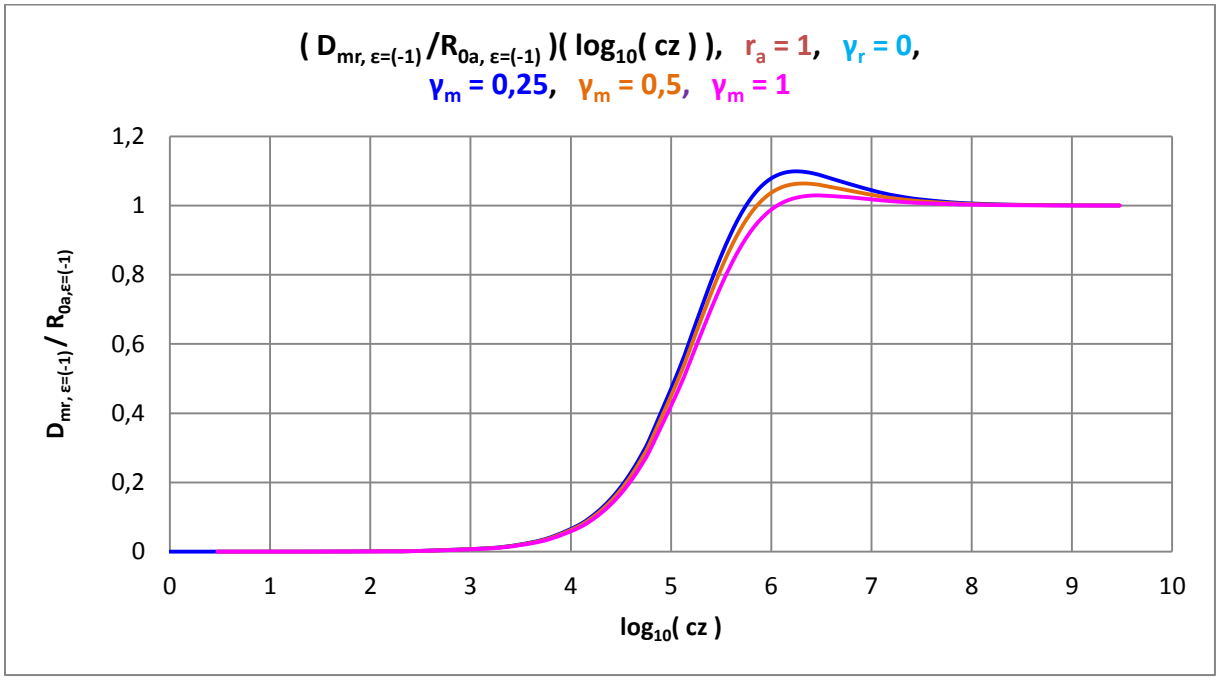

Figure 4. Redshift distance for different values of the parameters γ_m and $\gamma_r = 0$ as well as $r_a = 1$.

We see in all cases of γ_m used here, that $D_{mr,\varepsilon=(+1)}$ can be greater than $R_{0a,\varepsilon=(+1)}$ for some redshifts. But for z --> ∞ $D_{mr,\varepsilon=(+1)} = R_{0a,\varepsilon=(+1)}$ is reached always.

Fig. **5** shows the redshift distance (48) normalized to the distance $R_{0a,\varepsilon=(-1)}$ for various values of the parameter γ_r and $\gamma_m = 1$ as well as $r_a = 1$.

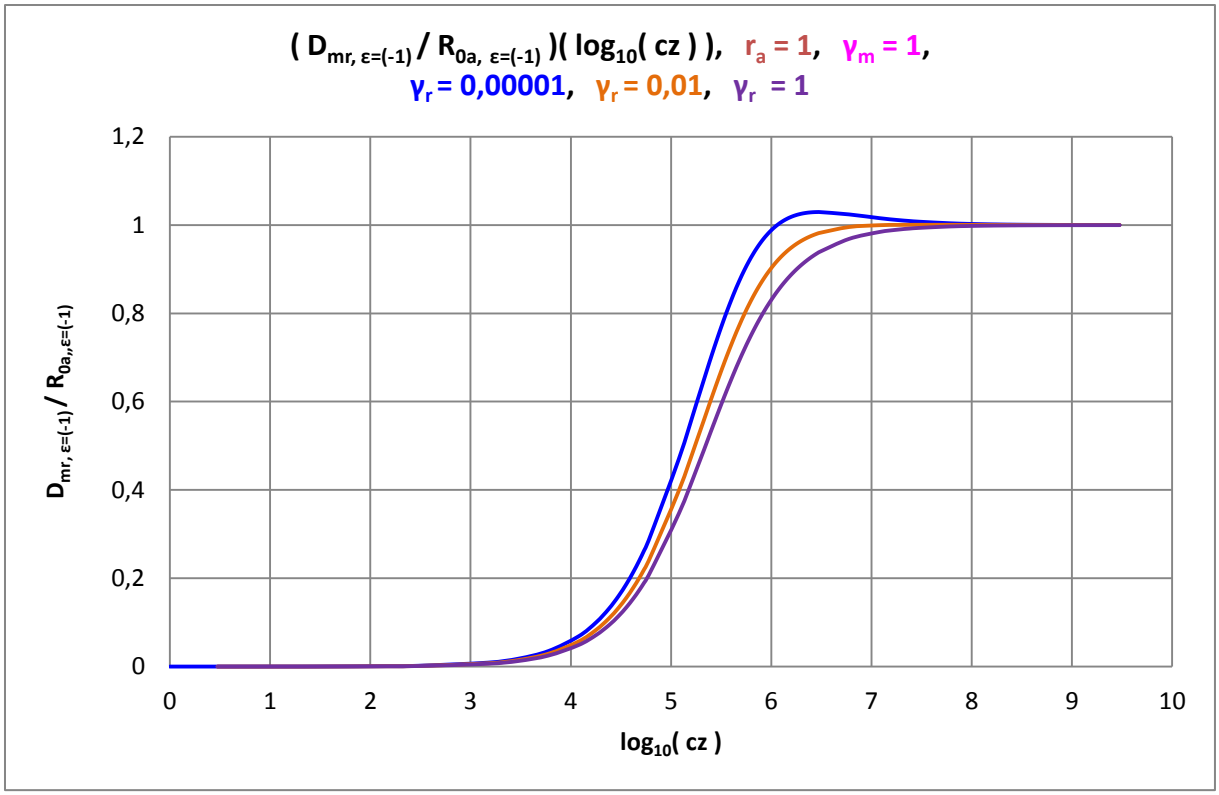

Figure 5. Redshift distance for different values of the parameter γ_r and $\gamma_m = 1$ as well as $r_a = 1$.

The curvature of all the curves is a direct consequence of the Friedmann equation.

The comparison of Eq. (48) and (48a), respectively, with a Hubble diagram thus determines the current radius $R_{0a,\varepsilon=(-1)} = a_0\chi_{a,\varepsilon=(-1)}$ of the Friedmann sphere (today's physical location of the observer).

2.3.2 The Hubble parameter

For calculating the Hubble parameter we make a Taylor series expansion of our redshift distance (48) up to first order in z and find

$$D_{mr,\varepsilon=(-1)}\left(z;R_{0a,\varepsilon=(-1)},\gamma_a,\gamma_m,\gamma_r\right)\approx R_{0a,\varepsilon=(-1)}\left(1+\frac{\gamma_a}{\sqrt{1+\gamma_m+\gamma_r}}\right)z \quad . \tag{49}$$

This results in

$$c_0 z \approx \frac{c_0}{R_{0a,\varepsilon=(-1)}\left(1+\frac{\gamma_a}{\sqrt{1+\gamma_m+\gamma_r}}\right)} D_{mr,\varepsilon=(-1)}\left(z; R_{0a,\varepsilon=(-1)}, \gamma_a, \gamma_m, \gamma_r\right) \quad . \tag{50}$$

This is how we find today's Hubble parameter

$$H_{0,mr,\varepsilon=(-1)}\left(R_{0a,\varepsilon=(-1)}, \gamma_a, \gamma_m, \gamma_r\right) \approx \frac{c_0}{R_{0a,\varepsilon=(-1)}\left(1+\frac{\gamma_a}{\sqrt{1+\gamma_m+\gamma_r}}\right)} \quad . \tag{51}$$

The today's Hubble parameter $H_{0a,mr,\varepsilon=(-1)}$ depends on the four parameters $R_{0a,\varepsilon=(-1)}$, γ_a, γ_m and γ_r and is in this form valid only for small redshifts because of the series expansion made. This means that this $H_{0a,mr,\varepsilon=(-1)}$ is only valid locally near the observer.

Neglecting γ_r in Eq. (51) we find

$$H_{0,m,\varepsilon=(-1)}\left(R_{0a,\varepsilon=(-1)}, \gamma_a, \gamma_m\right) \approx \frac{c_0}{R_{0a,\varepsilon=(-1)}\left(1+\frac{\gamma_a}{\sqrt{1+\gamma_m}}\right)} \qquad with \qquad \gamma_m = \frac{K_m}{a_0} \quad . \tag{52}$$

But if we set $\gamma_m = 0$ in Eq. (51) we get

$$H_{0,r,\varepsilon=(-1)}\left(R_{0a,\varepsilon=(-1)}, \gamma_a, \gamma_r\right) \approx \frac{c_0}{R_{0a,\varepsilon=(-1)}\left(1+\frac{\gamma_a}{\sqrt{1+\gamma_r}}\right)} \qquad with \qquad \gamma_r = \frac{K_r}{a_0^{\,2}} \quad . \tag{53}$$

The reciprocal of the Hubble parameter (51) is the Hubble time $t_{H0,mr,\varepsilon=(-1)}$ and yields

$$t_{H_{0,mr,\varepsilon=(-1)}}\left(R_{0a,\varepsilon=(-1)}, \gamma_a, \gamma_m, \gamma_r\right) = \frac{1}{H_{0,mr,\varepsilon=(-1)}} \approx \frac{R_{0a,\varepsilon=(-1)}}{c_0}\left(1+\frac{\gamma_a}{\sqrt{1+\gamma_m+\gamma_r}}\right) \quad . \tag{54}$$

2.3.3 The magnitude-redshift relation

The magnitude-redshift relation results by the general definition of the apparent magnitude $m_{mr,\varepsilon=(-1)}$

$$m_{mr,\varepsilon=(-1)} - m_{0a,\varepsilon=(-1)} = 5\log_{10}\frac{D_{mr,\varepsilon=(-1)}}{R_{0a,\varepsilon=(-1)}} \quad . \tag{55}$$

Here an apparent limit magnitude $m_{0a,\varepsilon=(-1)}$ was introduced instead of $R_{0a,\varepsilon=(-1)}$ which also changes with time. Substituting Eq. (48) into Eq. (55) then provides the sought magnitude-redshift relation

$$\begin{aligned} &m_{mr,\varepsilon=(-1)}\left(z; m_{0a,\varepsilon=(-1)}, \gamma_a, \gamma_m, \gamma_r\right) = \\ &= 5\log_{10}\left\{1-\frac{1}{(1+z)}\left\{1-\gamma_a \ln\left\{\frac{\left[\left(1+\frac{\gamma_m}{2}\right)+\sqrt{1+\gamma_m+\gamma_r}\right]}{\left\{\left[\frac{1}{(1+z)}+\frac{\gamma_m}{2}\right]+\sqrt{\frac{1}{(1+z)}\left[\frac{1}{(1+z)}+\gamma_m\right]+\gamma_r}\right\}}\right\}\right\}\right\} + m_{0a,\varepsilon=(-1)} \quad . \end{aligned} \tag{56}$$

The four free parameters $m_{0a,\varepsilon=(-1)}$, γ_a, γ_m and γ_r can be determined by direct comparison with a suitable magnitude-redshift diagram of astrophysical objects.

If we ignore the possible radiation density within our equation, we get the following simpler equation

$$\begin{aligned} &m_{m,\varepsilon=(-1)}\left(z; m_{0a,\varepsilon=(-1)}, \gamma_a, \gamma_m\right) = \\ &= 5\log_{10}\left\{1-\frac{1}{(1+z)}\left\{1-\gamma_a \ln\left\{\frac{\left[\left(1+\frac{\gamma_m}{2}\right)+\sqrt{1+\gamma_{mr}}\right]}{\left\{\left[\frac{1}{(1+z)}+\frac{\gamma_m}{2}\right]+\sqrt{\frac{1}{(1+z)}\left[\frac{1}{(1+z)}+\gamma_m\right]}\right\}}\right\}\right\}\right\} + m_{0a,\varepsilon=(-1)} \quad . \end{aligned} \tag{56a}$$

2.3.4 The angular size-redshift relation

This relation results in for larger distances over

$$\varphi = \arcsin\left(\frac{\delta_{\varepsilon=(-1)}}{D_{mr,\varepsilon=(-1)}}\right) \approx \frac{\delta_{\varepsilon=(-1)}}{D_{mr,\varepsilon=(-1)}} \tag{57}$$

to

$$\varphi_{mr,\varepsilon=(-1)}\left(z;\delta_{\varepsilon=(-1)}/R_{0a,\varepsilon=(-1)},\gamma_a,\gamma_m,\gamma_r\right)=$$
$$=\frac{\delta_{\varepsilon=(-1)}}{R_{0a,\varepsilon=(-1)}}\frac{1}{\left\{1-\frac{1}{(1+z)}\left\{1-\gamma_a\ln\left\{\frac{\left[\left(1+\frac{\gamma_m}{2}\right)+\sqrt{1+\gamma_m+\gamma_r}\right]}{\left\{\left[\frac{1}{(1+z)}+\frac{\gamma_m}{2}\right]+\sqrt{\frac{1}{(1+z)}\left[\frac{1}{(1+z)}+\gamma_m\right]+\gamma_r}\right\}}\right\}\right\}\right\}}\quad . \tag{58}$$

In this equation $\varphi_{mr,\varepsilon=(-1)}$ means the measurable angular size and $\delta_{\varepsilon=(-1)}$ the linear size of the observed extra-galactic object.

Setting $\gamma_r = 0$ we get

$$\varphi_{m,\varepsilon=(-1)}\left(z;\delta_{\varepsilon=(-1)}/R_{0a,\varepsilon=(-1)},\gamma_a,\gamma_m\right)=$$
$$=\frac{\delta_{\varepsilon=(-1)}}{R_{0a,\varepsilon=(-1)}}\frac{1}{\left\{1-\frac{1}{(1+z)}\left\{1-\gamma_a\ln\left\{\frac{\left[\left(1+\frac{\gamma_m}{2}\right)+\sqrt{1+\gamma_m}\right]}{\left\{\left[\frac{1}{(1+z)}+\frac{\gamma_m}{2}\right]+\sqrt{\frac{1}{(1+z)}\left[\frac{1}{(1+z)}+\gamma_m\right]}\right\}}\right\}\right\}\right\}}\quad . \tag{58a}$$

In logarithmic form Eq. (58) becomes to

$$\log_{10}\varphi_{mr,\varepsilon=(-1)}\left(z;\delta_{\varepsilon=(-1)}/R_{0a,\varepsilon=(-1)},\gamma_a,\gamma_m,\gamma_r\right)=$$
$$=\log_{10}\frac{\delta_{\varepsilon=(-1)}}{R_{0a,\varepsilon=(-1)}}-\log_{10}\left\{1-\frac{1}{(1+z)}\left\{1-\gamma_a\ln\left\{\frac{\left[\left(1+\frac{\gamma_m}{2}\right)+\sqrt{1+\gamma_m+\gamma_r}\right]}{\left\{\left[\frac{1}{(1+z)}+\frac{\gamma_m}{2}\right]+\sqrt{\frac{1}{(1+z)}\left[\frac{1}{(1+z)}+\gamma_m\right]+\gamma_r}\right\}}\right\}\right\}\right\}\quad . \tag{58b}$$

2.3.5 The number-redshift relation

We use here also Eq. (36) to calculate the number-redshift relation for curved spacetime, because the curvature is contained in the redshift distance.

If we introduce the redshift distance via Eq. (48)

$$V_{mr,\varepsilon=(-1)}\left(z;R_{0a,\varepsilon=(-1)},\gamma_a,\gamma_m,\gamma_r\right)=$$
$$=\frac{4\pi}{3}R_{0a,\varepsilon=(-1)}{}^3\left\{1-\frac{1}{(1+z)}\left\{1-\gamma_a\ln\left\{\frac{\left[\left(1+\frac{\gamma_m}{2}\right)+\sqrt{1+\gamma_m+\gamma_r}\right]}{\left\{\left[\frac{1}{(1+z)}+\frac{\gamma_m}{2}\right]+\sqrt{\frac{1}{(1+z)}\left[\frac{1}{(1+z)}+\gamma_m\right]+\gamma_r}\right\}}\right\}\right\}\right\}^3 \tag{59}$$

we get for the number-redshift relation

$$N_{mr,\varepsilon=(-1)}\left(z;N_{0a,\varepsilon=(-1)},\gamma_a,\gamma_m,\gamma_r\right)=$$
$$=N_{0a,\varepsilon=(-1)}\left\{1-\frac{1}{(1+z)}\left\{1-\gamma_a\ln\left\{\frac{\left[\left(1+\frac{\gamma_m}{2}\right)+\sqrt{1+\gamma_m+\gamma_r}\right]}{\left\{\left[\frac{1}{(1+z)}+\frac{\gamma_m}{2}\right]+\sqrt{\frac{1}{(1+z)}\left[\frac{1}{(1+z)}+\gamma_m\right]+\gamma_r}\right\}}\right\}\right\}\right\}^3, \tag{60}$$

where $N_{0a,\varepsilon=(-1)}$ means the expected number of objects in the whole light-path sphere $V_{0a,\varepsilon=(-1)}$ and besides

$$N_{0a,\varepsilon=(-1)}=V_{0a,\varepsilon=(-1)}\eta=\frac{4\pi}{3}R_{0a,\varepsilon=(-1)}{}^3\eta \qquad and \qquad N=V\eta \tag{61a, b}$$

applies. With η the number density was named.

In logarithmic form results

$$\log_{10}N_{mr,\varepsilon=(-1)}\left(z;N_{0a,\varepsilon=(-1)},\gamma_a,\gamma_m,\gamma_r\right)=$$
$$=3\log_{10}\left\{1-\frac{1}{(1+z)}\left\{1-\gamma_a\ln\left\{\frac{\left[\left(1+\frac{\gamma_m}{2}\right)+\sqrt{1+\gamma_m+\gamma_r}\right]}{\left\{\left[\frac{1}{(1+z)}+\frac{\gamma_m}{2}\right]+\sqrt{\frac{1}{(1+z)}\left[\frac{1}{(1+z)}+\gamma_m\right]+\gamma_r}\right\}}\right\}\right\}\right\}+\log_{10}N_{0a,\varepsilon=(-1)}\ . \tag{62}$$

If we ignore in Eq. (62) the possible radiation density within our equation, we find

$$\log_{10}N_{m,\varepsilon=(-1)}\left(z;N_{0a,\varepsilon=(-1)},\gamma_a,\gamma_m\right)=$$
$$=3\log_{10}\left\{1-\frac{1}{(1+z)}\left\{1-\gamma_a\ln\left\{\frac{\left[\left(1+\frac{\gamma_m}{2}\right)+\sqrt{1+\gamma_m}\right]}{\left\{\left[\frac{1}{(1+z)}+\frac{\gamma_m}{2}\right]+\sqrt{\frac{1}{(1+z)}\left[\frac{1}{(1+z)}+\gamma_m\right]}\right\}}\right\}\right\}\right\}+\log_{10}N_{0a,\varepsilon=(-1)}\ . \tag{63}$$

3. Derivation of further physical redshift distances

The starting point for the derivation of the further redshift distances are the following elementary general equations

$$(1+z)=\frac{a_0}{a_e} \qquad (19a) \qquad \textit{and} \qquad D=R_{0a}-R_{ee} \qquad (13)$$

$$\textit{and} \qquad (1+z)=\frac{a_0\chi_a}{a_e\chi_a}=\frac{R_{0a}}{R_{ea}} \qquad \textit{and} \qquad (1+z)=\frac{a_0\chi_e}{a_e\chi_e}=\frac{R_{0e}}{R_{ee}} \tag{64}$$

and

$$D_e=R_{ea}-R_{ee}=\frac{R_{0a}}{(1+z)}-(R_{0a}-D)=R_{0a}\left[\frac{1}{(1+z)}-1\right]+D$$
$$\textit{because of}$$
$$R_{ee}=R_{0a}-D \qquad \textit{and} \qquad R_{ea}=\frac{R_{0a}}{(1+z)} \tag{65}$$

and also

$$D_0=R_{0a}-R_{0e}=R_{0a}-(1+z)(R_{0a}-D)$$
$$\textit{because of}$$
$$R_{0e}=(1+z)(R_{0a}-D) \quad . \tag{66}$$

This results in the following further distances

$$R_{ee}=R_{0a}-D \qquad \textit{and} \qquad R_{ea}=\frac{R_{0a}}{(1+z)}$$
$$\textit{and} \qquad R_{0e}=(1+z)R_{ee}=(1+z)(R_{0a}-D) \quad . \tag{67}$$

R_{ee} is the distance at that time between the galaxy observed emitting the light and the origin of the coordinates at the time t_e the light was emitted (t_e: time at that time).

R_{ea} is the distance at that time of the observer's galaxy from the origin of the coordinates at the time t_e.

R_{0e} is the today's - at time t_0, at which the light is absorbed on the place of observer - distance of the light-emitting galaxy from the origin of the coordinates.

R_{0a} is today's distance of the galaxy containing the observer from the origin of the coordinates.

Hint:

We have not written above the second parts ",ε=(±1)" of indexes in all cases.

3.1 ε = (+1)

The further redshift distances become in the case of ε = (+1) concretely

$$R_{ee,mr,\varepsilon=(+1)}\left(z;R_{0a,\varepsilon=(+1)},\gamma_a,\gamma_m,\gamma_r\right)=$$
$$=\frac{R_{0a,\varepsilon=(+1)}}{(1+z)}\left\{1+\gamma_a\arcsin\left\{\frac{\left(\frac{\gamma_m}{2}-1\right)\sqrt{\gamma_r+\left[\gamma_m-\frac{1}{(1+z)}\right]\frac{1}{(1+z)}}-\left[\frac{\gamma_m}{2}-\frac{1}{(1+z)}\right]\sqrt{\gamma_r+\gamma_m-1}}{\left[\left(\frac{\gamma_m}{2}\right)^2+\gamma_r\right]}\right\}\right\} \tag{68}$$

and

$$R_{0e,mr,\varepsilon=(+1)}\left(z;R_{0a,\varepsilon=(+1)},\gamma_a,\gamma_m,\gamma_r\right)=$$
$$R_{0a,\varepsilon=(+1)}\left\{1+\gamma_a\arcsin\left\{\frac{\left(\frac{\gamma_m}{2}-1\right)\sqrt{\gamma_r+\left[\gamma_m-\frac{1}{(1+z)}\right]\frac{1}{(1+z)}}-\left[\frac{\gamma_m}{2}-\frac{1}{(1+z)}\right]\sqrt{\gamma_r+\gamma_m-1}}{\left[\left(\frac{\gamma_m}{2}\right)^2+\gamma_r\right]}\right\}\right\} \tag{69}$$

and of course too

$$R_{ea,mr,\varepsilon=(+1)}\left(z;R_{0a,\varepsilon=(+1)}\right)=\frac{R_{0a,\varepsilon=(+1)}}{(1+z)} \quad . \tag{70}$$

This distance is not depending on the parameters γ_a, γ_r and γ_m.

These distances from the origin of coordinates yield

$$D_{e,mr,\varepsilon=(+1)}\left(z;R_{0a,\varepsilon=(+1)},\gamma_a,\gamma_m,\gamma_r\right)=$$
$$=-\frac{R_{0a,\varepsilon=(+1)}}{(1+z)}\gamma_a\arcsin\left\{\frac{\left(\frac{\gamma_m}{2}-1\right)\sqrt{\gamma_r+\left[\gamma_m-\frac{1}{(1+z)}\right]\frac{1}{(1+z)}}-\left[\frac{\gamma_m}{2}-\frac{1}{(1+z)}\right]\sqrt{\gamma_r+\gamma_m-1}}{\left[\left(\frac{\gamma_m}{2}\right)^2+\gamma_r\right]}\right\} \quad . \tag{71}$$

$D_{e,mr,\varepsilon=(+1)}$ is the distance at the time t_e between the observed galaxy and the galaxy in which the observer is located.

Furthermore we find

$$D_{0,mr,\varepsilon=(+1)}\left(z;R_{0a,\varepsilon=(+1)},\gamma_a,\gamma_m,\gamma_r\right)=$$
$$=-R_{0a,\varepsilon=(+1)}\gamma_a \arcsin\left\{\frac{\left(\frac{\gamma_m}{2}-1\right)\sqrt{\gamma_r+\left[\gamma_m-\frac{1}{(1+z)}\right]\frac{1}{(1+z)}}-\left[\frac{\gamma_m}{2}-\frac{1}{(1+z)}\right]\sqrt{\gamma_r+\gamma_m-1}}{\left[\left(\frac{\gamma_m}{2}\right)^2+\gamma_r\right]}\right\} . \quad (72)$$

$D_{0,mr,\varepsilon=(+1)}$ is the today's distance between the two participating galaxies.

The following figures illustrate the equations for the further redshift distances, in which we have normalized all distances to $R_{0a,\varepsilon=(+1)}$.

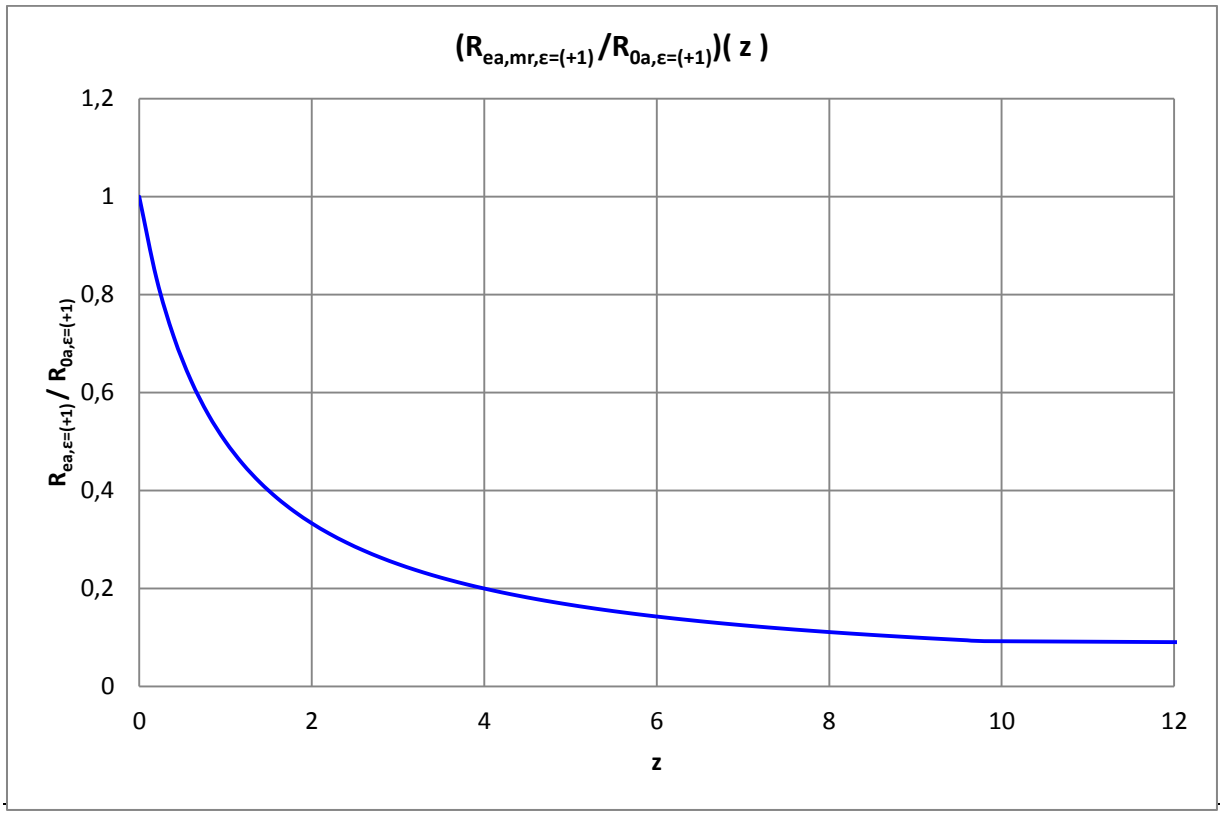

Figure 6. Redshift distance $R_{ea,mr,\varepsilon=(+1)}$ normalized to the distance $R_{0a,\varepsilon=(+1)}$.

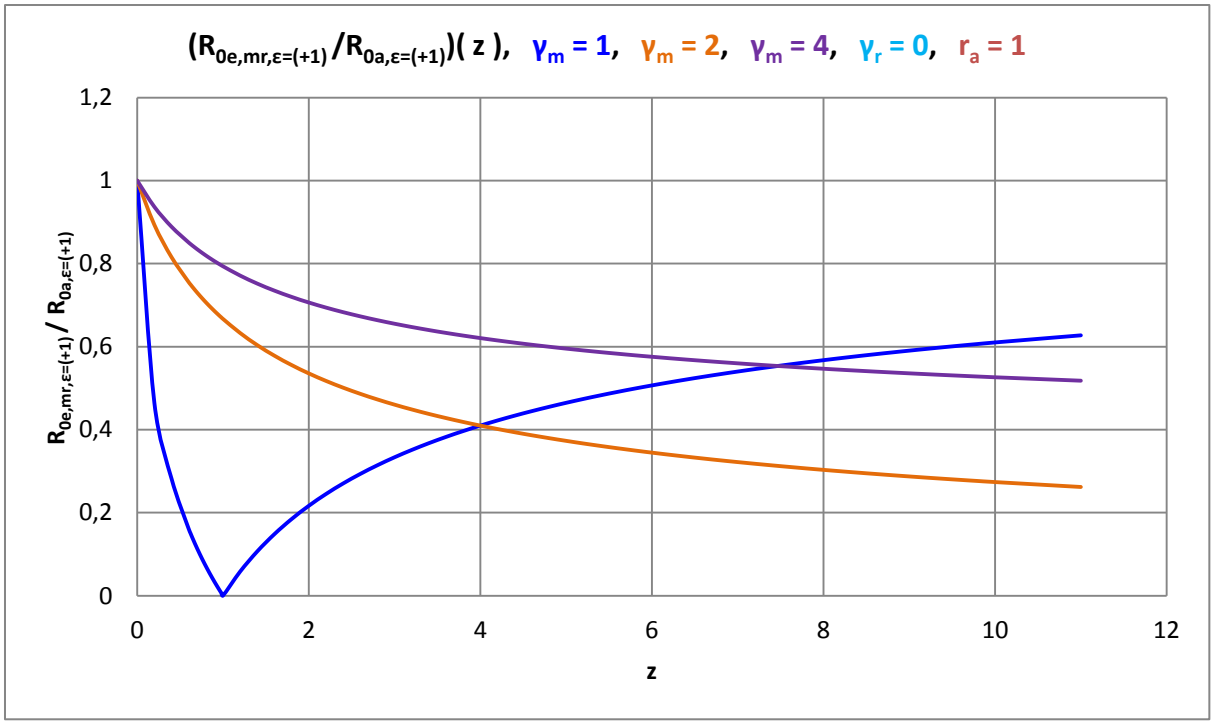

Figure 7. Redshift distance $R_{0e,mr,\varepsilon=(+1)}$ normalized to the distance $R_{0a,\varepsilon=(+1)}$ for various values of the parameter γ_m and $\gamma_r = 0$ as well as $r_a = 1$.

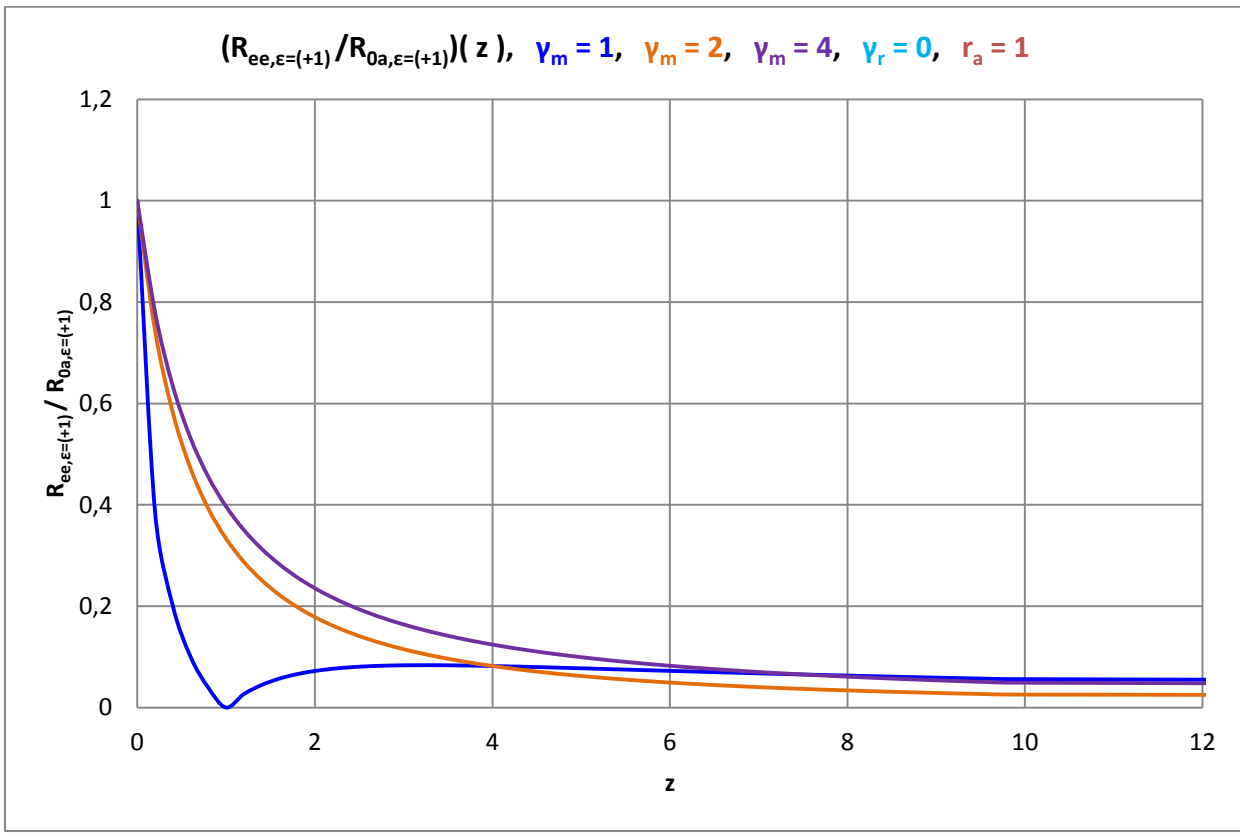

Figure 8. Redshift distance $R_{ee,mr,\varepsilon=(+1)}$ normalized to the distance $R_{0a,\varepsilon=(+1)}$ for different values of the parameter γ_m and $\gamma_r = 0$ as well as $r_a = 1$.

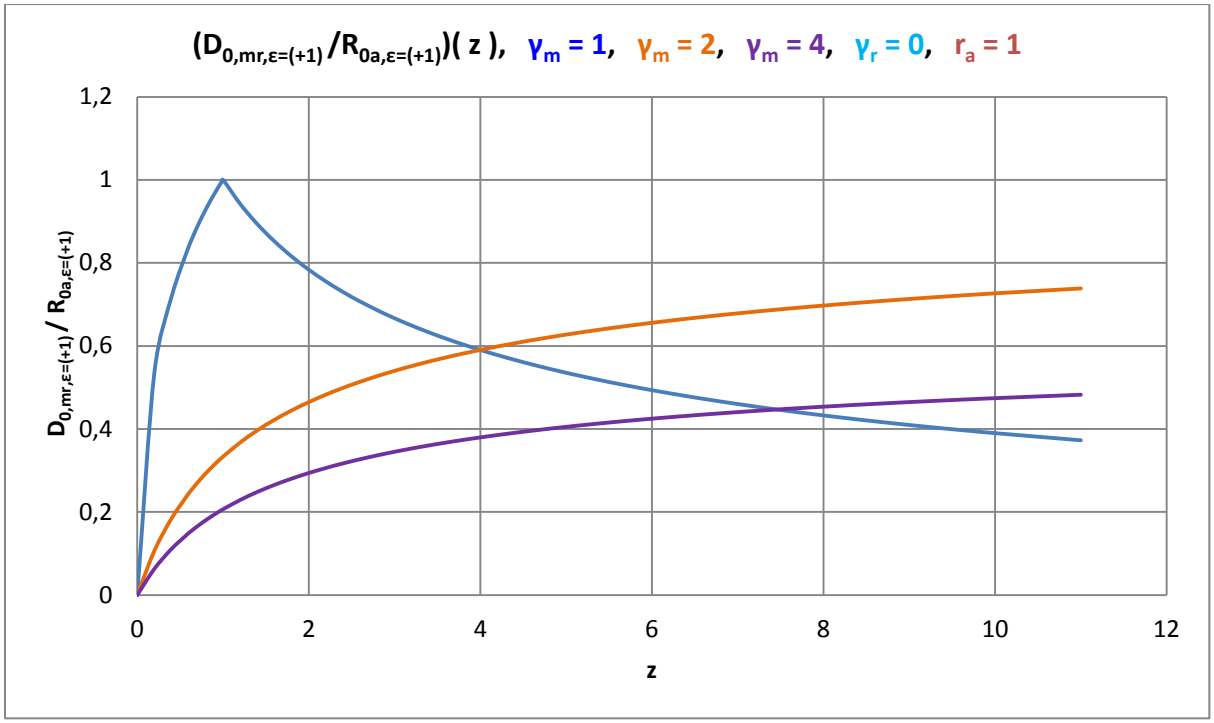

Figure 9. Today's redshift distance $D_{0,mr,\varepsilon=(+1)}$ normalized to the distance $R_{0a,\varepsilon=(+1)}$ for various values of the parameter γ_m and $\gamma_r = 0$ as well as $r_a = 1$.

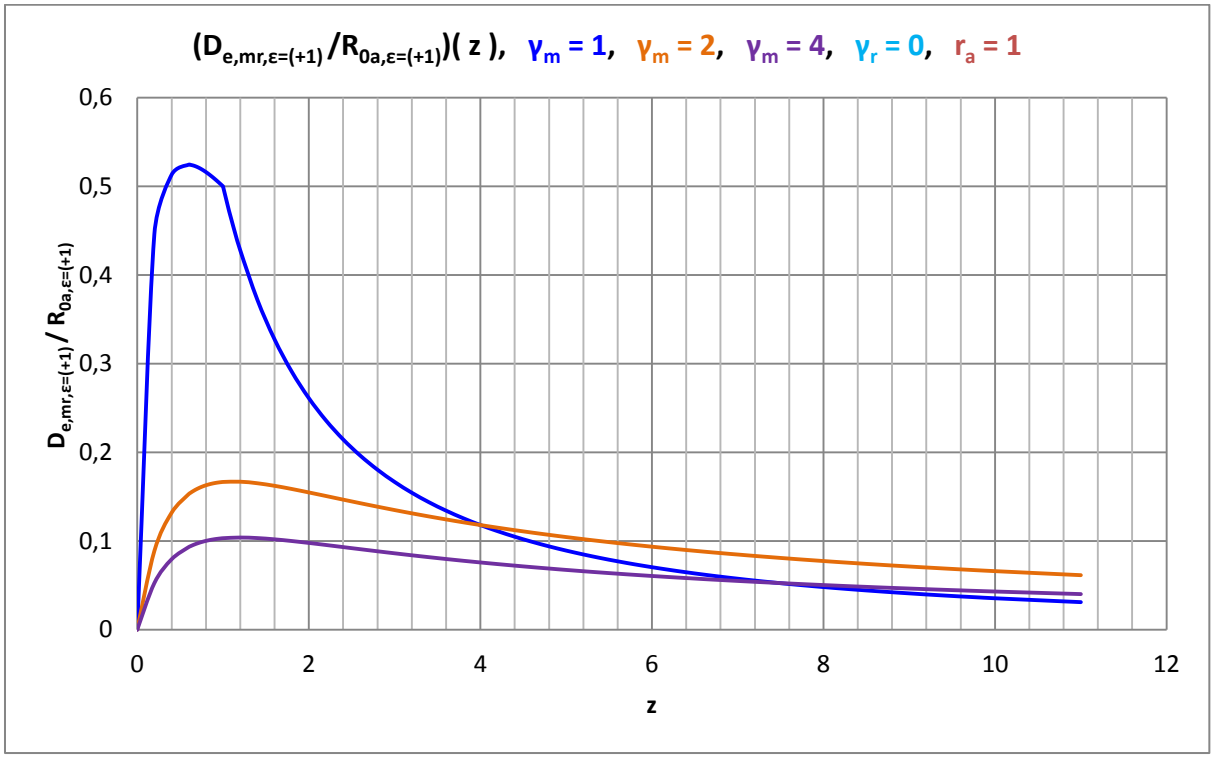

Figure 10. The redshift distance at that time $D_{e,mr,\varepsilon=(+1)}$ normalized to the distance $R_{0a,\varepsilon=(+1)}$ for various values of the parameter γ_m and $\gamma_r = 0$ as well as $r_a = 1$.

In the specialist literature, four of these redshift distances are not known and they cannot be derived there, respectively.

We will give concrete values for such redshift distances for the galaxy M87, 27 SN Ia and two other cosmological relevant objects below.

3.2 ε = (-1)

The further redshift distances become in the case of ε = (-1) concretely

$$R_{ee,mr,\varepsilon=(-1)}\left(z;R_{0a,\varepsilon=(-1)},\gamma_a,\gamma_m,\gamma_r\right)= \\ =\frac{R_{0a,\varepsilon=(-1)}}{(1+z)}\left\{1-\gamma_a\ln\left\{\frac{\left[\left(1+\frac{\gamma_m}{2}\right)+\sqrt{1+\gamma_m+\gamma_r}\right]}{\left\{\left[\frac{1}{(1+z)}+\frac{\gamma_m}{2}\right]+\sqrt{\frac{1}{(1+z)}\left[\frac{1}{(1+z)}+\gamma_m\right]+\gamma_r}\right\}}\right\}\right\} \tag{73}$$

and

$$R_{0e,mr,\varepsilon=(-1)}\left(z;R_{0a,\varepsilon=(-1)},\gamma_a,\gamma_m,\gamma_r\right)= \\ =R_{0a,\varepsilon=(-1)}\left\{1-\gamma_a\ln\left\{\frac{\left[\left(1+\frac{\gamma_m}{2}\right)+\sqrt{1+\gamma_m+\gamma_r}\right]}{\left\{\left[\frac{1}{(1+z)}+\frac{\gamma_m}{2}\right]+\sqrt{\frac{1}{(1+z)}\left[\frac{1}{(1+z)}+\gamma_m\right]+\gamma_r}\right\}}\right\}\right\} \tag{74}$$

and of course too

$$R_{ea,mr,\varepsilon=(-1)}\left(z;R_{0a,\varepsilon=(-1)}\right)=\frac{R_{0a,\varepsilon=(-1)}}{(1+z)} \quad . \tag{75}$$

This distance is not depending on the parameters γ_a, γ_r and γ_m.

These distances from the origin of coordinates yield

$$D_{e,mr,\varepsilon=(-1)}\left(z;R_{0a,\varepsilon=(-1)},\gamma_a,\gamma_m,\gamma_r\right)=$$
$$=\frac{R_{0a,\varepsilon=(-1)}}{(1+z)}\gamma_a\ln\left\{\frac{\left[\left(1+\frac{\gamma_m}{2}\right)+\sqrt{1+\gamma_m+\gamma_r}\right]}{\left\{\left[\frac{1}{(1+z)}+\frac{\gamma_m}{2}\right]+\sqrt{\frac{1}{(1+z)}\left[\frac{1}{(1+z)}+\gamma_m\right]+\gamma_r}\right\}}\right\}\quad . \tag{76}$$

$D_{e,mr,\varepsilon=(-1)}$ is the distance at the time t_e between the observed galaxy and the galaxy in which the observer is located.

Furthermore We find

$$D_{0,mr,\varepsilon=(-1)}\left(z;R_{0a,\varepsilon=(-1)},\gamma_a,\gamma_m,\gamma_r\right)=$$
$$=R_{0a,\varepsilon=(-1)}\gamma_a\ln\left\{\frac{\left[\left(1+\frac{\gamma_m}{2}\right)+\sqrt{1+\gamma_m+\gamma_r}\right]}{\left\{\left[\frac{1}{(1+z)}+\frac{\gamma_m}{2}\right]+\sqrt{\frac{1}{(1+z)}\left[\frac{1}{(1+z)}+\gamma_m\right]+\gamma_r}\right\}}\right\}\quad . \tag{77}$$

$D_{0,mr,\varepsilon=(-1)}$ is the today's distance between the two participating galaxies.

In the specialist literature, four of these redshift distances are not known and they cannot be derived there, respectively.

The following two figures illustrate the equations for the further redshift distances $D_{0,mr,\varepsilon=(-1)}$ and $D_{e,mr,\varepsilon=(-1)}$, respectively, in which we have normalized all distances to $R_{0a,\varepsilon=(-1)}$.

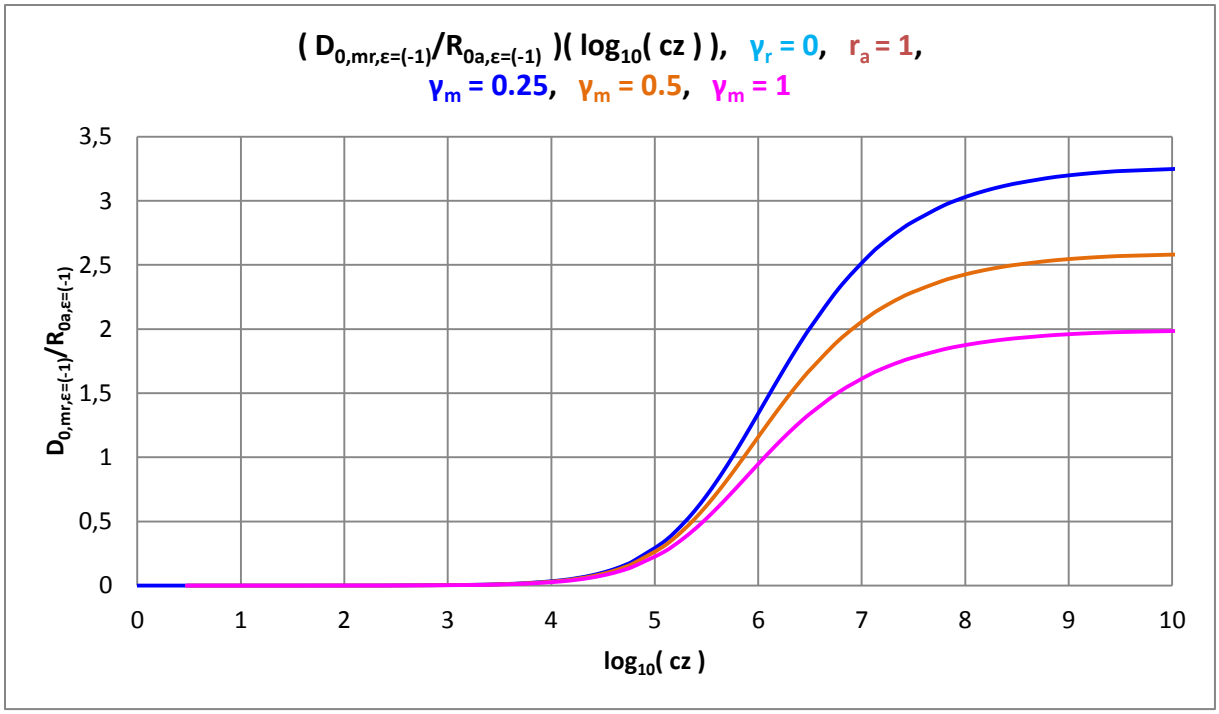

Figure 11. Today's redshift distance $D_{0,mr,\varepsilon=(-1)}$ normalized to the distance $R_{0a,\varepsilon=(-1)}$ for various values of the parameter γ_m and $\gamma_r = 0$ as well as $r_a = 1$.

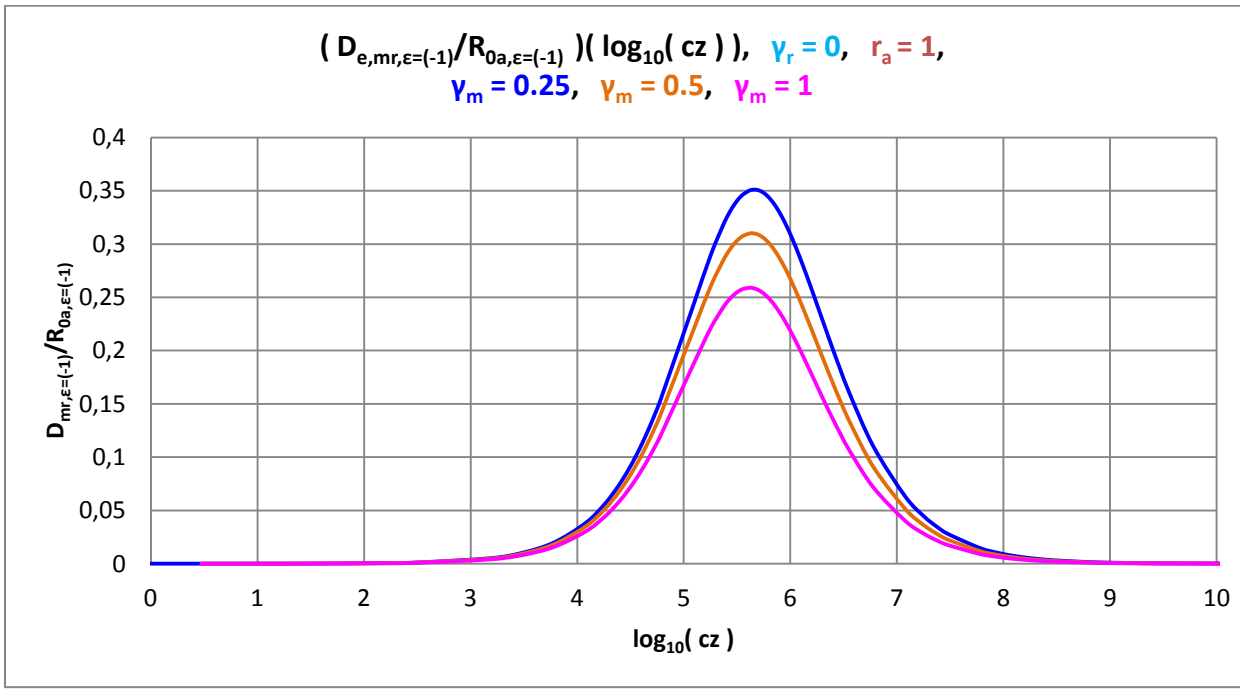

Figure 12. The redshift distance at that time $D_{e,mr,\varepsilon=(-1)}$ normalized to the distance $R_{0a,\varepsilon=(-1)}$ for various values of the parameter γ_m and $\gamma_r = 0$ as well as $r_a = 1$.

We will give concrete values for such redshift distances for the galaxy M87, 27 SN Ia and two other cosmological relevant objects below.

4. Determination of the parameter values

The present paper presents a theoretical derivation of redshift distances in the two possible curved spacetimes, which carry out without approximations for e.g. small redshifts z and is mainly of theoretical nature. The essay is therefore a theoretical offer to the observing cosmologists.

Nevertheless, in this chapter we will apply the theory presented here in detail to some measurement results of observational cosmology, whereby we only demonstrate the principle of evaluating the measurement data. For this reason, no more detailed error analyzes are carried out. We leave that to the interested experts of observational cosmology.

4.1 $\varepsilon = (+1)$

4.1.1 Magnitude-redshift relation

The apparent magnitude m depends according to Eq. (33) in addition to the measurable redshift z also on the four parameters $m_{0a,\varepsilon=(+1)}$, γ_a, γ_m and γ_r.

To find the values of the parameters, the quasar catalog by Véron-Cetty et al. [1] is suitable in which measured redshifts and apparent magnitudes of 132,975 quasars are given.

Fig. 13 shows all these quasars in a single magnitude-redshift diagram, where we have used $\log_{10}(cz)$ on the axis of ordinates.

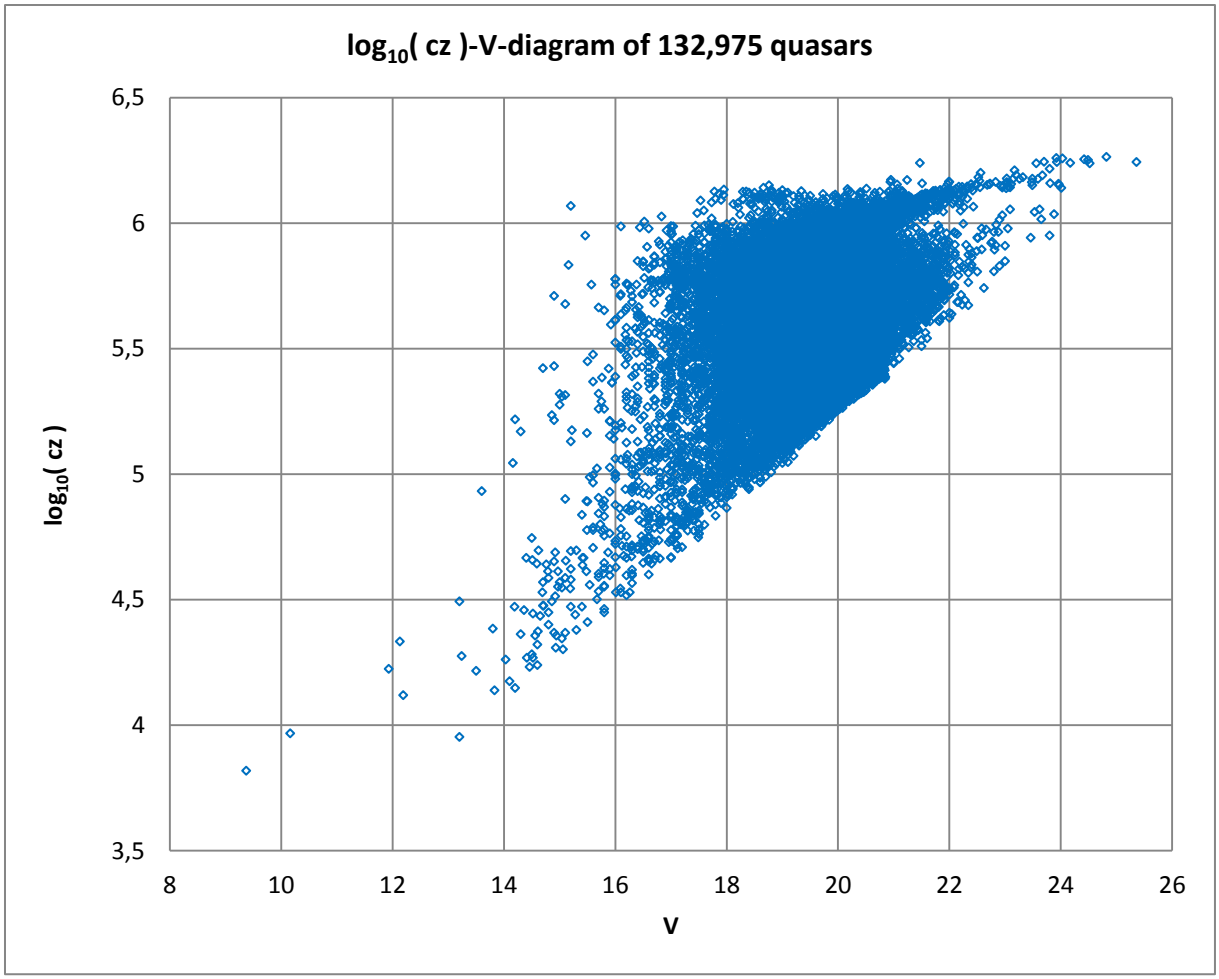

Figure 13. Magnitude-redshift diagram for all 132,975 quasars according to M.-P. Véron-Cetty et al. [1].

A clear edge exists on the right side of the accumulation of measurement points, which indicates minimum apparent magnitudes for associated redshifts. The apparent magnitudes are usually up to far to the left of this edge inside the diagram.

If we form redshift intervals with mean values of the redshifts and the corresponding mean values for the apparent magnitudes, this fact leads to a clear curvature of the mean value curve in the direction of the redshift axis. This curvature should be explained by means of a valid astrophysical theory. More precisely: The theory has to explain the curvature! This suggests that our redshift distance [i.e. ultimately Eq. (33)] could be suitable for the measured values.

It is precisely this strange magnitude-redshift diagram, which was stimulating us to think about cosmological distance determinations for many years [9].

To evaluate the quasar data set, we first create 75 z-intervals with 1,773 quasars each. For these intervals, we calculate the mean values $\langle z_i \rangle$ and the associated mean values $\langle m_i \rangle$ of the quasars.

We use the following χ^2-function

$$\chi^2(p_k) = \frac{1}{(N-1)} \sum_{i=1}^{N} \left[m_{th,i}(p_k) - m_{obs,i} \right]^2 \tag{78}$$

for our evaluation of the data.

The abbreviation p_k with k = 1, 2, 3, 4 stands for the four parameters we are looking for, $m_{0a,\varepsilon=(+1)}$, γ_a, γ_m and γ_r.

If we use our magnitude-redshift relation (33), the χ^2-function looks more concrete

$$\chi^2(z; m_{0a,\varepsilon=(+1)}, \gamma_a, \gamma_m, \gamma_r) = \frac{1}{(N-1)} \sum_{i=1}^{N} \{ X_i + m_{0a,\varepsilon=(+1)} - m_{obs,i} \}^2$$

with

$$X_i = 5 \log_{10} \left\{ 1 - \frac{1}{(1+z)} \left\{ 1 + \gamma_a \arcsin \left\{ \frac{\left(\frac{\gamma_m}{2} - 1 \right) \sqrt{\gamma_r + \frac{1}{(1+z)} \left[\gamma_m - \frac{1}{(1+z)} \right]} - \left[\frac{\gamma_m}{2} - \frac{1}{(1+z)} \right] \sqrt{\gamma_r + \gamma_m - 1}}{\left[\left(\frac{\gamma_m}{2} \right)^2 + \gamma_r \right]} \right\} \right\} \right\} \tag{78a}$$

and $z = z_i$.

Using the quasar data and the usual mathematical procedure, we find the parameters to be $m_{0a,\varepsilon=(+1)} = 20.1912$, $\gamma_m = 1.8116$ and $r_a = 1$. We have specialized our analysis to $\gamma_r = 0$ because the radiation density plays obvious no role today.

Fig. 14 shows the result of the mean value formation and the adaptation of our theory to the curvature of the mean value curve.

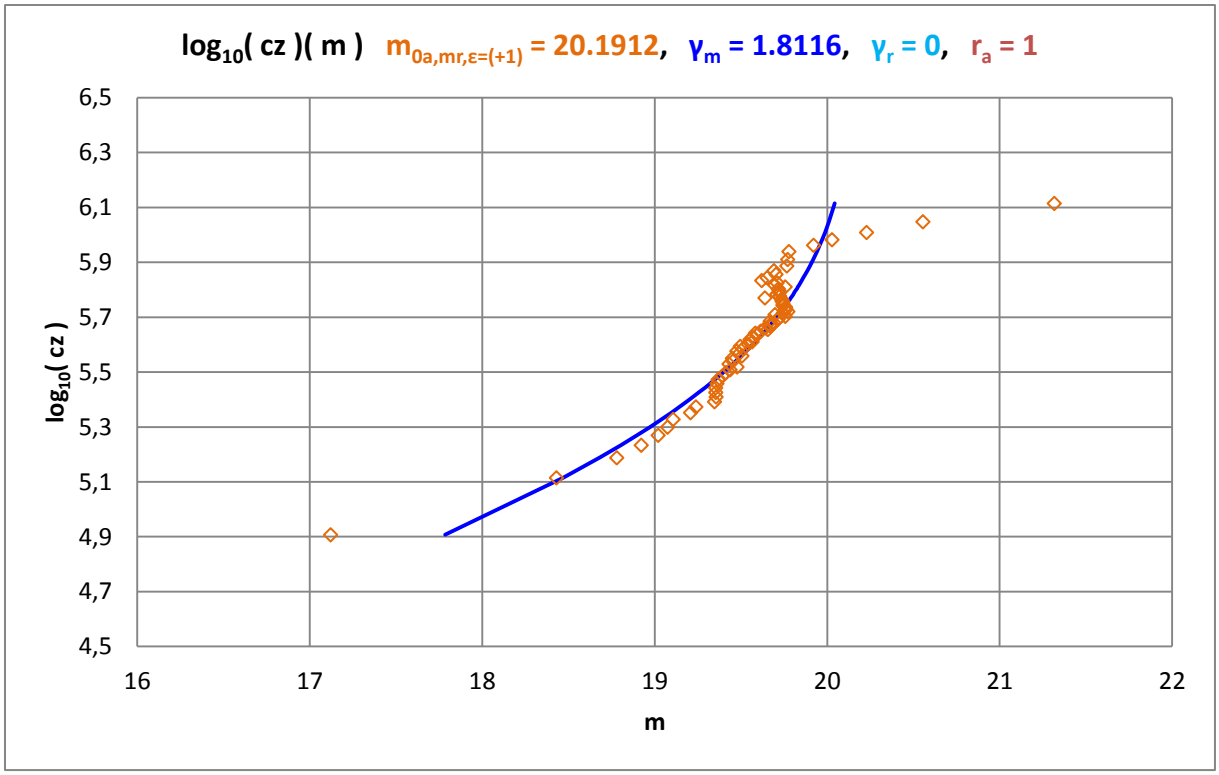

Figure 14. Magnitude-redshift diagram for 132,975 quasars according to M.-P. Véron-Cetty et al. [1].

A possible interpretation of the measured magnitude-redshift relation may be:
The quasars came in to being historically slowly as relatively few and weakly luminous objects at a point in time that corresponds to about $z \approx 4.3$ (development effect). The quasars later behaved as our theory expects in curved space and moved with time - i.e. for decreasing redshifts z - on average along the theoretical curve (in the diagram from top right diagonally to bottom left). The quasars have gradually died out in the recent past and became relatively bright in this process.

4.1.2 Number-redshift relation

We use the following variance to evaluate the number-redshift relation

$$\chi^2(p_k) = \frac{1}{(N-1)} \sum_{i=1}^{N} \left[N_{th,i}(p_k) - N_{obs,i} \right]^2 \quad . \tag{79}$$

The abbreviation p_k with k = 1, 2, 3, 4 stands for the four parameters we are looking for, $N_{0a,\varepsilon=(+1)}$, γ_a, γ_m and γ_r.

If we insert our number-redshift relation (40), the Eq. (79) reads concrete

$$\chi^2\left(z; N_{0a,\,\varepsilon=(+1)}, \gamma_a, \gamma_m, \gamma_r\right) = \frac{1}{(N-1)} \sum_{i=1}^{N} \left\{X_i - N_{obs,i}\right\}^2$$

with

$$X_i = N_{0a,\,\varepsilon=(+1)} \left\{1 - \frac{1}{(1+z)} \left\{1 + \gamma_a \arcsin\left\{ \frac{\left(\frac{\gamma_m}{2} - 1\right)\sqrt{\gamma_r + \frac{1}{(1+z)}\left[\gamma_m - \frac{1}{(1+z)}\right]} - \left[\frac{\gamma_m}{2} - \frac{1}{(1+z)}\right]\sqrt{\gamma_r + \gamma_m - 1}}{\left[\left(\frac{\gamma_m}{2}\right)^2 + \gamma_r\right]} \right\}\right\}\right\}^3 \qquad (79a)$$

and $z = z_i$.

Using this simple χ^2-function, we find $N_{0a,\varepsilon=(+1)}$ = 126,789 for the theoretically expected total number of quasars, if we use the value γ_m = 1.8116 found via the magnitude-redshift relation. Furthermore we have used γ_r = 0 and r_a = 1.

The expected number $N_{0a,\varepsilon=(+1)}$ = 126,789 is slightly smaller than the actual number of quasars measured within the catalogue of M.-P. Véron-Cetty et al. [1].
May be that the reason for this is the use of the simple Eq. (36) for the flat volume during the derivation of the number-redshift relation.

Fig. 15 shows the graphic result.

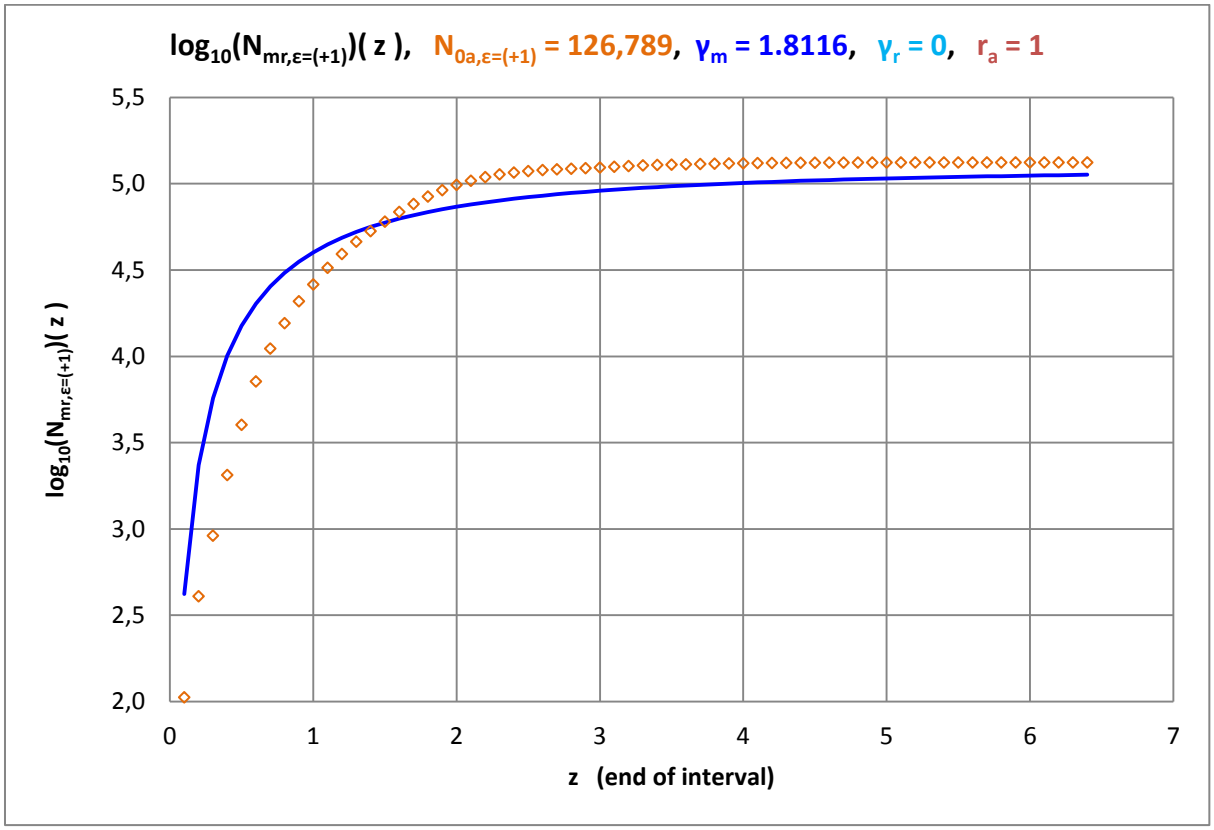

Figure 15. Number-redshift diagram for the 132,975 quasars according to M.-P. Véron-Cetty et al. [1].

Table 11 in the appendix shows the numbers N_i summed up in the redshift intervals z_i of the quasars according to [1].

4.1.3 Angular size-redshift relation

In this case, we use the measurement data from K. Nilsson et al. [2] to find an average linear size of the cosmic objects measured there.

The starting point is the variance

$$\chi_\varphi{}^2(p_k) = \frac{1}{(N-1)} \sum_{i=1}^{N} \left[\varphi_{th,i}(p_k) - \varphi_{obs,i}\right]^2 \quad . \tag{80}$$

The abbreviation p_k with k = 1, 2, 3, 4 stands for the four parameters we are looking for, $\delta_{\varepsilon=(+1)}/R_{0a,\varepsilon=(+1)}$, γ_a, γ_m and γ_r.

If we use our angular size-redshift relation (35), the Eq. (80) reads concrete (setting $\gamma_r = 0$)

$$\chi_\varphi{}^2\left(z_i; \delta_{\varepsilon=(+1)}/R_{0a,\varepsilon=(+1)}, \gamma_a, \gamma_m\right) = \frac{1}{(N-1)} \sum_{i=1}^{N} \left\{ \frac{\delta_{\varepsilon=(+1)}}{R_{0a,\varepsilon=(+1)}} X_i - \varphi_{obs,i} \right\}^2$$

with

$$X_i = \frac{1}{\left\{1 - \frac{1}{(1+z_i)} \left\{1 + \gamma_a \arcsin\left\{ \frac{\left(\frac{\gamma_m}{2} - 1\right)}{\sqrt{1+z_i}} \sqrt{\gamma_m - \frac{1}{(1+z_i)}} - \left[\frac{\gamma_m}{2} - \frac{1}{(1+z_i)}\right] \sqrt{\gamma_m - 1} \right\} \right\} \right\}} \quad . \tag{80a}$$

$$\left(\frac{\gamma_m}{2}\right)^2$$

The comparison of the theory with the measurement data using $\gamma_m = 1.8116$, $\gamma_r = 0$ and $r_a = 1$ results in a value of $\delta_{\varepsilon=(+1)}/R_{0a,\varepsilon=(+1)} = 5.9592 \times 10^{-5}$.

Fig. 16 shows the graphic result.

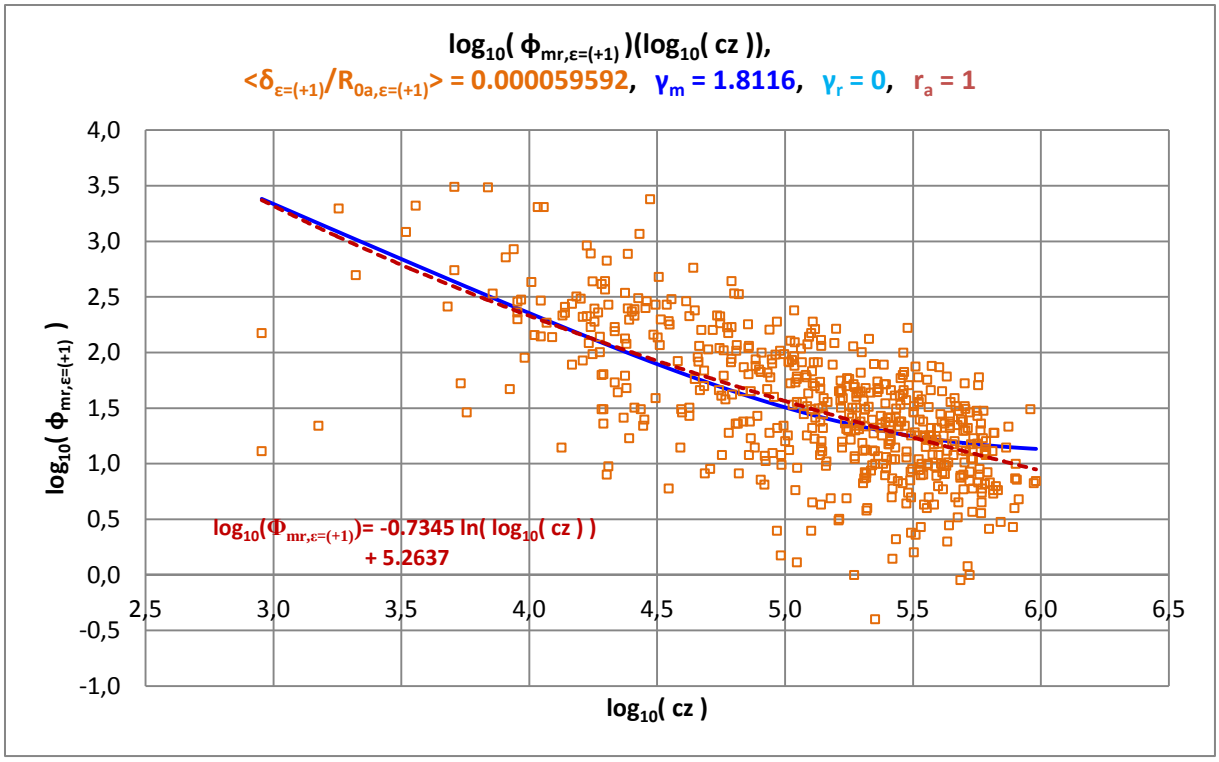

Figure 16. Angular size-redshift diagram according to K. Nilsson et al. [2].

The determination of the linear size $\delta_{\varepsilon=(+1)}$ requires the knowledge of $R_{0a,\varepsilon=(+1)}$. Because the absolute magnitudes are known for some SN Ia (which differ strangely enough slightly from one another), we can determine $R_{0a,\varepsilon=(+1)}$ using a magnitude-redshift diagram of these cosmic objects. We will carry out this within the next chapter.

4.1.4 Fixing of $R_{0a,\varepsilon=(+1)}$ with the help of SN Ia

By W. L. Freedman et al. [3], data from a total of 27 SN Ia were made available, with the help of which we can determine both the distance $R_{0a,\varepsilon=(+1)}$ - a current physical distance - and, as a main result, the today's Hubble parameter $H_{0a,mr,\varepsilon=(+1)}$.

The data we are interested in are the distance modules (μ_{TRGB} and μ_{Ceph}, respectively), the maximum apparent magnitudes (m_{CSP_B0} and m_{SC_B}, respectively) and the radial velocities V_{NED}, from which the redshifts z_{NED} can be calculated.

The methods taken into account in [3] for determining the maximum apparent magnitude and thus the associated absolute magnitude are different, which is why somewhat different values are given for one and the same SN Ia. For our purposes, we calculate the mean values from these data and assign them to the relevant SN Ia.

We calculate the absolute magnitudes M_i of the SN Ia$_i$ using (μ_{TRGB} - m_{CSP_B0}) and (μ_{Ceph} - m_{SC_B}), respectively, and then we always calculate an average value $<M_i>$ if both value pairs are specified for one and the same SN Ia.

From all the absolute magnitudes obtained in this way, we finally form the mean value of the absolute magnitude to be <M> ≈ -19.24, which enables us to determine the distance $R_{0a,\varepsilon=(+1)}$ with the aid of the parameter $m_{0a,\varepsilon=(+1)}$, which results from the magnitude-redshift diagram of the SN Ia. The simple equation used for this is

$$R_{0a,\varepsilon=(+1)} = 10^{\frac{\left(m_{0a,\varepsilon=(+1)} - M\right)}{5}+1} \quad . \tag{81}$$

The graphic result is shown in Fig. 17.

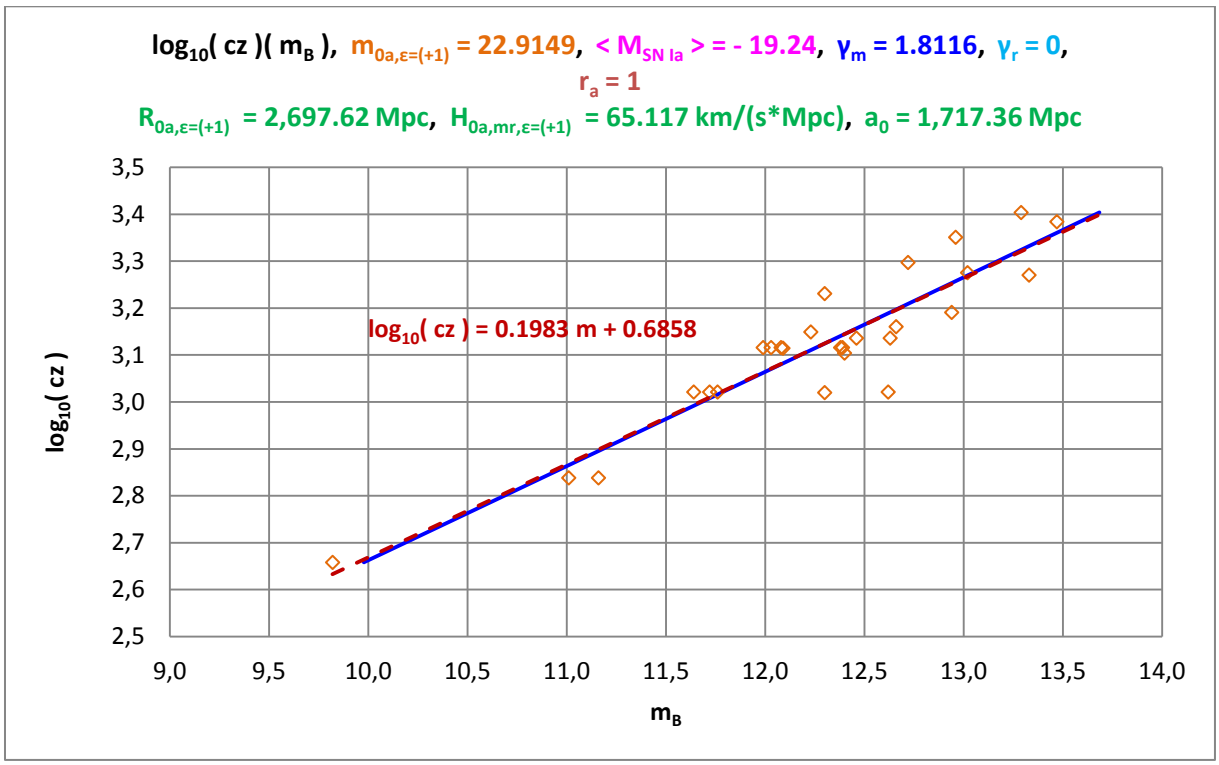

Figure 17. Magnitude-redshift diagram for 27 SN Ia according to W. L. Freedman et al. [3].

The theoretical curve (blue) lies exactly on the linear trend line (dashed in red) with the equation given in the figure.

Finding $m_{0a,\varepsilon=(+1)} \approx 22.9149$ and using the mean value of the absolute brightness <M> = -19.24, the distance $R_{0a,\varepsilon=(+1)} \approx 2{,}697.62$ Mpc we are ultimately looking for is the essential result of this data analysis.
We get furthermore $a_0 \approx 1{,}717.36$ Mpc. This value can be calculated with Eq. (23) using $R_{0a,\varepsilon=(+1)}$ and γ_a found.

With the help of the value of $R_{0a,\varepsilon=(+1)}$ and taking the Eq. (28), which is an approximation for small redshifts, the today's Hubble parameter $H_{0a,m,\varepsilon=(+1)} \approx 65.117$ km/(s·Mpc) results, if we neglect the radiation density how before always. This value is slightly below the Planck value (2018) with $H_{0,Planck} \approx 67.66$ km/(s·Mpc) [4].

In Table 12 of the appendix, all the values we have used for the magnitude-redshift diagram of the 27 SN Ia are compiled.

Using Eq. (5b) we can write

$$\rho_{0m} = \frac{3{c_0}^2 K_{0m}}{8\pi G}\frac{1}{{a_0}^3} \quad . \tag{82}$$

Inserting the second equation of equations (23) we get as result for the today's mass density

$$\rho_{0m} = \frac{3{c_0}^2}{8\pi G}\frac{\gamma_m}{{a_0}^2} \qquad because\ of \qquad K_{0m} = a_0\gamma_m \quad . \tag{83}$$

With the help of the parameters γ_m and $R_{0a,\varepsilon=(+1)}$ determined by us, we find $\rho_{0m,\varepsilon=(+1)} \approx 1.037 \times 10^{-30}$ g/cm^3 for today's matter density inside the closed universe with $\varepsilon = (+1)$.

Via

$$M_{Fs,\varepsilon=(+1)} = \frac{4\pi}{3}{R_{0a,\varepsilon=(+1)}}^3\rho_{0m} = \frac{{c_0}^2}{2G}\frac{\gamma_m}{{a_0}^2}{R_{0a,\varepsilon=(+1)}}^3 = \frac{{c_0}^2}{2G}\frac{\gamma_m}{{\gamma_a}^2}R_{0a,\varepsilon=(+1)} \tag{84}$$

$$because\ of \qquad {a_0}^2 = {\gamma_a}^2{R_{0a,\varepsilon=(+1)}}^2$$

the constant mass of the Friedmann sphere - so called by us - results in $M_{Fs,\varepsilon=(+1)} \approx 2.506 \times 10^{54}$ g.

Because we generally do not consider the accuracy within this paper, we simply specify the decimal places with up to three places, whereby the mathematical analysis of the data usually delivers more decimal digits.

With the known value $R_{0a,\varepsilon=(+1)} \approx 2{,}697.62$ Mpc we can calculate the mean linear size of the Nilsson objects [2] to be $\delta_{\varepsilon=(+1)} \approx 0.161$ Mpc, because we have found $\delta_{\varepsilon=(+1)}/R_{0a,\varepsilon=(+1)} = 5.959 \times 10^{-5}$ for them.
Using known $R_{0a,\varepsilon=(+1)}$ and γ_m, of course, all linear dimensions of these objects can be calculated using their angular size and redshift if they could be measured.

4.1.5 Calculation of the further redshift distances for SN Ia

Because we were able to determine $R_{0a,\varepsilon=(+1)}$, we can graphically display all the further redshift distances in a form, which is not normalized to $R_{0a,\varepsilon=(+1)}$. The result is shown in Fig. 18, using the values we found for our parameters γ_a, γ_m and $R_{0a,\varepsilon=(+1)}$ and $\gamma_r = 0$.

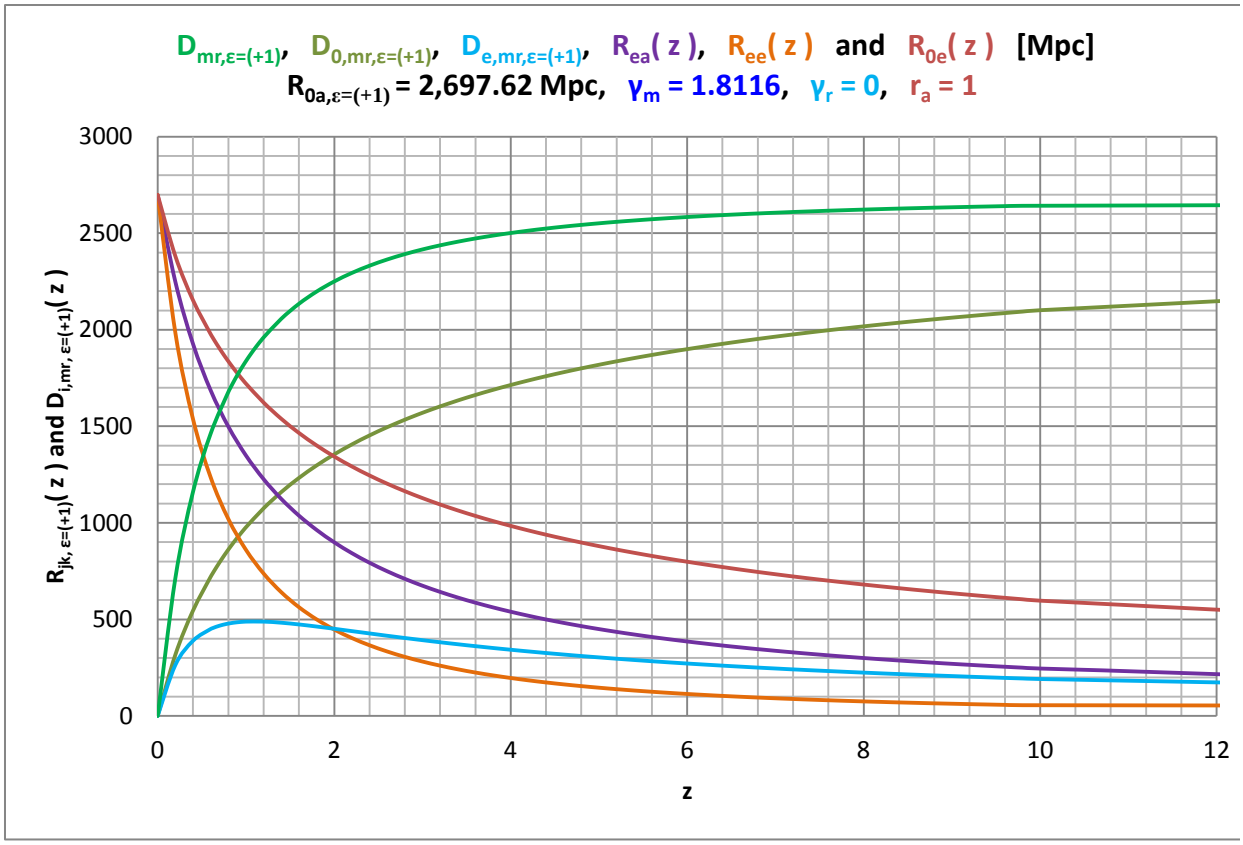

Figure 18. Redshift distance $D_{mr,\varepsilon=(+1)}$ (real light path) and all further redshift distances $D_{i,mr,\varepsilon=(+1)}$ (i = 0, e) and R_{jk} (j = 0, e; k = e, a) as a function of the redshift up to z = 12.

We have neglected in the Fig. 18 the part "mr,ε=(+1)" of indexes for all R_{jk}.

To interpret Fig. 18:

a) For redshift z going towards infinity the distance $D_{mr,\varepsilon=(+1)}$ goes to $R_{0a,\varepsilon=(+1)}$.

This means that no observer can observe objects for which is $D_{mr,\varepsilon=(+1)} > R_{0a,\varepsilon=(+1)} \approx 2{,}697.62$ Mpc.

b) The light path distance $D_{mr,\varepsilon=(+1)} = R_{0a,\varepsilon=(+1)} - R_{ee,mr,\varepsilon=(+1)}$ is always greater than the distances $D_{0,mr,\varepsilon=(+1)}$ (today's) and $D_{e,mr,\varepsilon=(+1)}$ (time at that time).

In particular, the light path $D_{mr,\varepsilon=(+1)}$ is not equal to the today's distance $D_{0,mr,\varepsilon=(+1)}$ between two astrophysical objects.

c) The distances $R_{jk,mr,\varepsilon=(+1)}$ are physical distances from an origin coordinates and develop directly with the change in the scale parameter a(t) over time. For large redshifts, the scale parameter was correspondingly small and, as a result, the associated physical distances were also correspondingly small.

d) The distance at that time $D_{e,mr,\varepsilon=(+1)}$ is interesting: It shows a maximum for a specific redshift and approaches zero for very large redshifts.

Table 1 summarizes all calculated redshift distances of the 27 SN Ia used by us for analyzing the data.

SN Ia	R_{ea}	R_{ee}	R_{0e}	R_{0a}	D_e	D_0	D	z

1980N	2,685.91	2,677.69	2,689.35	2,697.62	8.23	8.27	19.93	0.004356347
1981B	2,688.20	2,681.58	2,690.96	2,697.62	6.63	6.65	16.04	0.003502423
1981D	2,685.91	2,677.69	2,689.35	2,697.62	8.23	8.27	19.93	0.004356347
1989B	2,691.43	2,687.07	2,693.24	2,697.62	4.36	4.37	10.55	0.002298257
1990N	2,688.20	2,681.58	2,690.96	2,697.62	6.63	6.65	16.04	0.003502423
1994D	2,688.20	2,681.58	2,690.96	2,697.62	6.63	6.65	16.04	0.003502423
1994ae	2,683.72	2,673.96	2,687.80	2,697.62	9.76	9.81	23.66	0.005176915
1995al	2,680.75	2,668.92	2,685.70	2,697.62	11.84	11.91	28.70	0.006291019
1998aq	2,685.36	2,676.75	2,688.96	2,697.62	8.62	8.66	20.87	0.004563157
1998bu	2,691.43	2,687.07	2,693.24	2,697.62	4.36	4.37	10.55	0.002298257
2001el	2,688.23	2,681.62	2,690.98	2,697.62	6.61	6.63	16.00	0.003492416
2002fk	2,680.95	2,669.25	2,685.84	2,697.62	11.70	11.78	28.37	0.006217635
2003du	2,676.00	2,660.85	2,682.34	2,697.62	15.15	15.27	36.77	0.008078922
2005cf	2,677.57	2,663.53	2,683.46	2,697.62	14.05	14.16	34.09	0.007485178
2006dd	**2,685.91**	**2,677.69**	**2,689.35**	**2,697.62**	**8.23**	**8.27**	**19.93**	**0.004356347**
2007af	2,679.89	2,667.45	2,685.09	2,697.62	12.44	12.52	30.17	0.006614576
2007on	2,685.91	2,677.69	2,689.35	2,697.62	8.23	8.27	19.93	0.004356347
2007sr	2,682.39	2,671.69	2,686.86	2,697.62	10.70	10.76	25.93	0.005677261
2009ig	2,675.00	2,659.17	2,681.64	2,697.62	15.84	15.97	38.45	0.008452514
2011by	2,685.36	2,676.75	2,688.96	2,697.62	8.62	8.66	20.87	0.004563157
2011fe	2,693.53	2,690.65	2,694.73	2,697.62	2.88	2.89	6.97	0.001517717
2011iv	2,685.91	2,677.69	2,689.35	2,697.62	8.23	8.27	19.93	0.004356347
2012cg	2,688.20	2,681.58	2,690.96	2,697.62	6.63	6.65	16.04	0.003502423
2012fr	2,685.95	2,677.75	2,689.37	2,697.62	8.21	8.24	19.87	0.004343005
2012ht	2,684.66	2,675.55	2,688.46	2,697.62	9.11	9.15	22.07	0.004826672
2013dy	2,684.99	2,676.11	2,688.69	2,697.62	8.88	8.92	21.51	0.004703254
2015F	2,686.23	2,678.22	2,689.57	2,697.62	8.01	8.05	19.40	0.0042396

Table 1. Redshift distance D and the further redshift distances D_i and R_{jk} of all 27 SN Ia.

We have neglected here the part "mr,ε=(+1)" of indexes in all cases.

To interpret the distances from Table 1:

For a more detailed explanation, we take into account the SN Ia 2006dd, for example, and use it to interpret the meaning of the distances in the table.

The "light-travel time" always means the time interval between the emission of light (the time at that time $t_{e,2006dd}$) by the SN Ia 2006dd and today (t_0), i.e. $\Delta t_{2006dd} = t_0 - t_{e,2006dd}$. This light-travel time is generally different for all observable cosmic objects, here especially for the individual SN Ia 2006dd we will consider.

a) The today's (t_0) distance between the selected SN Ia 2006dd and us as observers is $D_{0,mr,\varepsilon=(+1)} \approx 8.27$ Mpc.
b) The distance at that time (t_e) between this SN Ia 2006dd and us as observers was $D_{e,mr,\varepsilon=(+1)} \approx 8.23$ Mpc.
According to this, the distance between the two cosmic objects has increased by about 0.04 Mpc during the light-travel time Δt_{2006dd}.
c) The SN Ia 2006dd has been shifted expansively away from the origin of the coordinates by $\Delta R_e = R_{0e} - R_{ee} \approx$ 11.66 Mpc during the light-travel time due to the time-dependent scale parameter a(t).
d) The galaxy with us as observers has been expansively shifted away from the origin of the coordinates by $\Delta R_a = R_{0a} - R_{ea} \approx 11.71$ Mpc during the light-travel time due to a(t).
The difference between the two displacement distances is of course the increase in the distance between the two cosmic objects noted above.
e) The real light path (redshift distance) covered by the photons within the interval of time Δt_{2006dd} is $D_{mr,mr,\varepsilon=(+1)} \approx 19.93$ Mpc. It is unequal to the other mentioned distances D_i and greater than these.

4.1.6 Evaluation of the data from the black hole in M87

For the sake of simplicity, we summarize the data taken from the specialist literature on the galaxy M87 containing a black hole (BH) in it in the first line of Table 2 {see [5] and [6]}.
The second line lists the data specified in this paper, which usually differ from those in the specialist literature.

	D [Mpc]	**M_B [mag]**	**z**	**m_B [mag]**	**Θ_{BH} [µas]**	**$\delta/2 = R_S$ [pc]**	**M_{BH} [g]**
literature	16.9 / 16.8	-23.5	0.004283	9.6	42		1.2928E+43
we	19.60	-21.860				1.995268E-03	4.1469E+43

Table 2. Summary of data from galaxy M87 containing a black hole in it.

The theory was adapted to the measured angle size Θ_{BH} given in the specialist literature. Overall, a larger redshift distance $D_{mr,\varepsilon=(+1)}$, a smaller absolute magnitude M_B and a little bigger value of mass M_{BH} of the black hole follow.

Table 3 lists the values found by means of our theory for all redshift distances R_{jk}, D_i and D, respectively.

[Mpc]	**R_{ea}**	**R_{ee}**	**R_{0e}**	**R_{0a}**	**D_e**	**D_0**	**D**
we	2,686.12	2,678.02	2,689.49	2,697.62	8.09	8.13	19.60
literature	---	---	---	---	---	---	16.8

Table 3. Redshift distances D_i, D and R_{jk} belonging to the black hole in M87.

From these values, the expansion-related shifts in distance of the galaxy M87 and of the galaxy with us as observers can be calculated, which took place during the time of light travel.

The theory from the specialist literature does not know the most distances listed in Table 3. Therefore, they cannot be calculated using this theory and not determined in terms of value.

The distance $D_{mr,\varepsilon=(+1)}$ differs because of the physical meaning: In our theory, $D_{mr,\varepsilon=(+1)}$ is the real physical light path, which is not the case in the astrophysical specialist literature.

We briefly interpret the meaning of the distances listed in Table 3, whereby the light-travel time is again defined as described in former chapter:

a) The today's (t_0) distance between the BH or the galaxy M87 and us as observers is $D_{0,mr,\varepsilon=(+1)} \approx 8.13$ Mpc.

b) The distance at that time (t_e) between the BH (or M87) and us as observers was $D_{e,mr,\varepsilon=(+1)} \approx 8.09$ Mpc.

Accordingly, the distance between the two cosmic objects has increased by about 0.04 Mpc during the light-travel time $\Delta t_{BH,M87} = t_0 - t_{e,BH,M87}$.

c) The BH (or M87) has been shifted expansively away from the origin of the coordinates by $\Delta R_e = R_{0e} - R_{ee} \approx 11.47$ Mpc during the light-travel time due to the time-dependent scale parameter a(t).

d) The galaxy with us as observer was expansively shifted away from the origin of the coordinates by $\Delta R_a = R_{0a} - R_{ea} \approx 11.50$ Mpc during the light-travel time due to a(t).

e) The real light path (redshift distance) covered by the photons during the interval of time $\Delta t_{BH,M87}$ is $D_{mr,\varepsilon=(+1)} \approx 19.60$ Mpc. It is unequal to the other mentioned distances D_i and greater than these.

Fig. 19 shows the various calculated distances in a clear form.

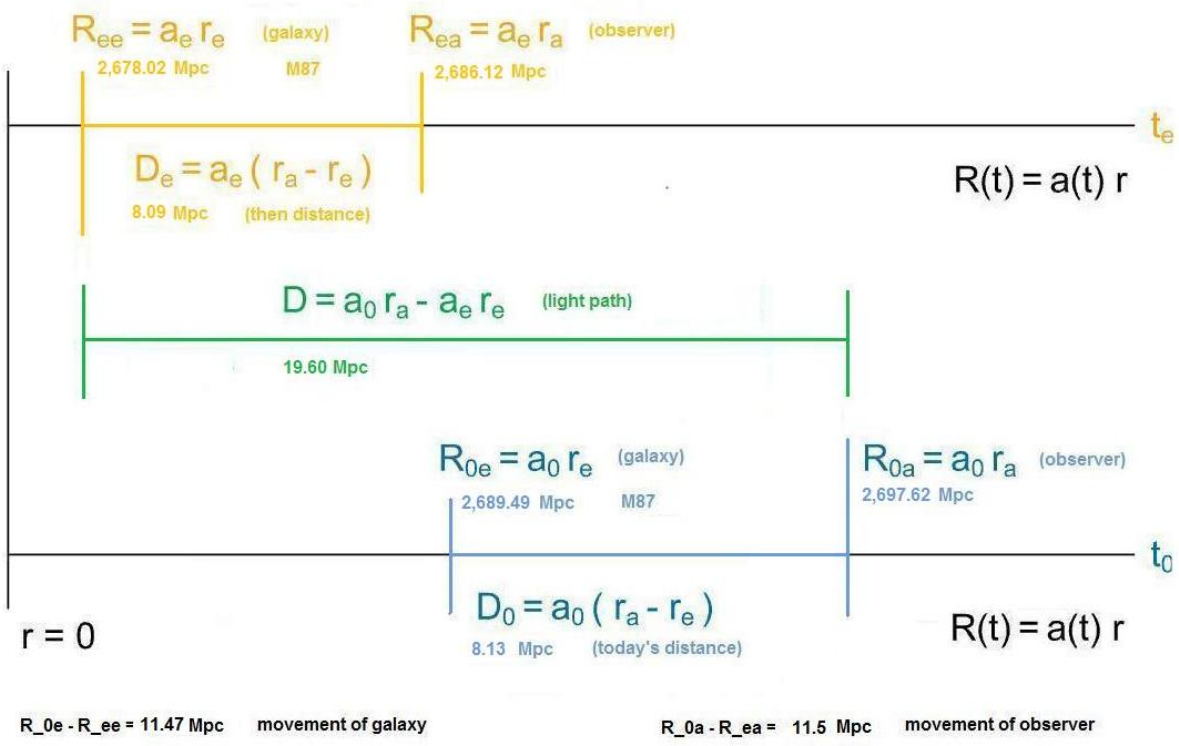

Figure 19. Visualization of the distances D_i, D and R_{jk} with regard to M87 and observer.

The distances are not drawn to scale here.

4.1.7 Maximum values known today: Galaxy UDFj-39546284 and Quasar J0313

The galaxy UDFj-39546284 [8] currently holds the record among the galaxies with a redshift of z = 10.3, while the quasar J0313 [7] with z = 7.642 holds the analog record among the quasars.

Table 4 shows all the corresponding distances R_{jk}, D_i and D together using Mpc as unit of measurement.

object name	z	D	D_0	D_e	R_{ee}	R_{0e}	R_{ea}	R_{0a}	object
J0313	7.642	2,616.77	1,998.96	231.31	80.84	698.66	312.15	2,697.62	quasar
UDFj-39546284	10.300	2,645.71	2,111.08	186.82	51.91	586.54	238.73	2,697.62	galaxy

Table 4. All calculated redshift distances R_{jk}, D_i and D for the two cosmic objects with the maximum redshifts and for us as observer.

Table 5 summarizes the spatial shifts of the two objects chosen and the observer with respect to the origin of coordinates due to the expansion during the associated light travel times.

object name	$R_{0e} - R_{ee}$	$R_{0a} - R_{ea}$	object
J0313	617.82	2,385.47	quasar
UDFj-39546284	534.63	2,458.89	galaxy

Table 5. Expansion-related shifts in the distance of the quasar and the galaxy and of the observer [Mpc].

We have already explained above how the tables have to be interpreted.

Fig. 20 shows the distances $D_{i,mr,\varepsilon=(+1)}$ and $D_{mr,\varepsilon=(+1)}$ of the three special astrophysical objects analyzed in this paper in one diagram, whereby we have entered all numerical values for the distances in Mpc.

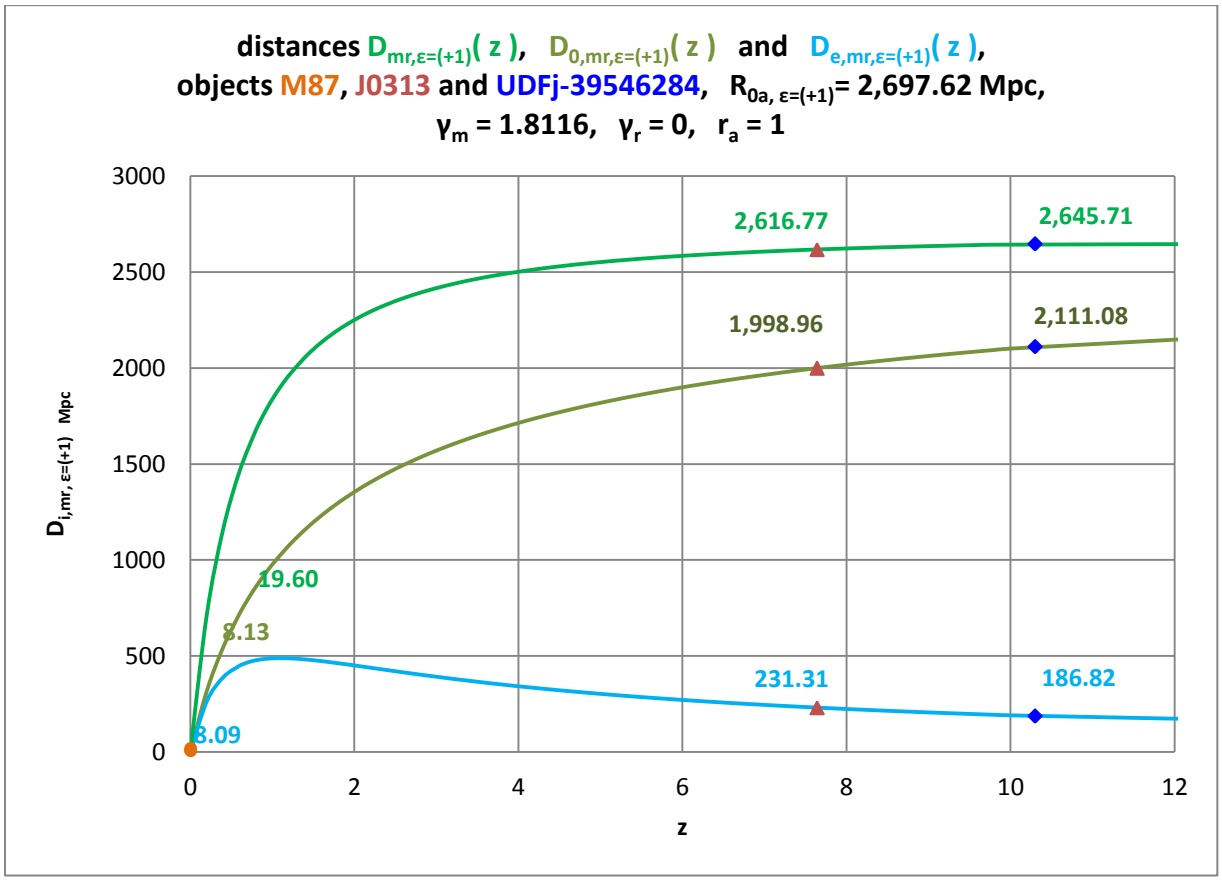

Figure 20. All distances $D_{i,mr,\varepsilon=(+1)}$ and $D_{mr,\varepsilon=(+1)}$ for M87, J0313 and UDFj-39546284.

The middle curve shows the today's distances $D_{0,mr,\varepsilon=(+1)}$ of the three objects from us as observers. These distances are clearly shorter than the associated light paths $D_{mr,\varepsilon=(+1)}$ of these objects.

4.2 $\varepsilon = (-1)$

4.2.1 Magnitude-redshift relation

The apparent magnitude m depends according to Eq. (56) in addition to the measurable redshift z also on the four parameters $m_{0a,\varepsilon=(-1)}$, γ_a, γ_m and γ_r.

To analyze the quasar catalog by Véron-Cetty et al. [1] we use the same redshift intervals with mean values of the redshifts and the corresponding mean values for the apparent magnitude how this was done in chapter with ε = (+1).

We use the same χ^2-function Eq. (78) for the evaluation of the measurement values.
The introduced abbreviation p_k with k = 1, 2, 3, 4 stands here for the four parameters we are looking for, $m_{0a,\varepsilon=(-1)}$, γ_a, γ_m and γ_r.

Using our magnitude-redshift relation (56), the χ^2-function looks concrete

$$\chi^2\left(z; m_{0a,\varepsilon=(-1)}, \gamma_a, \gamma_m, \gamma_r\right) = \frac{1}{(N-1)} \sum_{i=1}^{N} \left\{ X_i + m_{0a,\varepsilon=(-1)} - m_{obs,i} \right\}^2$$

with

$$X_i = 5 \log_{10} \left\{ 1 - \frac{1}{(1+z)} \left\{ 1 - \gamma_a \ln \left\{ \frac{\left[\left(1 + \frac{\gamma_m}{2} \right) + \sqrt{1 + \gamma_m + \gamma_r} \right]}{\left\{ \left[\frac{1}{(1+z)} + \frac{\gamma_m}{2} \right] + \sqrt{\frac{1}{(1+z)} \left[\frac{1}{(1+z)} + \gamma_m \right] + \gamma_r} \right\}} \right\} \right\} \right\} \tag{85}$$

and $z = z_i$.

Using again the quasar data and the usual mathematical procedure, we find the parameters to be $m_{0a,\varepsilon=(-1)}$ = 20.17575, γ_m = 0.160004 and r_a = 2.8225. We have specialized our analysis to γ_r = 0 because the radiation density plays obvious no role today.

Fig. 21 shows the result of the mean value formation and the adaptation of our theory to the curvature of the mean value curve.

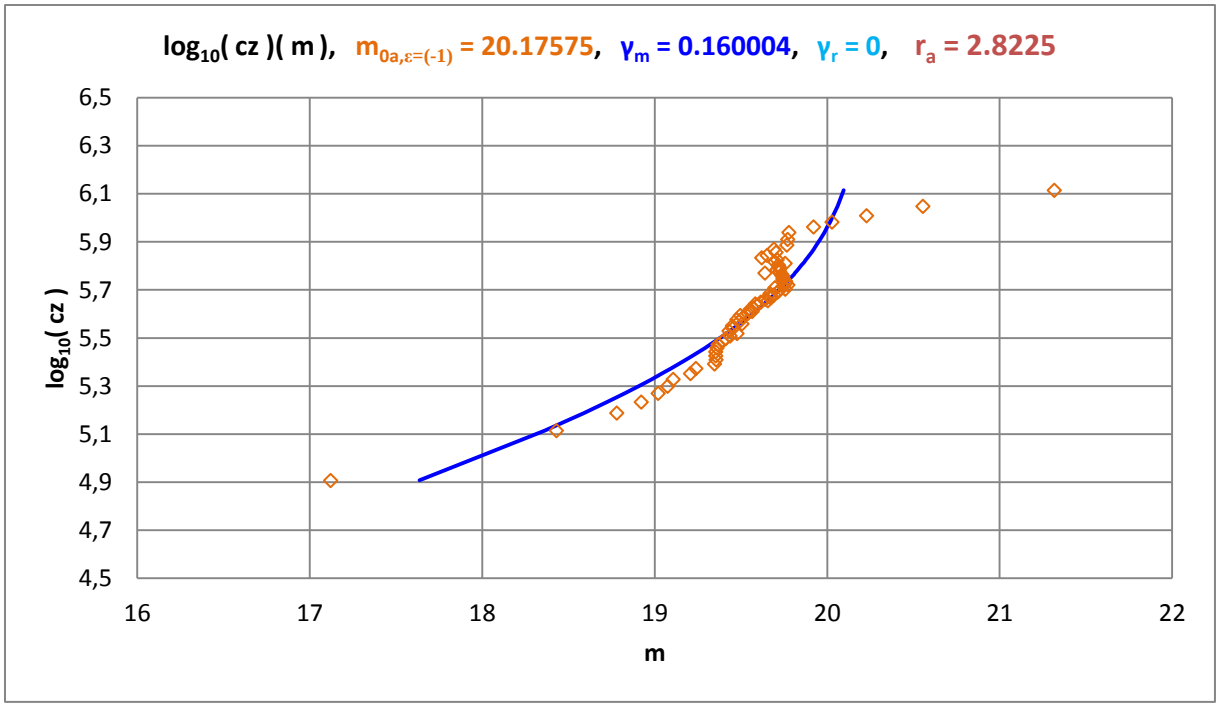

Figure 21. Magnitude-redshift diagram for 132,975 quasars according to M.-P. Véron-Cetty et al. [1].

We have given a possible interpretation of the measured magnitude-redshift relation in the chapter with ε = (+1).

4.2.2 Number-redshift relation

We use here also Eq. (79) to evaluate the number-redshift relation.

The introduced abbreviation p_k with k = 1, 2, 3, 4 stands here for the four parameters we are looking for, $N_{0a,\varepsilon=(-1)}$, γ_a, γ_m and γ_r.

If we insert our number-redshift relation (60), the Eq. (79) reads here concrete

$$\chi^2\left(z; N_{0a,\varepsilon=(-1)}, \gamma_a, \gamma_m, \gamma_r\right) = \frac{1}{(N-1)} \sum_{i=1}^{N} \left\{X_i - N_{obs,i}\right\}^2 \quad .$$

with

$$X_i = N_{0a,\varepsilon=(-1)} \left\{1 - \frac{1}{(1+z)} \left\{1 - \gamma_a \ln \left\{ \frac{\left[\left(1+\frac{\gamma_m}{2}\right) + \sqrt{1+\gamma_m+\gamma_r}\right]}{\left\{\left[\frac{1}{(1+z)} + \frac{\gamma_m}{2}\right] + \sqrt{\frac{1}{(1+z)}\left[\frac{1}{(1+z)} + \gamma_m\right] + \gamma_r}\right\}} \right\}\right\}\right\}^3 \qquad (86)$$

and $z = z_i$.

Using this simple χ^2-function, we find $N_{0a,\varepsilon=(-1)}$ = 121,138 for the theoretically expected total number of quasars, if we use the value γ_m = 0.160004 found via the magnitude-redshift relation. Furthermore we have used γ_r = 0 and r_a = 2.8225.

The expected number $N_{0a,\varepsilon=(-1)}$ = 121,138 is slightly smaller than the number of quasars measured and listed within the catalogue of M.-P. Véron-Cetty et al. [1].
May be that the reason for this is the use of the simple Eq. (59) for the flat volume during the derivation of the number-redshift relation.

Fig. 22 shows the graphic result.

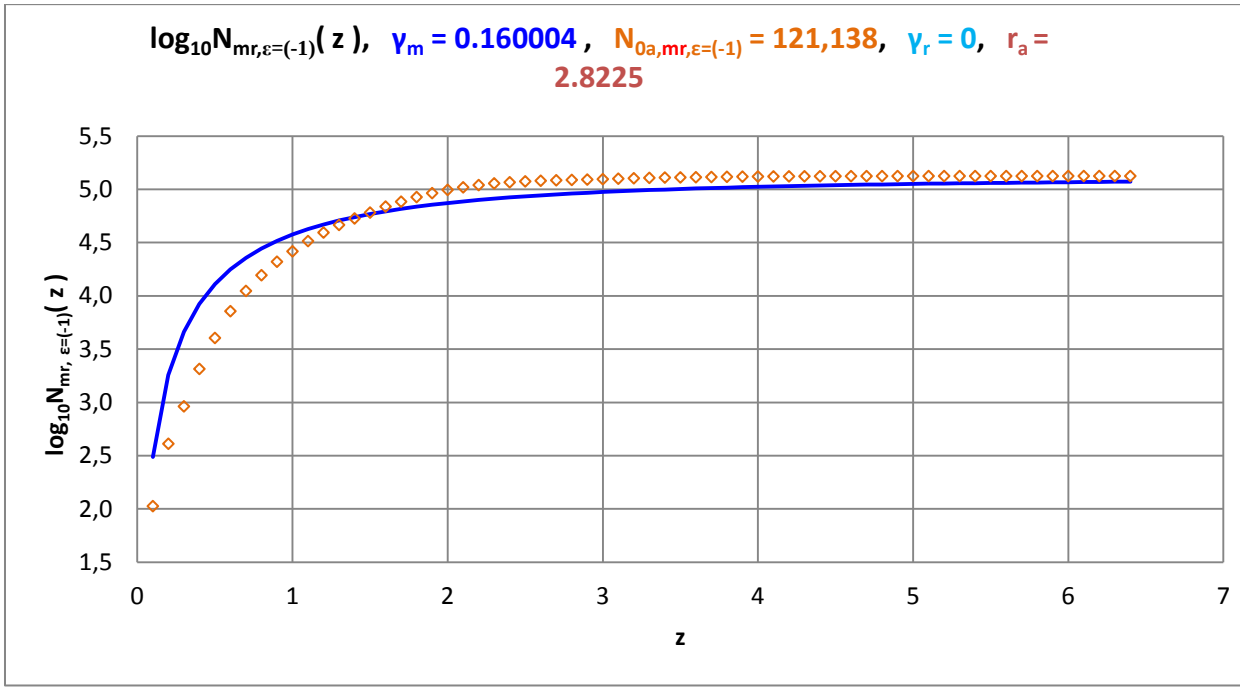

Figure 22. Number-redshift diagram for the 132,975 quasars according to M.-P. Véron-Cetty et al. [1].

4.2.3 Angular size-redshift relation

We use here also the measurement data from K. Nilsson et al. [2] to find an average linear size of the cosmic objects measured there.

The starting point is here also the Eq. (80).
The introduced abbreviation p_k with k = 1, 2, 3, 4 stands now for the four parameters we are looking for, $\delta_{\varepsilon=(-1)}/R_{0a,\varepsilon=(-1)}$, γ_a, γ_m and γ_r.

If we use our angular size-redshift relation (58), the Eq. (80) reads concrete (setting γ_r = 0)

$$\chi_{\varphi}^{\,2}\left(z;\delta_{\varepsilon=(-1)}/R_{0a,\varepsilon=(-1)},\gamma_a,\gamma_m\right)=\frac{1}{(N-1)}\sum_{i=1}^{N}\left\{\frac{\delta_{\varepsilon=(-1)}}{R_{0a,\varepsilon=(-1)}}X_i-\varphi_{obs,i}\right\}^2$$

with

$$X_i=\frac{1}{\left\{1-\frac{1}{(1+z)}\left\{1-\gamma_a\ln\left\{\frac{\left[\left(1+\frac{\gamma_m}{2}\right)+\sqrt{1+\gamma_m+\gamma_r}\right]}{\left\{\left[\frac{1}{(1+z)}+\frac{\gamma_m}{2}\right]+\sqrt{\frac{1}{(1+z)}\left[\frac{1}{(1+z)}+\gamma_m\right]+\gamma_r}\right\}}\right\}\right\}\right\}} \qquad (87)$$

and $z=z_i$.

The comparison of the theory with the measurement data using γ_m = 0.160004, γ_r = 0 and r_a = 2.8225 results in a value of $\delta_{\varepsilon=(-1)}/R_{0a,\varepsilon=(-1)}$ = 5.7488 x 10^{-5}.

Fig. 23 shows the graphic result.

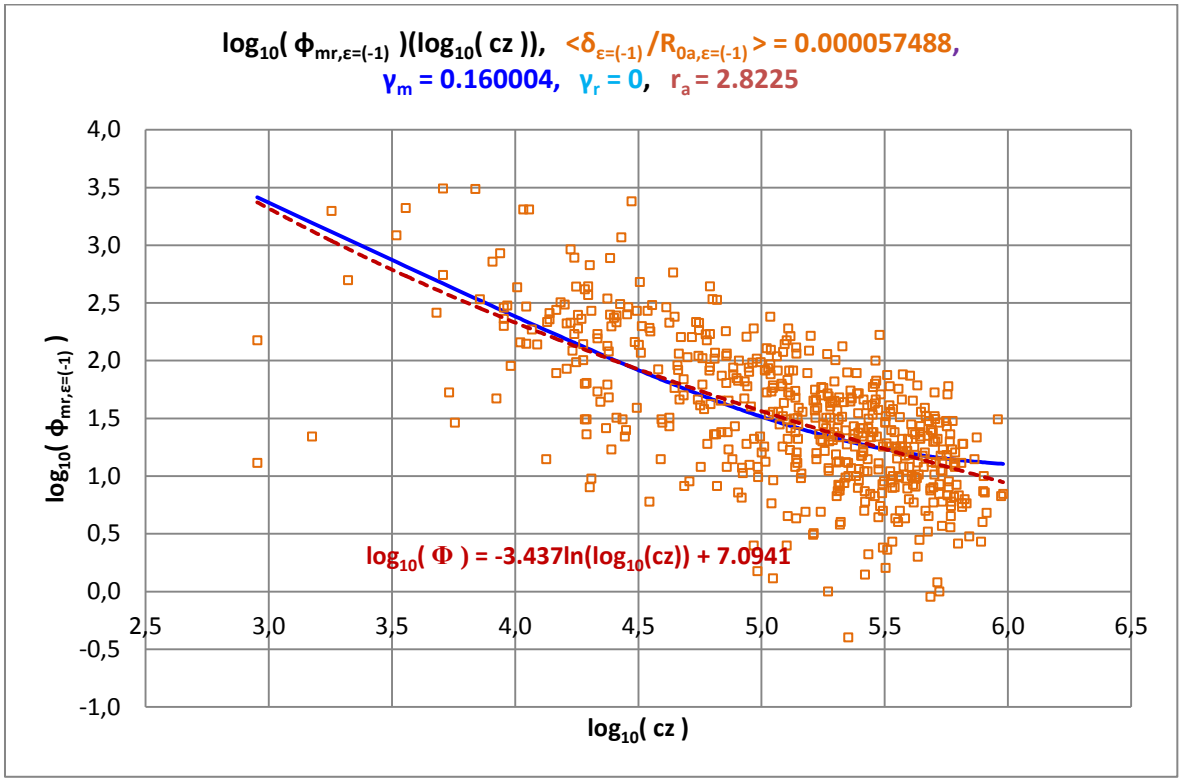

Figure 23. Angular size-redshift diagram according to K. Nilsson et al. [2].

The determination of the linear size $\delta_{\varepsilon=(-1)}$ requires the knowledge of $R_{0a,\varepsilon=(-1)}$. Because the absolute magnitudes are known for some SN Ia, we can determine $R_{0a,\varepsilon=(-1)}$ using a magnitude-redshift diagram of these cosmic objects. We will do that in the next chapter.

4.2.4 Fixing of $R_{0a,\varepsilon=(-1)}$ with the help of SN Ia

Here we use also the data given by W. L. Freedman et al. [3] for our analysis. The goal is to find the values of distance $R_{0a,\varepsilon=(-1)}$ and the today's Hubble parameter $H_{0a,mr,\varepsilon=(-1)}$.

The simple equation used for this task is

$$R_{0a,\varepsilon=(-1)} = 10^{\frac{\left(m_{0a,\varepsilon=(-1)} - M\right)}{5}+1} \quad . \tag{88}$$

The graphic result is shown in Fig. 24.

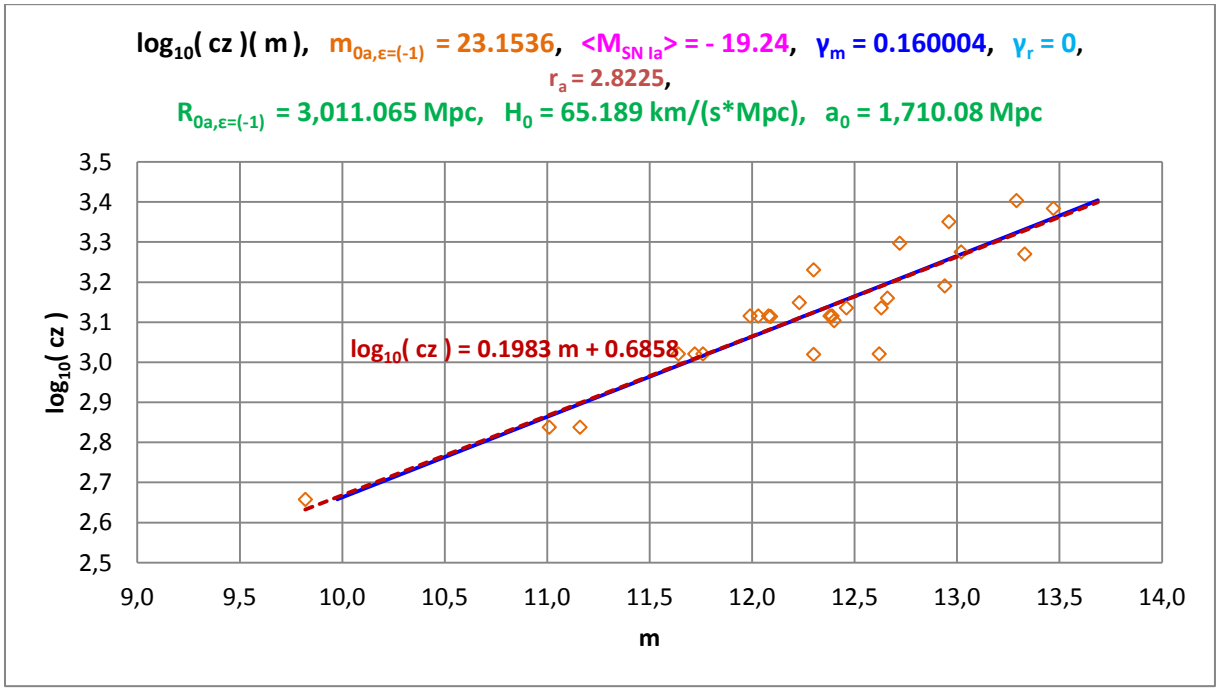

Figure 24. Magnitude-redshift diagram for 27 SN Ia according to W. L. Freedman et al. [3].

The theoretical curve (blue) lies exactly on the linear trend line (dashed in red) with the equation given in the figure.

Finding $m_{0a,\varepsilon=(-1)} \approx 23.1536$ and using the mean value of the absolute brightness <M> = -19.24, the distance $R_{0a,\varepsilon=(-1)} \approx$ 3,011.065 Mpc we are ultimately looking for is the essential result of this data analysis.
We get furthermore $a_0 \approx 1{,}710.08$ Mpc. This value can be calculated with Eq. (49) using $R_{0a,\varepsilon=(-1)}$ and γ_a found.

With the help of the value of $R_{0a,\varepsilon=(-1)}$ and taking the Eq. (51), which is an approximation for small redshifts, the today's Hubble parameter $H_{0a,m,\varepsilon=(-1)} \approx 65.189$ km/(s·Mpc) results, if we neglect the radiation density how before also. This value is slightly below the Planck value (2018) with $H_{0,Planck} \approx 67.66$ km/(s·Mpc) [4].

With the help of Eq. (82) we can calculate the today's matter density $\rho_{0m,\varepsilon=(-1)}$.

Using the parameters γ_m and $R_{0a,\varepsilon=(-1)}$ determined by us, we find $\rho_{0m,\varepsilon=(-1)} \approx 9.24 \times 10^{-32}$ g/cm^3 for today's matter density inside the open universe with $\varepsilon = (-1)$.

Via Eq. (84) the constant mass of the Friedmann sphere - so called by us - results in $M_{Fs,\varepsilon=(-1)} \approx 3.10 \times 10^{53}$ g.

With the known value $R_{0a,\varepsilon=(-1)} \approx 3{,}011.06$ Mpc we can calculate the mean linear size of the Nilsson objects [2] to be $\delta_{\varepsilon=(-1)} \approx 0.1731$ Mpc, because we have found $\delta_{\varepsilon=(-1)}/R_{0a,\varepsilon=(-1)} = 5.7488 \times 10^{-5}$ for them.
Using known $R_{0a,\varepsilon=(-1)}$ and γ_m, of course, all linear dimensions of these objects can be calculated using their angular size and redshift if they could be measured.

4.2.5 Calculation of the further redshift distance for SN Ia

Because we were able to determine $R_{0a,\varepsilon=(-1)}$, we can graphically display the further redshift distances $D_{e,mr,\varepsilon=(-1)}$, $D_{0,mr,\varepsilon=(-1)}$ and $D_{mr,\varepsilon=(-1)}$ in a form, which is not normalized to $R_{0a,\varepsilon=(-1)}$. The result is shown in Fig. 25, using the values we found for our parameters γ_a, γ_m and $R_{0a,\varepsilon=(-1)}$ and setting $\gamma_r = 0$.

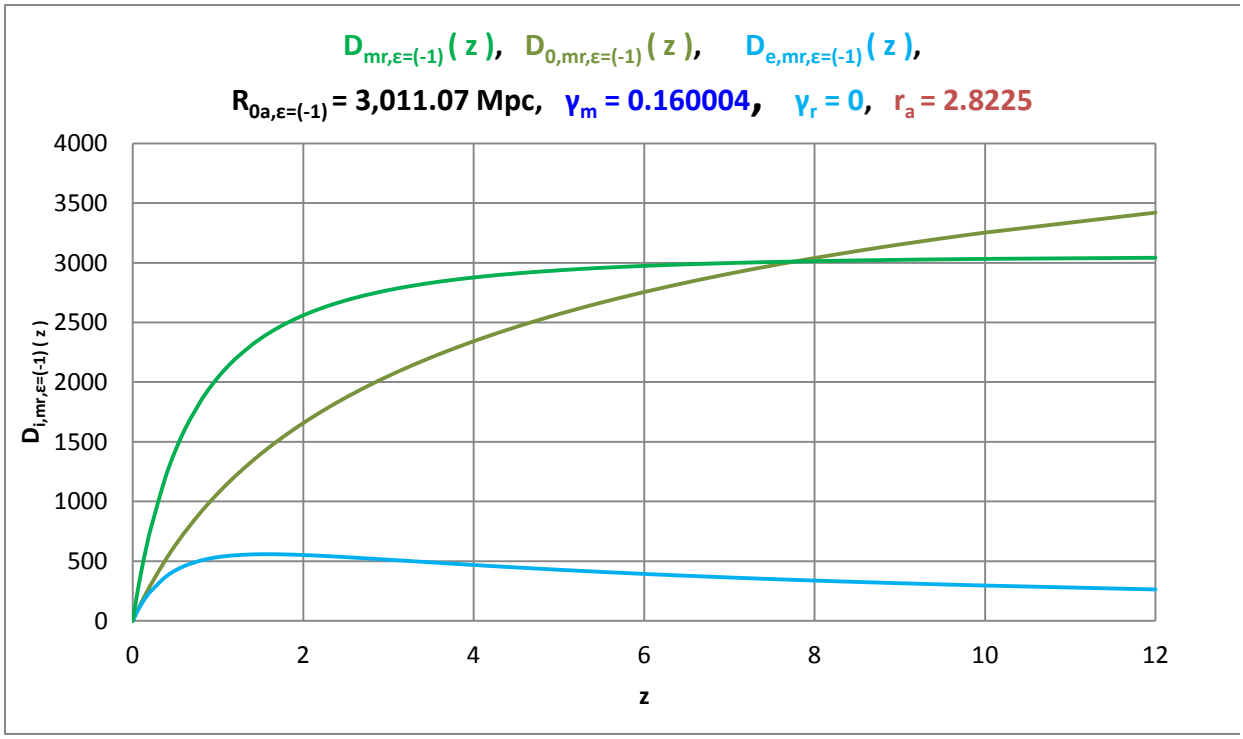

Figure 25. Redshift distance $D_{mr,\varepsilon=(-1)}$ (real light path) and the two further redshift distances $D_{e,mr,\varepsilon=(-1)}$ and $D_{0,mr,\varepsilon=(-1)}$ as a function of the redshift up to z = 12.

To interpret Fig. 25:

a) For $D_{mr,\varepsilon=(-1)}$, going to $R_{0a,\varepsilon=(-1)}$ the redshift z goes towards infinity. This means that no observer can observe objects for which is $D_{mr,\varepsilon=(-1)} > R_{0a,\varepsilon=(-1)} \approx 3{,}011.07$ Mpc.

b) The light path distance $D_{mr,\varepsilon=(-1)}$ can for bigger redshifts be smaller than the today's distances $D_{0,mr,\varepsilon=(-1)}$.

d) The distance at that time $D_{e,mr,\varepsilon=(-1)}$ is interesting: It shows a maximum for a specific redshift and approaches zero for very large redshifts.

Table 6 summarizes all calculated redshift distances of the 27 SN Ia used by us.

SN Ia	$D_{e,mr,\varepsilon=(-1)}$	$D_{0,mr,\varepsilon=(-1)}$	$D_{mr,\varepsilon=(-1)}$	z
1980N	6.87	6.90	19.93	0.00435635
1981B	5.53	5.55	16.04	0.00350242
1981D	6.87	6.90	19.93	0.00435635
1989B	3.64	3.64	10.54	0.00229826
1990N	5.53	5.55	16.04	0.00350242
1994D	5.53	5.55	16.04	0.00350242
1994ae	8.15	8.20	23.66	0.00517692
1995al	9.89	9.96	28.72	0.00629102
1998aq	7.19	7.23	20.87	0.00456316
1998bu	3.64	3.64	10.54	0.00229826

2001el	5.52	5.53	15.99	0.00349242
2002fk	9.78	9.84	28.38	0.00621764
2003du	12.67	12.77	36.80	0.00807892
2005cf	11.75	11.84	34.12	0.00748518
2006dd	**6.87**	**6.90**	**19.93**	**0.00435635**
2007af	10.40	10.47	30.18	0.00661458
2007on	6.87	6.90	19.93	0.00435635
2007sr	8.94	8.99	25.93	0.00567726
2009ig	13.25	13.36	38.49	0.00845251
2011by	7.19	7.23	20.87	0.00456316
2011fe	2.40	2.41	6.97	0.00151772
2011iv	6.87	6.90	19.93	0.00435635
2012cg	5.53	5.55	16.04	0.00350242
2012fr	6.85	6.88	19.87	0.00434301
2012ht	7.61	7.64	22.07	0.00482667
2013dy	7.41	7.45	21.51	0.00470325
2015F	6.69	6.72	19.40	0.0042396

Table 6. Redshift distance $D_{mr,\varepsilon=(-1)}$ and the further redshift distances $D_{e,mr,\varepsilon=(-1)}$ and $D_{o,mr,\varepsilon=(-1)}$ of all 27 SN Ia.

To interpret the distances from Table 6:

For a more detailed explanation, we take into account the SN Ia 2006dd, for example, and use it to interpret the meaning of the distances in the table.

The "light-travel time" always means here also the time interval between the emission of light (the time at that time $t_{e,2006dd}$) by the SN Ia 2006dd and today (t_0), i.e. $\Delta t_{2006dd} = t_0 - t_{e,2006dd}$. This light-travel time is generally different for all observable cosmic objects, here especially for the individual SN Ia 2006dd we will consider.

a) The today's (t_0) distance between the selected SN Ia 2006dd and us as observers is $D_{0,mr,\varepsilon=(-1)} \approx 6.90$ Mpc.
b) The distance at that time (t_e) between this SN Ia 2006dd and us as observers was $D_{e,mr,\varepsilon=(-1)} \approx 6.87$ Mpc.
According to this, the distance between the two cosmic objects has increased by about 0.03 Mpc during the light-travel time Δt_{2006dd}.
c) The real light path (redshift distance) covered by the photons within the interval of time Δt_{2006dd} is $D_{mr,mr,\varepsilon=(-1)} \approx 19.93$ Mpc. It is unequal to the other mentioned distances D_i and greater than these.

4.2.6 Evaluation of the data from the black hole in M87

For the sake of simplicity, we summarize the data taken from the specialist literature on the galaxy M87 containing a black hole (BH) in it in the first line of Table 7 {see [5] and [6]}.
The second line lists the data specified in this paper, which usually differ from those in the literature.

	D [Mpc]	**M_B [mag]**	**z**	**m_B [mag]**	**Θ_{BH} [µas]**	**$\delta/2 = R_S$ [pc]**	**M_{BH} [g]**
literature	16.9 / 16.8	-23.5	0.004283	9.6	42		1.2928E+43
we	19.60	-21.861				1.995223E-03	4.1468E+43

Table 7. Summary of data from galaxy M87 containing a black hole in it.

The theory was adapted to the measured angle size Θ_{BH} given in the specialist literature. Overall, a larger redshift distance $D_{mr,\varepsilon=(-1)}$, a smaller absolute magnitude M_B and a similar value of mass M_{BH} of the black hole follow.

Table 8 lists the values found by means of our theory for all redshift distances R_{jk}, D_i and D, respectively.

[Mpc]	$D_{e,mr,\varepsilon=(-1)}$	$D_{0,mr,\varepsilon=(-1)}$	$D_{mr,\varepsilon=(-1)}$
we	6.76	6.78	19.60
literature	---	---	16.8

Table 8. Redshift distances $D_{e,mr,\varepsilon=(-1)}$, $D_{0,mr,\varepsilon=(-1)}$ and $D_{mr,\varepsilon=(-1)}$ belonging to the black hole in M87.

The theory from the specialist literature does not know two of the distances listed in Table 8. Therefore, they cannot be calculated using this theory and not determined in terms of value.

The distance $D_{mr,\varepsilon=(-1)}$ differs because of the physical meaning: In our theory, $D_{mr,\varepsilon=(-1)}$ is the real physical light path, which is not the case in the astrophysical specialist literature.

We briefly interpret the meaning of the distances listed in Table 8, whereby the light-travel time is again defined as described in a former chapter:
a) The today's (t_0) distance between the BH or the galaxy M87 and us as observers is $D_{0,mr,\varepsilon=(-1)} \approx 6.78$ Mpc.
b) The distance at that time (t_e) between the BH (or M87) and us as observers was $D_{e,mr,\varepsilon=(-1)} \approx 6.76$ Mpc.
Accordingly, the distance between the two cosmic objects has increased by about 0.02 Mpc during the light-travel time $\Delta t_{BH,M87} = t_0 - t_{e,BH,M87}$.
c) The real light path (redshift distance) covered by the photons during the interval of time $\Delta t_{BH,M87}$ is $D_{mr,\varepsilon=(-1)} \approx 19.60$ Mpc. It is unequal to the other mentioned distances D_i and greater than these.

4.2.7 Maximum values known today: Galaxy UDFj-39546284 and Quasar J0313

Similar to the chapter ε = (+1) the table 9 shows the resulting distances $D_{e,mr,\varepsilon=(-1)}$, $D_{0,mr,\varepsilon=(-1)}$ and $D_{mr,\varepsilon=(-1)}$ (in Mpc) belonging to the two cosmic objects J0313 and UDFj-39546284.

object name	z	$D_{mr,\varepsilon=(-1)}$	$D_{0,mr,\varepsilon=(-1)}$	$D_{e,mr,\varepsilon=(-1)}$	object
J0313	7.642	3,009.20	2,994.94	346.56	quasar
UDFj-39546284	10.300	3,034.90	3,280,36	290.30	galaxy

Table 9. Redshift distances $D_{e,mr,\varepsilon=(-1)}$, $D_{0,mr,\varepsilon=(-1)}$ and $D_{mr,\varepsilon=(-1)}$ of the two cosmic objects with the maximum redshifts.

We have already explained above how the tables have to be interpreted.

Fig. 26 shows the distances $D_{e,mr,\varepsilon=(-1)}$, $D_{0,mr,\varepsilon=(-1)}$ and $D_{mr,\varepsilon=(-1)}$ of the three special astrophysical objects analyzed in this paper in one diagram, whereby we have entered all numerical values for the distances in Mpc.

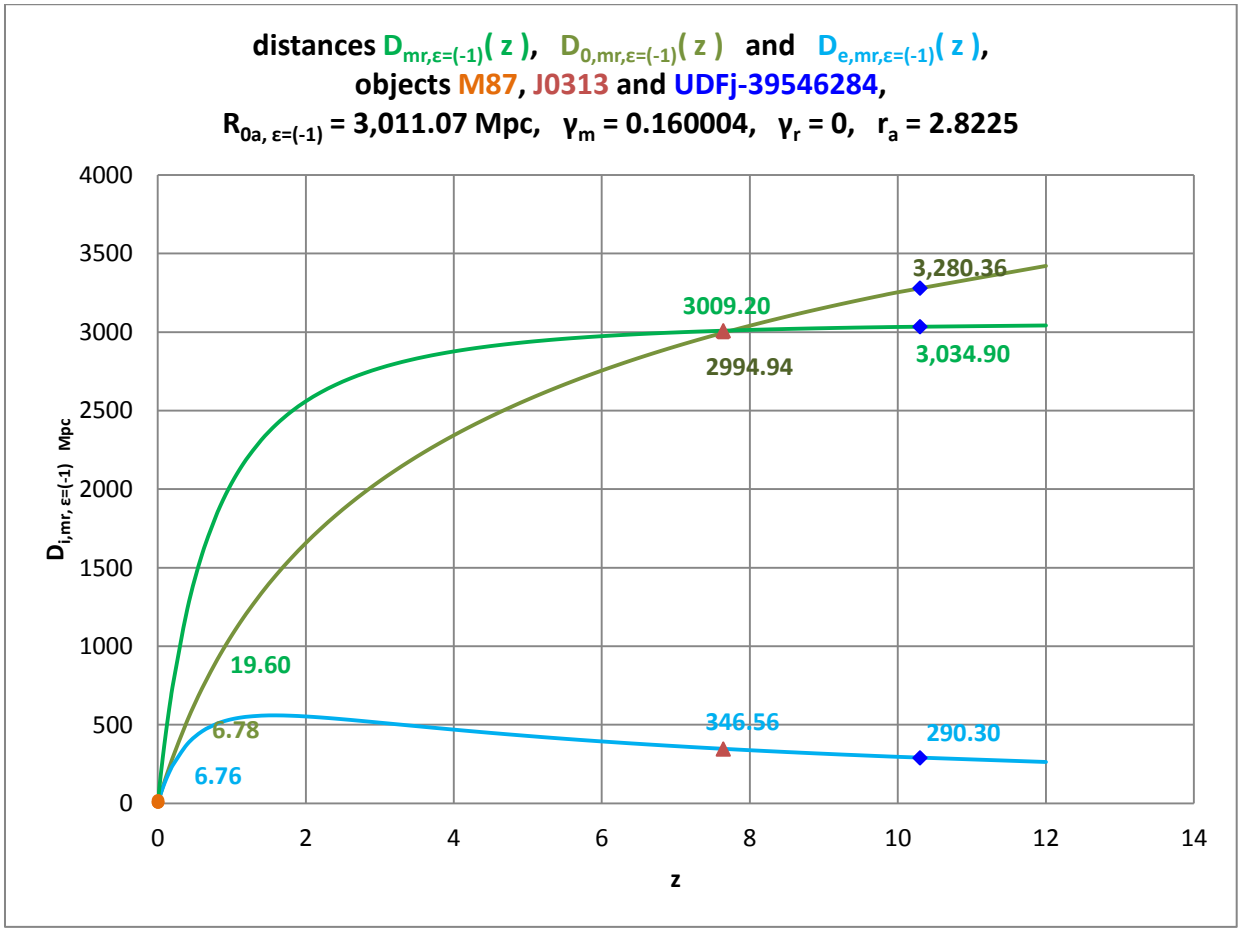

Figure 26. Redshift distances $D_{e,mr,\varepsilon=(-1)}$, $D_{0,mr,\varepsilon=(-1)}$ and $D_{mr,\varepsilon=(-1)}$ for M87, J0313 and UDFj-39546284.

The middle (beginning left) curve shows the today's distances $D_{0,mr,\varepsilon=(-1)}$ of the three objects from us as observers.

We see that this today's distance $D_{0,mr,\varepsilon=(-1)}$ can be clearly larger than the associated light path $D_{mr,\varepsilon=(-1)}$ of the cosmic objects. This effect concerns in our case here the galaxy UDFj-39546284 with z = 10.300.
The data of the quasar J0313 with z = 7.642 show that the light-way distance $D_{mr,\varepsilon=(+1)}$ = 3,009.20 is only a little bigger as the today's distance $D_{0,mr,\varepsilon=(-1)}$ = 2,994.94.

5. Hubble parameter again

In this chapter, we discuss only on the case of the closed universe with ε = (+1). The other possible case with ε = (-1) can treated similar.

At this point we explicitly point out that our equation of today's Hubble parameter - which also only applies to very small redshifts - differs significantly from the definition (!) used in the specialist literature. The equations for both are

$$H_{0a,mr,\varepsilon=(+1)}\left(R_{0a,\varepsilon=(+1)},\gamma_a,\gamma_m,\gamma_r\right)\approx\frac{c_0}{R_{0a,\varepsilon=(+1)}\left(1+\frac{\gamma_a}{\sqrt{\gamma_r+\gamma_m-1}}\right)}\qquad(we)$$

and

$$H_{0a,lit}=\frac{\dot{a}_0}{a_0}=\frac{\dot{a}_0\chi_{a,\varepsilon=(+1)}}{a_0\chi_{a,\varepsilon=(+1)}}=\frac{\dot{R}_{0a,\varepsilon=(+1)}}{R_{0a,\varepsilon=(+1)}}\qquad\chi_{a,\varepsilon=(+1)}=const\qquad(literature)\quad.\tag{89}$$

For an arbitrary point in time t this reads

$$H_{a,mr,\varepsilon=(+1)}(t)\approx\frac{c_0}{a(t)\chi_{a,\varepsilon=(+1)}\left(1+\frac{\gamma_a}{\sqrt{\gamma_r+\gamma_m-1}}\right)}\qquad(we)$$

$$H_{a,lit}(t)=\frac{\dot{a}(t)}{a(t)}\frac{\chi_{a,\varepsilon=(+1)}}{\chi_{a,\varepsilon=(+1)}}\qquad(literature)\quad.\tag{89a}$$

The index a generally indicates the spatial proximity to the observer, meaning $\chi = \chi_{a,\varepsilon=(+1)} = \arcsin(r_a)$.

In our theory, the numerator contains the constant physical speed of light c_0 in vacuum, while the current, i.e. the variable spatial expansion speed da/dt is found at this place in the specialist literature.

In a more recent past - time t_x - our distance from the origin of coordinats $R_{xa,\varepsilon=(+1)} < R_{0a,\varepsilon=(+1)}$ was slightly smaller than the current one and the Hubble parameter H_{xa} was therefore correspondingly larger.

Furthermore, in the case of the Hubble parameter in specialist literature, the - actually non-physical - spatial expansion speed da/dt can have been arbitrarily large in the past and, in addition, the scale parameter a(t) arbitrarily small.
Both types of Hubble parameters therefore show a completely different behavior!

In addition, our Hubble parameter is actually made up of physical quantities, while the Hubble parameter in the astrophysical literature is only defined using the non-physical scale parameter a(t), although to the latter can be assigned a suitable unit of measurement - e.g. Mpc. This means that a(t) alone per se is not a physical distance. This meaning only applies to the real physical distance $R(t)_{a,\varepsilon=(+1)} = a(t)\chi_{a,\varepsilon=(+1)}$ and the differences that can be calculated from it.

The Hubble parameter is the proportionality factor between the so called Hubble speed $V = c_0 z$ and a distance, i.e. the actual Hubble law applies

$$V = c_0 z = H_{0a,mr,\varepsilon=(+1)} D_{\varepsilon=(+1),Hubble} \approx \frac{c_0}{R_{0a,\varepsilon=(+1)}\left(1+\frac{\gamma_a}{\sqrt{\gamma_r+\gamma_m-1}}\right)} D_{\varepsilon=(+1),Hubble} \qquad (we)$$

and

$$V_{lit} = c_0 z = H_{0a,lit} D_{lit,Hubble} = \frac{\dot{a}_0}{a_0} D_{lit,Hubble} = \frac{\dot{R}_{0a,\varepsilon=(+1)}}{R_{0a,\varepsilon=(+1)}} D_{lit,Hubble} \qquad (literature) \quad . \tag{90}$$

For the redshift z it simply follows therefore

$$z = \frac{H_{0a,\varepsilon=(+1)}}{c_0} D_{\varepsilon=(+1),Hubble} \approx \frac{1}{\left(1+\frac{\gamma_a}{\sqrt{\gamma_r+\gamma_m-1}}\right)} \frac{D_{\varepsilon=(+1),Hubble}}{R_{0a,\varepsilon=(+1)}} \qquad (we)$$

and

$$z = \frac{H_{0a,lit}}{c_0} D_{lit,Hubble} = \frac{\dot{a}_0}{c_0} \frac{D_{lit,Hubble}}{a_0} = \frac{\dot{R}_{0a,\varepsilon=(+1)}}{c_0} \frac{D_{lit,Hubble}}{R_{0a,\varepsilon=(+1)}} \qquad (literature) \quad . \tag{91}$$

In the specialist literature, the redshift z is therefore depending on the ratio of the current speed of the observer (his galaxy) related to an origin of the coordinates to the speed of light in the product with the ratio of an object distance $D_{lit,Hubble}$ and the current distance of the observer's galaxy from an origin of the coordinates.

Our redshift, on the other hand, is depending on the ratio of the light path distance $D_{\varepsilon=(+1),Hubble}$ and the current distance $R_{0a,\varepsilon=(+1)}$ of the observer galaxy from an origin of the coordinates and is besides proportional to the factor that contains the parameters γ_a, γ_m and γ_r.

Overall, it is somewhat unclear in the specialist literature what exactly corresponds to the distance $D_{lit,Hubble}$.

Note:

Of course, it can be set $\gamma_r = 0$ in equations (89) to (91) in case of neglecting the radiation matter.

Fig. 27 shows the difference between our non-approximated redshift distance $D_{mr,\varepsilon=(+1)}$ and the linear Hubble redshift distance $D_{\varepsilon=(+1),Hubble}$ [compare Eq. (26)] that is an approximated one.

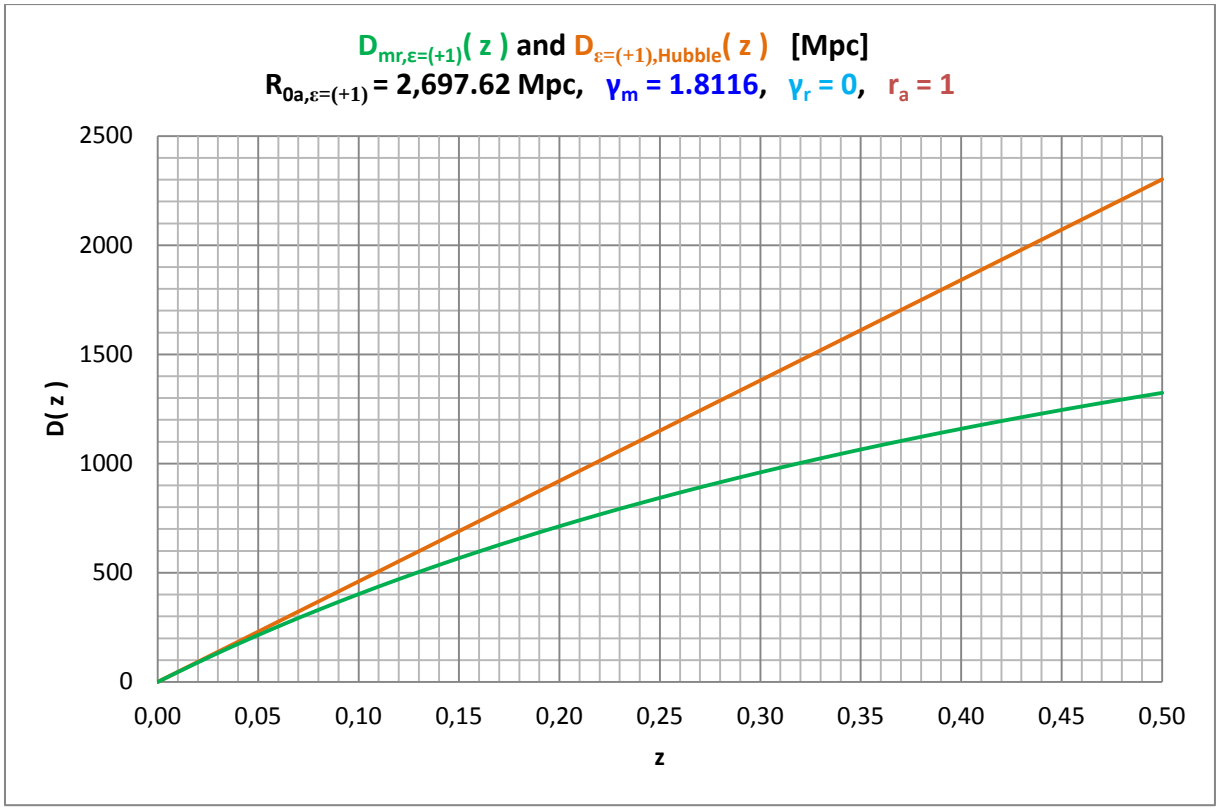

Figure 27. Non-approximated redshift distance $D_{mr,\varepsilon=(+1)}$ compared to the linear Hubble redshift distance $D_{\varepsilon=(+1),Hubble}$.

It can be seen that the two curves already clearly separate from each other at $z \approx 0.025$, and that Hubble's law results in distances $D_{\varepsilon=(+1),Hubble}$ that are significantly too large for larger redshifts, so that it is no longer applicable from around this value.

Recall:

Of course, it should be noted that the Hubble parameter $H_{0a,\varepsilon=(+1)}$ in our theory results from an approximation for small redshifts z.

6. Concluding remarks

The Fig. 28 summarizes all three possible redshift distances, which we have calculated in this paper and in paper [12], respectively, in one diagram.

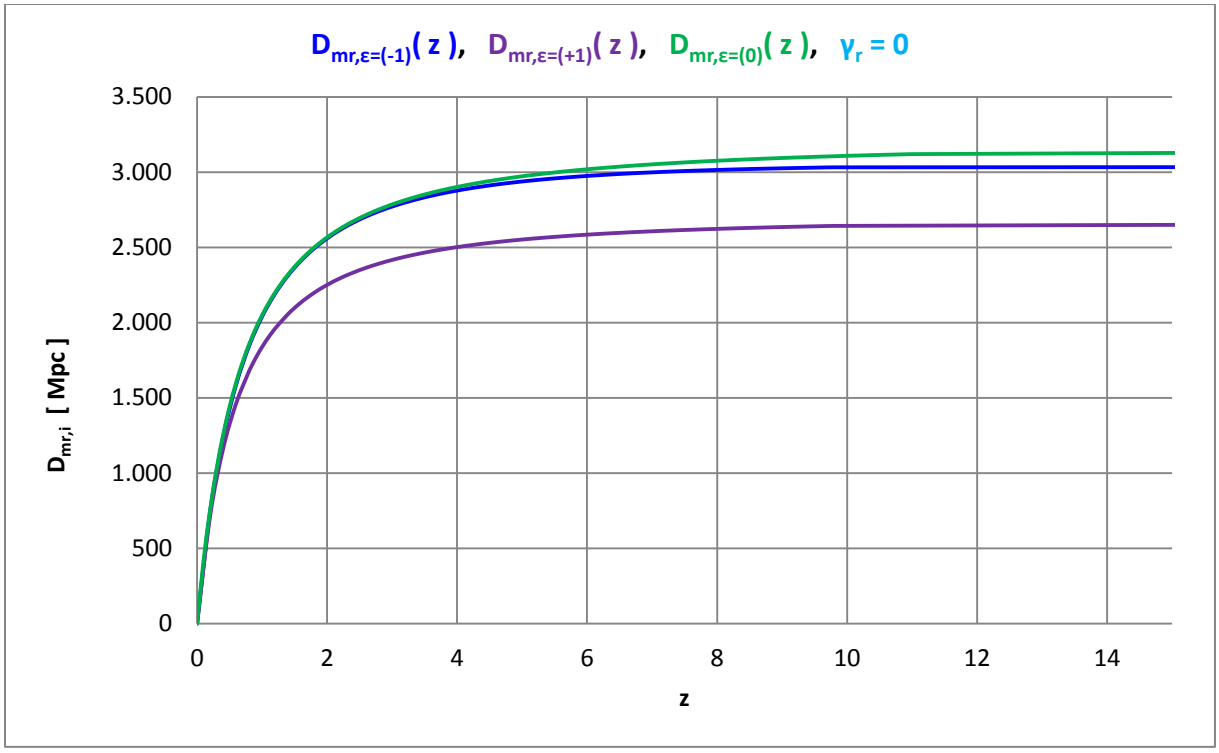

Figure 28. all redshift distances - real light ways - together in one diagram without normalization to R_{0a}.

We see that differences between the three curves occur only for relatively big redshifts. This shows us, that we have to analyze more data especially containing more bigger redshifts to can distinguish between the mathematical possible types of the universe.

All three real light pathes $D_{mr,\varepsilon=(\pm1,0)}$ of the photons through the expanding universe correspond to dynamic distances and appear therefore as apparent distances. These distances are in general not identical to the today's distances $D_{0,mr,\varepsilon=(\pm1,0)}(z)$ between the cosmic objects.

For every conceivable observer, the cosmic objects are not radial-spatially, where they appear at first glance!
In cosmology, nothing is what it seems to be if we look at distances and therefore in the past.

Of course, all cosmological relevant astrophysical objects have today's distances $D_{0,mr,\varepsilon=(\pm1,0)}$. However, these distances are not observable, but we can calculate them. Photons that are emitted at these distances from the observed galaxy cannot have reached us so far.

Note of thanks:

I would like to thank my wife for the long-standing toleration and the corresponding endurance of my almost constant virtual absence. What would I be without her?!

7. Appendix

In this table appendix, we provide the essential data that we have used and some of the data that we have edited or generated for general purposes.

$< V >_i$	$< z >_i$	$< V >_i$	$< z >_i$	$< V >_i$	$< z >_i$
17.12072194	0.269543711	19.5118161	1.28508799	19.7439932	1.86740102
18.42994924	0.434725324	19.4960406	1.30997857	19.7431839	1.90379949
18.77986464	0.514410603	19.5406994	1.33635871	19.73815	1.91629442
18.92177101	0.571495206	19.5648675	1.36044896	19.7370051	1.94113536
19.01993232	0.621120135	19.5526283	1.38646193	19.6390299	1.96661139
19.07454597	0.665043993	19.5667343	1.41249746	19.7247377	1.99498872
19.10685279	0.710045685	19.5917766	1.43823632	19.7073435	2.02761873
19.20756345	0.750830795	19.5835759	1.46348111	19.7225437	2.05895826
19.23878173	0.788362662	19.6146701	1.4877084	19.7209927	2.09067964
19.34673999	0.823077834	19.6560914	1.50872984	19.7166723	2.12286464
19.35605189	0.857111675	19.6421545	1.53039989	19.7562211	2.15726452
19.35379019	0.889902425	19.6730062	1.55031021	19.6955838	2.1915251
19.35354202	0.925268472	19.669718	1.57141117	19.7102256	2.23148844
19.36111675	0.958962211	19.691489	1.59370615	19.6203328	2.27565595
19.36687535	0.99085674	19.6689622	1.61663057	19.6516638	2.32895262
19.39208122	1.021072758	19.7130344	1.64024196	19.7034969	2.39616356
19.41216018	1.049862944	19.7208742	1.66227637	19.6915454	2.47184715
19.43737733	1.076128596	19.7568415	1.68460462	19.7660462	2.57089058
19.47736041	1.10186802	19.6973942	1.70912747	19.7708009	2.71401918
19.4307727	1.129618161	19.7453187	1.7323057	19.7781162	2.90122279
19.45345178	1.157690919	19.7723632	1.75403384	19.9208291	3.05796277
19.4499718	1.18469656	19.7568754	1.77625888	20.0279357	3.20401523
19.50609701	1.208890017	19.7599436	1.79742358	20.2283362	3.40521263
19.48940778	1.233098139	19.7587704	1.82113988	20.5549521	3.7254264
19.47597857	1.259028765	19.7435195	1.84394303	21.3169261	4.34427862

Table 10. Mean values from the quasar data set used according to [1].

Hint:

$\langle z \rangle_i$ (with i = 1, 2, ..., 75) are the 75 mean values of the redshifts of the quasars in the redshift intervals formed.
$\langle V \rangle_i$ are the associated 75 mean values of the apparent visual magnitude of the quasars.

z_i (end of interval)	N_i	z_i (end of interval)	N_i
0.24669	622	3.45369	128,884
0.49338	3,891	3.70038	130,205
0.74008	12,827	3.94708	131,357
0.98677	25,495	4.19377	132,019
1.23346	41,724	4.44046	132,432
1.48015	58,818	4.68715	132,669
1.72685	78,456	4.93385	132,848
1.97354	97,109	5.18054	132,902
2.22023	110,358	5.42723	132,924
2.46692	117,810	5.67392	132,932
2.71362	121,463	5.92062	132,949
2.96031	123,820	6.16731	132,972
3.20700	126,835	6.41400	132,977

Table11. Numbers N_i summed up in the redshift intervals z_i of the quasars according to [1].

SN Ia	μ_{TRGB}	μ_{Ceph}	μ or $\langle\mu\rangle$	m_{CSP_B0}	m_{SC_B}	m_B or $\langle m_B \rangle$	M_i or $\langle M_i \rangle$	V_{NED}	z
1980N	31.46		31.46	12.08		12.08	-19.38	1,306.00	0.004356347
1981B	30.96	30.91	**30.94**	11.64	11.62	**11.63**	**-19.31**	1,050.00	0.003502423
1981D	31.46		31.46	11.99		11.99	-19.47	1,306.00	0.004356347
1989B	30.22		30.22	11.16		11.16	-19.06	689.00	0.002298257
1990N		31.53	31.53	12.62	12.42	**12.52**	**-19.01**	1,050.00	0.003502423
1994D	31.00		31.00	11.76		11.76	-19.24	1,050.00	0.003502423
1994ae	32.27	32.07	**32.17**	12.94	12.92	**12.93**	**-19.24**	1,552.00	0.005176915
1995al	32.22	32.50	**32.36**	13.02	12.97	**13.00**	**-19.37**	1,886.00	0.006291019
1998aq		31.74	31.74	12.46	12.24	**12.35**	**-19.39**	1,368.00	0.004563157
1998bu	30.31		30.31	11.01		11.01	-19.30	689.00	0.002298257
2001el	31.32	31.31	**31.32**	12.30	12.20	**12.25**	**-19.07**	1,047.00	0.003492416
2002fk	32.50	32.52	**32.51**	13.33	13.20	**13.27**	**-19.25**	1,864.00	0.006217635
2003du		32.92	32.92	13.47	13.47	**13.47**	**-19.45**	2,422.00	0.008078922
2005cf		32.26	32.26	12.96	13.01	**12.99**	**-19.28**	2,244.00	0.007485178
2006dd	31.46		31.46	12.38		12.38	-19.08	1,306.00	0.004356347
2007af	31.82	31.79	**31.81**	12.72	12.70	**12.71**	**-19.10**	1,983.00	0.006614576

2007on	31.42		31.42	12.39		12.39	-19.03	1,306.00	0.004356347
2007sr	31.68	31.29	**31.49**	12.30	12.24	**12.27**	**-19.22**	1,702.00	0.005677261
2009ig		32.50	32.50	13.29	13.46	**13.38**	**-19.13**	2,534.00	0.008452514
2011by		31.59	31.59	12.63	12.49	**12.56**	**-19.03**	1,368.00	0.004563157
2011fe	29.08	29.14	**29.11**	9.82	9.75	**9.79**	**-19.33**	455.00	0.001517717
2011iv	31.42		31.42	12.03		12.03	-19.39	1,306.00	0.004356347
2012cg	31.00	31.08	**31.04**	11.72	11.55	**11.64**	**-19.41**	1,050.00	0.003502423
2012fr	31.36	31.31	**31.34**	12.09	11.92	**12.01**	**-19.33**	1,302.00	0.004343005
2012ht		31.91	31.91	12.66	12.70	**12.68**	**-19.23**	1,447.00	0.004826672
2013dy		31.50	31.50	12.23	12.31	**12.27**	**-19.23**	1,410.00	0.004703254
2015F		31.51	31.51	12.40	12.28	**12.34**	**-19.17**	1,271.00	0.0042396
						<M>=	**-19.24**		

Table 12. Summary of the data which we have used from the 27 SN Ia according to [3].

SN Ia values that can be traced back to a mean value are marked in green (bold).
The individual meanings of the data can be found in the article mentioned.

The data for the angular-size redshift diagram can be found in full in [2].

References

[1] M.-P. Véron-Cetty and P. Véron, A Catalogue of Quasars and Active Nuclei, 13th edition, March 2010, http://www.obs-hp.fr/catalogues/veron2_13/veron2_13.html

[2] K. Nilsson, M. J. Valtonen, J. Kotilainen and T. Jaakkola, Astro. J. 413 (1993), 453.

[3] W. L. Freedman u. a., The Carnegie-Chicago Hubble Program. VIII. An Independent Determination of the Hubble Constant Based on the Tip of the Red Giant Branch, arXiv.org:1907.05922

[4] The Planck Collaboration: Planck 2018 results. VI. Cosmological parameters, arXiv:1807.06209

[5] The Event Horizon Telescope Collaboration, The Astrophysical Journal Letters, 875:L1 (17pp), 2019 April 10, https://doi.org/10.3847/2041-8213/ab0ec7

[6] de.wikipedia.org/wiki/Messier_87, retrieved 18.12.2021

[7] de.wikipedia.org/wiki/Quasar, retrieved 18.12.2021

[8] de.wikipedia.org/wiki/UDFj-39546284, retrieved 18.12.2021

[9] G. Dautcourt, Was sind Quasare?, S. 68, Abb. 18, BSB B.G. Teubner Verlagsgesellschaft, 4. Auflage 1987

[10] A. Sandage, R. G. Kron, and M. S. Longair, The Deep Universe, Springer-Verlag, 1995, (Saas-Fee Advanced Course 23, Lecture Notes 1993, Swiss Society for Astrophysics and Astronomy, Publishers: B. Binggeli and R. Buser).

[11] St. Haase, New derivation of redshift distance without using power expansions, Fundamental Journal of Modern Physics, Volume 17, Issue 1, 2022, Pages 1-40
This paper is available online at http://www.frdint.com/

[12] St. Haase, Redshift distances in flat Friedmann-Lemaître-Robertson-Walker spacetime, viXra:2201.0168
